

UNIVERSITY OF OKLAHOMA  
GRADUATE COLLEGE

STUDY AND DEVELOPMENT OF IN-SITU CO<sub>2</sub> ENHANCED OIL RECOVERY

A DISSERTATION  
SUBMITTED TO THE GRADUATE FACULTY  
in partial fulfillment of the requirements for the  
Degree of  
DOCTOR OF PHILOSOPHY

By

SHUOSHI WANG  
Norman, Oklahoma  
2018

STUDY AND DEVELOPMENT OF IN-SITU CO<sub>2</sub> ENHANCED OIL RECOVERY

A DISSERTATION APPROVED FOR THE  
MEWBOURNE SCHOOL OF PETROLEUM AND GEOLOGICAL ENGINEERING

BY

---

Dr. Bor-Jier (Ben) Shiau, Chair

---

Dr. Jeffrey H. Harwell

---

Dr. Xingru Wu

---

Dr. Ahmad Jamili

---

Dr. Rouzbeh Ghanbarnezhad Moghanloo

© Copyright by SHUOSHI WANG 2018  
All Rights Reserved.

This dissertation is dedicated to my family for their constant encouragement

## **Acknowledgments**

I would like to express my heartiest gratitude to my advisor Dr. Benjamin Shiau for his continuous support and guidance on my Ph.D. research. With countless patient discussions and suggestions, he led me to the frontier of my interested topic. I always had enough freedom to explore each clue emerged along the route of my research. All the failed tests had been transferred to knowledge with his strong academic background. Dr. Shiau's comments and revisions to my paper are invaluable. It is a pleasure to work with him. I am also grateful to Dr. Jeffrey Harwell. The constructive suggestions inspired me to address the problems wisely. My curiosity of the science became to meaningful experimental design with his instructions.

I would also like to appreciate my committee members, Dr. Xingru Wu, Dr. Ahmad Jamili and Dr. Rouzbeh Ghanbarnezhad Moghanlo for their in-depth advice. The conversations with Dr. Xingru Wu were always enlightening. His knowledge and experience could show me a comprehensive view of my problem. Dr. Ahmad Jamili was the one who made me interested in CO<sub>2</sub> enhanced oil recovery research. He showed me a world that was worth studying. Dr. Rouzbeh Ghanbarnezhad Moghanlo was always supportive and helpful during my graduate study.

I want to express my gratitude to the DeepStar Consortium for financial support of this work. I would also like to express my thanks to Dr. Mohannad Kadhum for his inputs and the initial ideas.

I would also like to say thank you to all my colleagues in the Applied Surfactant Lab, Changlong, Sangho, Keren, Na for all the training and helping on the experiment work.

I would also like to thank my friends at OU, Yixin, Luchao, Wei, Li, Xiaochun, Tengfei, Ting and many others who made my life in OU joyful and colorful.

At last, many thanks to my parents, Qingbiao Wang and Jian Zhang, for their endless love.

# Table of Contents

Acknowledgments .....	iv
Table of Contents .....	vi
List of Tables .....	ix
List of Figures.....	x
Abstract.....	xiii
Chapter 1 : Overview.....	1
1.1 CO <sub>2</sub> Enhanced Oil Recovery .....	2
1.2 In Situ CO <sub>2</sub> EOR .....	4
Chapter 2 : Development of In-Situ CO <sub>2</sub> Generation Formulations for Enhanced Oil Recovery.....	8
2.1 Introduction .....	8
2.2 Materials .....	14
2.2.1 Chemicals .....	14
2.2.2 Porous Media.....	15
2.2.3 Apparatus.....	16
2.3 Experiment Procedure .....	17
2.4 Result and Discussion.....	19
2.4.1 Low Pressure tests (<80 psig).....	20
2.4.2 Intermediate Pressure Tests (1500 Psig) .....	23
2.4.3 High Pressure Tests (4000 psig).....	31
2.4.4 Core Flooding.....	34
2.4.5 Dilute Concentration of Gas Generating Agent .....	36

2.5 Summary.....	37
2.6 Conclusion.....	39
Chapter 3 : In-Situ CO <sub>2</sub> Generation for EOR by Using Urea as A Gas Generation Agent	
.....	41
3.1 Introduction .....	41
3.2 Materials.....	47
3.3 Experiment Procedure .....	48
3.4 Results and Discussion.....	51
3.4.1 Effect of Injection Flow Rate .....	52
3.4.2 Effect of Injection Pressure .....	53
3.4.3 Effect of Oil with Different Properties .....	59
3.4.4 Presence of Divalent Ions .....	62
3.4.5 Effect of Gas Generating Agent Concentration.....	64
3.4.6 Urea Solution PVT Test .....	65
3.5 Summary.....	67
3.6 Conclusion.....	68
Chapter 4 : In-Situ CO <sub>2</sub> Enhanced Oil Recovery: Parameters Affecting Reaction	
Kinetics and Recovery Performance .....	70
4.1 Introduction .....	70
4.2 Materials.....	74
4.2.1 Chemicals .....	74
4.2.2 Porous Media & Apparatus .....	75
4.3 Experimental.....	75



4.3.1 Urea Hydrolysis and Catalytic Reactions .....	75
4.3.2 Sand pack flooding with the presence of divalent ions .....	76
4.4 Results and Discussion .....	79
4.4.1 Urea Hydrolysis Kinetics .....	79
4.4.2 Flow through Tests Data Interpretation and Conditions .....	81
4.4.3 The Suitable Chemical Concentrations .....	84
4.4.4 The Optimized Injection Strategy .....	90
4.4.5 Impact of High Divalent Ions Level .....	93
4.4.6 Low Temperature .....	96
4.5 Summary .....	98
4.6 Conclusion .....	99
Chapter 5 : Conclusions and Recommendations .....	101
References .....	104
Appendix A: Representative Data .....	113

## List of Tables

Table 2-1 Physical properties of the oils used in the experiments (at 25°C and atmospheric pressure).....	15
Table 2-2 Test groups.....	19
Table 2-3 All Tests result summary .....	37
Table 3-1 literature reported CWI and in situ CO <sub>2</sub> generation tests.....	47
Table 3-2 Physical properties of the oils used in the experiments (at 25°C and atmospheric pressure).....	48
Table 3-3 Composition of Artificial Seawater .....	48
Table 3-4 Column test conditions.....	51
Table 4-1 The brine composition .....	77
Table 4-2 Experiment Conditions .....	83
Table 4-3 pH measurement of the aqueous effluent for test 1-5 .....	89
Table 4-4 Tertiary Recovery Summary .....	98
Table A.1 Chapter 2 test 11 .....	113
Table A. 2 Chapter 3 test 3.....	114
Table A. 3 Chapter 4 test 4.....	115

## List of Figures

Figure 1-1 Energy consumption increases over the projection for all fuels[1] .....	1
Figure 1-2 Active world, U.S., and Permian basin CO <sub>2</sub> EOR project counts[2].....	2
Figure 1-3 Plot showing U.S. oil production in barrels per day associated with various enhanced oil recovery .....	3
Figure 1-4 Measured and CO <sub>2</sub> solubility in Bakken stock tank oil/Brine sample at different equilibrium pressures and two constant temperatures of $T = 25$ and $40$ °C[5]..	5
Figure 2-1 CO <sub>2</sub> concentration as a function of distance[36].....	12
Figure 2-2 Schematic sand pack column flooding test for in situ CO <sub>2</sub> generation EOR	16
Figure 2-3 tertiary recovery stage Oil Saturation vs. PV for tertiary recovery stages of test 1.....	20
Figure 2-4 tertiary recovery stage Oil Saturation vs. PV for tertiary recovery stages of test 2 and test 3 .....	21
Figure 2-5 tertiary recovery stage Oil Saturation vs Time plot of test 4.....	23
Figure 2-6 tertiary recovery stage Oil Saturation vs. PV plot of test 5, test 6 and test 7 dash line stands for no flow stage.....	25
Figure 2-7 Test 6 and Test 7 Cumulative Gas Volume and Oil saturation VS PV .....	28
Figure 2-8 Produced oil composition change of test 6(DeepStar oil at 1500 psi).....	29
Figure 2-9 tertiary recovery stage Oil Saturation vs PV plot of test 8 and test 9 dash line stands for no flow stage .....	31
Figure 2-10 Oil Saturation vs. Time plot of core flooding for Test 11 DeepStar Oil 1300 psi Core flooding with shut-in.....	34

Figure 2-11 Oil Saturation vs Time plot of Low Gas Generating Agent Concentration Test 10 Earlsboro Oil 5% gas generating agent slug 1500 psi with shut-in.....	36
Figure 2-12 Oil Saturation reduction plot .....	38
Figure 2-13 tertiary recovery .....	39
Figure 3-1 Oil Saturation vs. PV for tertiary recovery stages, operating at different flow rate, NaCl 5% Brine, 1500 psi and 120°C with Earlsboro oil .....	52
Figure 3-2 Oil Saturation vs. PV for tertiary recovery stages, operating at different pressure, NaCl 5% Brine, velocity of 13.6 inches/day and 120°C with Earlsboro oil ...	54
Figure 3-3 Normal alkane composition changing in test 1(top) and test 3(bottom). The analyses for high pressure test (4,000 psi, Test 3) were carried out in triplicates for the individual sample to generate standard deviations in the curves. ....	56
Figure 3-4 Oil Saturation vs. PV for tertiary recovery stages, operating with different oils at 1500 psi, NaCl 5% Brine, 13.6 inches/day and 120°C .....	59
Figure 3-5 Oil Saturation vs. PV for tertiary recovery stages, operating with seawater/NaCl,1500 psi, 13.6 inches/day and 120°C with Earlsboro oil .....	62
Figure 3-6 Oil Saturation vs. PV for tertiary recovery stages, operating with different Urea concentration, NaCl 5% Brine, 1500 psi, 13.6 inches/day and 120 °C with Earlsboro oil .....	64
Figure 3-7 The 5 wt. % NaCl solution base case .....	65
Figure 3-8 The 5 wt.% NaCl and 10 wt.% urea solution tested case .....	66
Figure 3-9 Oil saturation change and tertiary recovery for all the tests .....	67
Figure 4-1 Temperature dependence of the rate constant for Urea hydrolysis .....	80

Figure 4-2 Oil saturation VS time for different urea concentration injection (Test1-5)  
The dashed lines between the dots indicate the injection of the gas generating agent slug. .... 85

Figure 4-3 Effect of the gas generating agent concentration on the tertiary recovery of each shut-in stage and total tertiary recovery ..... 87

Figure 4-4 Oil saturation VS time plot of 5 wt.% Urea injections with different injection strategy. The dashed lines between the dots indicate the injection of the gas generating agent slug. Cases: 5% Urea 1 PV flow through 1 PV Shut in(Test 6), 5% Urea 2 PV flow through (Test 7) and 5% Urea 1+1 PV shut-in (Test 3)..... 90

Figure 4-5 Oil saturation VS time plot of 10 wt.% Urea injections with different injection strategy. The dashed lines between the dots indicate the injection of the gas generating agent slug. Cases: 10% Urea 1 PV flow through 1 PV Shut in (Test 8), 10% Urea 2 PV flow through (Test 9) and 10% Urea 1+1 PV shut-in (Test 4)..... 91

Figure 4-6 Oil saturation VS time plot of 10 wt.% Urea with API brine and 10 wt.% Urea with seawater. Cases: 10% Urea API Brine 1+1PV Shut in (Test 10) and 10% Urea 1+1PV Shut in (Test 4)..... 95

Figure 4-7 Oil saturation VS time plot of 35 wt.% urea injection at 80°C and 2.5 wt.% urea injection at 120°C. Cases: 35% Urea 80°C 1+1PV Shut in (Test 11) and 2.5% Urea 1+1PV Shut in (Test 2)..... 97

Figure 4-8 Conversion factor of all the tests. .... 99

## Abstract

While the injection of CO<sub>2</sub> has great potential for increasing oil production, this potential is limited by site conditions and operational constraints such as the lack of proper infrastructure, limited cheap CO<sub>2</sub> sources, viscous fingering, gravity override at the targeted zones, and others. The alternative methodologies which can successfully deliver CO<sub>2</sub> through gas generation in situ, with superior improved oil recovery (IOR) performance, while offering reasonable chemical cost is explored to mitigate some of these common limitations.

In this study, the ammonium carbamate and urea are considered as the new compounds capable of generating CO<sub>2</sub> in situ. Their self-reaction ignition properties make the single fluid injection possible and reduce the complexity of the injection system. With exceptional water solubility (up to 40 wt.% for ammonium carbamate and 50% for urea at room temperature), ammonium carbamate and urea can be thermally endothermically hydrolyzed to CO<sub>2</sub> and NH<sub>3</sub> after equilibration under reservoir conditions. Because of their CO<sub>2</sub> producing capacity and reasonable cost-benefit, they appear to be a promising candidate for delivering CO<sub>2</sub> to increase oil recovery.

In this work, the performance of injected aqueous chemical solutions was evaluated in a series of bench experiments to mimic tertiary oil recovery (perform test after the residual oil saturation was established by water flooding). One-dimensional sand pack tests and core flooding experiments were operated at different pre-set conditions: the flow rate varied from 0.03 to 0.3 ml/min, CO<sub>2</sub> generating chemical concentrations from 1 to 35 wt%, pressures from 0 to 4000 psig, , temperature from 80 to 133 °C and different API gravity oils were used, varying from 27 to 57.3.

The eluted crude oil and brine samples from these tests were collected and analyzed to assess the change of oil properties and brine chemistry influenced by the thermally produced CO<sub>2</sub> and NH<sub>3</sub>. In addition, the reaction rates of urea hydrolysis were tested separately using a microwave reactor to compare the kinetics of urea hydrolysis reactions via varying reaction temperatures.

Most importantly, results of injecting chemical solution (as low as 1 % solution) showed tertiary recovery performance (as high as 50%) as compared to the similar in situ CO<sub>2</sub> generation EOR(2.4% to 18.8%) approaches proposed by others. Because of the reservoir brine compatibility of urea, even under high levels of divalent ions( Ca<sup>+2</sup> 7000 ppm), the experiment showed no detectable effect of brine composition on the recovery and/or any occurrence of formation damage. The post-reacted solution showed a solution pH about 10 because of the formation of NH<sub>3</sub> (and NH<sub>4</sub>OH). Compositional analyses of the eluted oil also revealed different trends as compared to typical CO<sub>2</sub> flooding, indicating additional benefits of this new CO<sub>2</sub> delivery method resulted from the produced ammonia and its impact on the wettability of the solid surfaces. The economic feasibility and operational advantages of this newly developed method were demonstrated in this work. In brief, results of this work served further as a proof of concept for designing in situ CO<sub>2</sub> generation formulations for tertiary oil recovery at both onshore and offshore fields under proper conditions. It can be a guide to select the suitable reservoir condition, oil property, chemical concentration and injection strategy.

## Chapter 1: Overview

Fossil fuels remain to meet most of the world's energy demand in the recent years with the fast growth of the renewable energy. Based on the projection from Figure 1-1, petroleum and other liquids account for the most considerable part of the energy source with its share reducing from 33% in 2015 to 31% in 2040. Petroleum is growing 0.7% per year, compared with the coal's 0.1% per year growth.

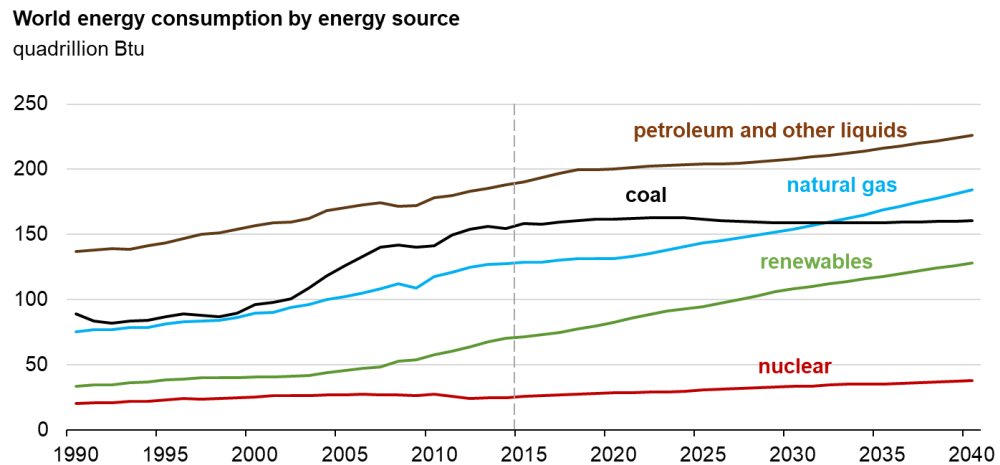


**Figure 1-1 Energy consumption increases over the projection for all fuels[1]**

The oil consumption is currently around 98.4 million barrels per day and continuously increasing with time. Therefore, the exploration of the new oil reservoirs and enhancing the recovery of the proved reserves are still necessary to meet the future world energy demand. After the well is drilled into the reservoir, the first stage of hydrocarbon production is the primary recovery. The natural energy of the oil reservoir is driving the hydrocarbons to the wellbore. Once the energy of the reservoir is depleted during the primary recovery, the water/gas injection will be applied as the secondary recovery



method. At this stage, the purpose of the injection is to maintain the reservoir pressure and displace the oil to the wellbore. After the first two stages of the hydrocarbon production, the reservoir produces around 15% to 40 % of the original oil in place.

Tertiary recovery starts when secondary recovery is not efficient in the oil production. Thermal methods, gas injection, microbial methods and chemical flooding are used in the tertiary recovery stage.

### 1.1 CO<sub>2</sub> Enhanced Oil Recovery

CO<sub>2</sub>-EOR is an efficient method that can increase oil production after primary and secondary phase of production. At the same time, it is a CO<sub>2</sub> storage option to reduce the emissions of CO<sub>2</sub>.

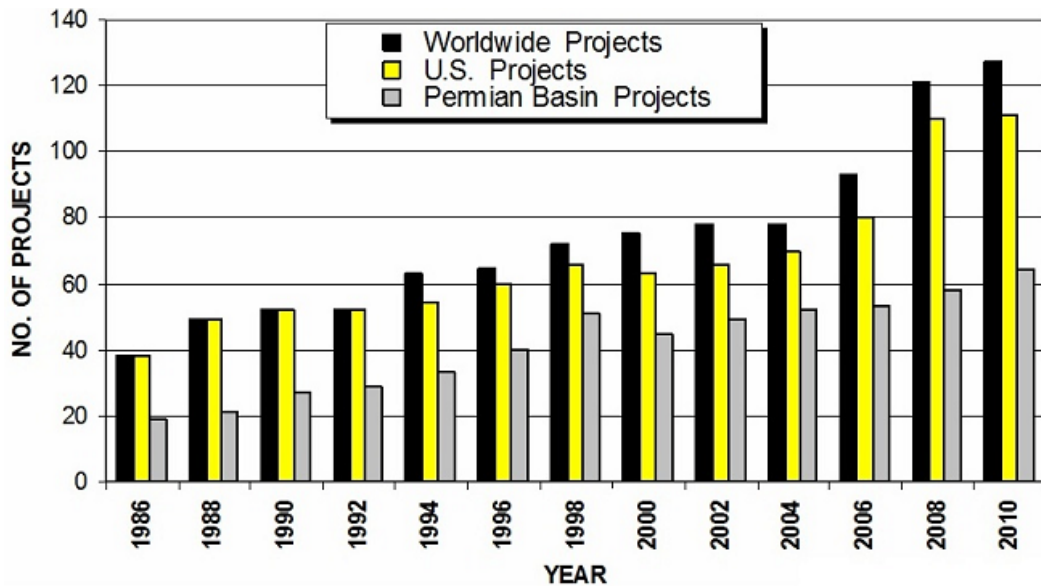


**Figure 1-2 Active world, U.S., and Permian basin CO<sub>2</sub> EOR project counts[2]**

Figure 1-2 shows that U.S. has the largest amount of active CO<sub>2</sub> EOR project in the world. The supply of CO<sub>2</sub> leads the project expansion of the Permian Basin. Based on

the records from active EOR projects within the United States, oil production from CO<sub>2</sub>-EOR has continued to increase compared to other EOR methods (Figure 1-3).

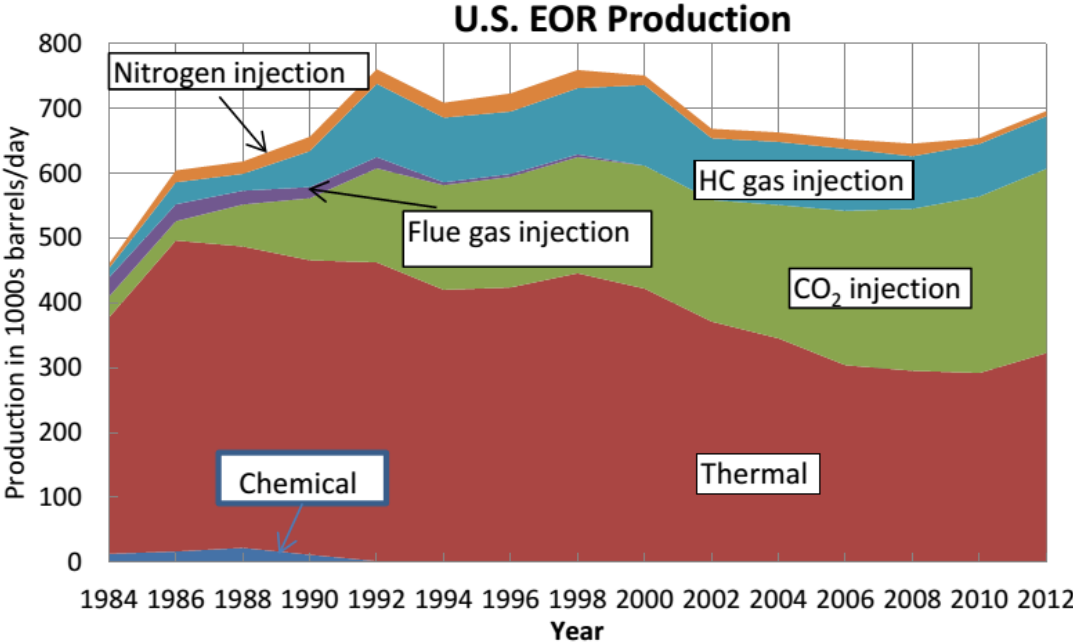


**Figure 1-3 Plot showing U.S. oil production in barrels per day associated with various enhanced oil recovery (EOR) methods[3]**

The CO<sub>2</sub> flooding improves oil recovery by lowering interfacial tension, swelling the oil, reducing oil viscosity, and the CO<sub>2</sub> miscible and immiscible displacement between oil and CO<sub>2</sub>.

$$E = E_D E_V \dots \dots \dots (1.1)$$

Where

*E*, Overall displacement efficiency

*E<sub>D</sub>*, Microscopic displacement efficiency

*E<sub>V</sub>*, Macroscopic displacement efficiency

The macroscopic displacement efficiency is a measure of how well the displacing fluid has come in contact with the oil-bearing parts of the reservoir. The microscopic displacement efficiency is a measure of how well the displacing fluid mobilizes the residual oil once the fluid has come in contact with the oil[4]. Despite the lack of CO<sub>2</sub> source and transporting infrastructure, the low viscosity and low density of the CO<sub>2</sub> are resulting in high mobility ratio. Even the microscopic displacement efficiency of CO<sub>2</sub> flooding is high. The viscous fingering and gravity override cause an early breakthrough. Low macroscopic displacement efficiency is leaving much of the residual oil uncontacted after the CO<sub>2</sub> flooding. The sweep efficiency of the CO<sub>2</sub> flooding is still a primary drawback to the tertiary recovery.

### **1.2 In Situ CO<sub>2</sub> EOR**

The concept of the In situ CO<sub>2</sub> EOR(ICE) is to deliver the CO<sub>2</sub> to the reservoir by injecting a chemical solution that releases CO<sub>2</sub> at reservoir condition. The availability of CO<sub>2</sub> and high mobility of the gas slug issues are resolved in ICE process. Since ammonia is generated as a by-product of the ICE chemical hydrolysis, it is expected that besides all the benefits from carbonated water injection(CWI), the positive effects on the tertiary recovery from ammonia molecules are introduced in ICE.

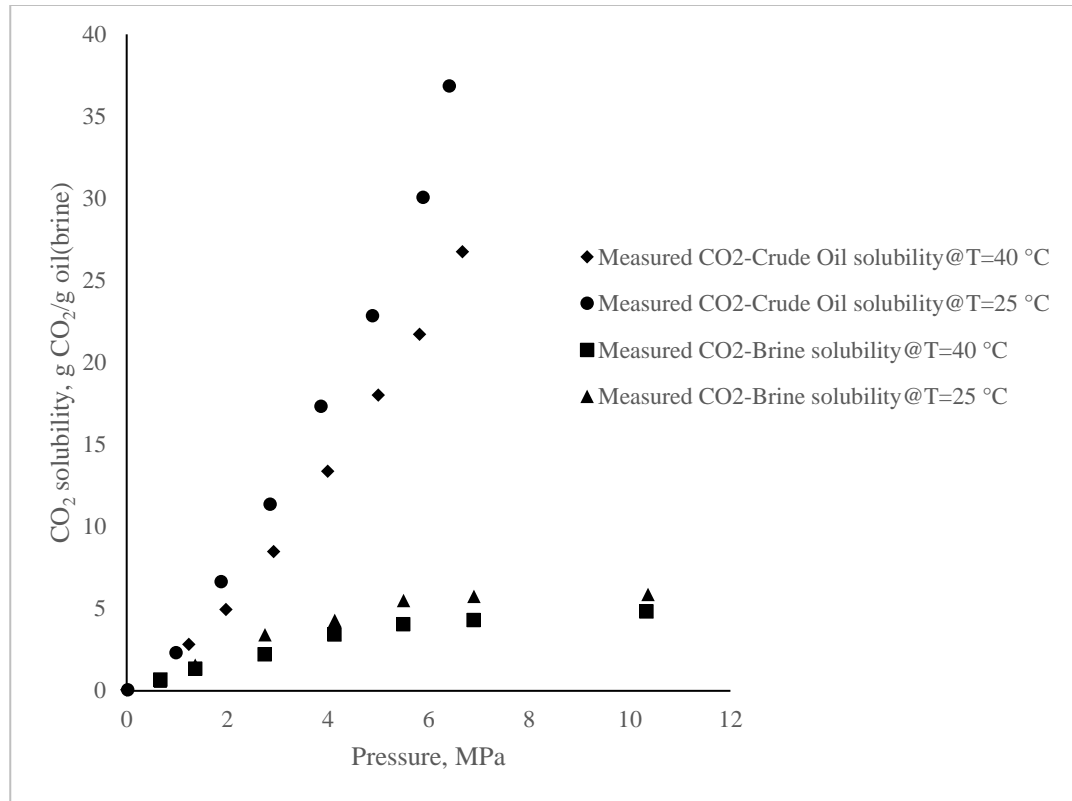


**Figure 1-4 Measured and CO<sub>2</sub> solubility in Bakken stock tank oil/Brine sample at different equilibrium pressures and two constant temperatures of  $T = 25$  and  $40$  °C[5]**

From the Figure 1-4, large CO<sub>2</sub> solubility contrast between brine and oil is observed[5].

The salinity of the tested brine is 0.35 mole NaCl/kg water. The MW of the tested Bakken stock tank oil is 223 g/mole. Most of the formed CO<sub>2</sub> in the aqueous phase can migrate to the oil phase. After the chemical decomposition and CO<sub>2</sub> migration, the involved tertiary recovery mechanisms are oil swelling and oil viscosity reduction from CO<sub>2</sub> dissolution, wettability alteration and alkalinity benefits from ammonia.

In this dissertation, the work focuses on the development of an efficient ICE formulation. Chapter 2 proposed the ammonium carbamate as the gas generating agent.

The cool aqueous amines CO<sub>2</sub> capture process forms ammonium carbamate. On the

contrary, heating the ammonium carbamate aqueous solution releases CO<sub>2</sub>. This phenomenon makes delivering the CO<sub>2</sub> to the targeted reservoir by injecting the aqueous solution indirectly possible. The CO<sub>2</sub> production from the ammonium carbamate hydrolysis was observed. The concentrated solution was used to enhance the tertiary recovery in the sand pack and Brea core. The proof of concept of the newly proposed technique was provided in a broad range of testing condition. ICE showed behavior that CO<sub>2</sub> flooding and CWI did not have. The work of this chapter was published on the Energy & Fuels after peer review.

Chapter 3 focuses on using urea as the gas generating agent to explore a better divalent cations tolerance. The urea can also be hydrolyzed at reservoir condition to release CO<sub>2</sub>. It is commercially available in large quantity in the fertilizer industry. The tertiary recovery ability of the concentrated urea solution was evaluated at reservoir conditions with different brine and oil. Other than the proof of concept for the tertiary recovery, the urea solution showed superior divalent cations compatibility that ammonium carbamate did not have when it mixed with sea water. This work was published on the Fuel after peer review.

Chapter 4 continues the research on urea ICE system. The kinetic parameters of the urea hydrolysis reaction were determined for optimization and pilot test design. The concentration of the urea slug was optimized based on different criteria. As a tertiary recovery method, the optimized case exhibited low chemical cost compared with the surfactant flooding. The hypothesis based on the reaction kinetics was proved, which could expand the ICE operating envelope (salinity and temperature). The chapter was accepted by 2018 SPE Improved Oil Recovery Conference and had been submitted

to Fuel for peer review.

Chapter 5 presents some conclusions of this work and recommendation for the future

ICE studies.

## **Chapter 2: Development of In-Situ CO<sub>2</sub> Generation Formulations for Enhanced Oil Recovery**

### **2.1 Introduction**

The CO<sub>2</sub> flooding is one of the most proven tertiary Enhanced Oil Recovery (EOR) methods and has been increasingly used in the US and other regions [3, 6]. The injected CO<sub>2</sub> could exhibit impressive microscopic displacement efficiency, mostly conducted at or above the minimum miscibility pressure(MMP) conditions, but frequently suffers adverse performance in macroscopic displacement. Because of the large density contrast between the oil displaced and CO<sub>2</sub>, severe gravity segregation may lead to significant gas override because of less favorable mobility ratio and poor sweep of oil. Some proposed use of the Water Alternating Gas (WAG) process to mitigate the bypass issues of CO<sub>2</sub> injection [7, 8]

Sometimes, the WAG-modified process is unlikely to become economically viable, largely due to the presence of thick formation [5]. Many optimization efforts are required for acceptable economic feasibility on the WAG process[7, 9]. Carbonated Water Injection (CWI), viz. injecting water with dissolved CO<sub>2</sub>, offered an alternative to address the problem of the WAG. The CWI technique had been demonstrated both in laboratory studies [10-12] and field pilot tests [13-15]. CWI is a single aqueous phase injection that has similar sweep efficiency as water flooding. In comparison with conventional CO<sub>2</sub> flooding and CO<sub>2</sub> WAG, only minor modification of the existing water injection system is required using a CWI system. For example, a pressurized

mixing tank for dissolving CO<sub>2</sub> at surface facilities can easily achieve the CWI modification for an ongoing water flooding project.

In general, the levels of gas water ratio (GWR) of CWI are largely controlled by reservoir condition.[16, 17]. Previously Shu [16] proposed that additional chemical promoters can be introduced in CWI application to improve aqueous solubility of CO<sub>2</sub> dramatically. Examples of the promoters, such as mono- or di-ethanolamine, ammonia, carbonates (Na, K), hydroxides (Na, K), phosphate (K), diaminoisopropanol, di- and tri-ethanolamine were studied in the CWI application. Addition of promoter likely increases the complexity of the CWI system. In practical, the availability of low-cost CO<sub>2</sub> source will be the key economic consideration for any CO<sub>2</sub>-based projects.

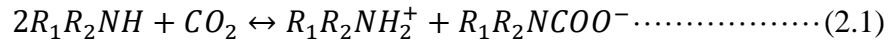
To address some of the issues mentioned above, in-situ CO<sub>2</sub> generation for EOR application were investigated in recent years. A variety of CO<sub>2</sub> generated compounds, including aluminum carbamide, ammonium carbamate, sodium carbonate and ammonium bicarbonate were developed [18-25]. A few of field scale pilot tests were also reported even for offshore reservoirs ( Li, Ma, Liu, Zhang, Jia and Liu [25]). The gas generation mechanism of the previously developed system involved complex reaction or involved multiple recovery mechanisms, for example, low interfacial tension (IFT) surfactant flooding in conjunction with CO<sub>2</sub> generation, co-injection with polymer, or alkaline, acidizing treatment combined with CO<sub>2</sub> flooding.

Increasing the complexity of prior systems developed somewhat limited their economic feasibility of the project. In this work, a new CO<sub>2</sub> generation methodology is explored to further eliminate the shortcomings of current In Situ CO<sub>2</sub> generation formulations. The potential benefits of these new approaches include:



- i. Not relying on the natural CO<sub>2</sub> source and CO<sub>2</sub> transportation pipeline.
- ii. Better sweep efficiency than that of CO<sub>2</sub> WAG.
- iii. High GWR comparing to limited GWR of CWI[10, 26, 27]
- iv. Self-initiation gas generation ability versus sequential injection of the gas generating reagents and acid slug system (a complex fluid system)
- v. Simple and cheap in operations (no additional polymer, surfactant or alkaline required)
- vi. Reasonable recovery performance either above or below minimum miscibility pressure conditions.

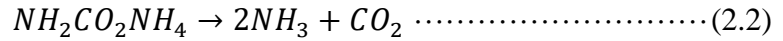
Some of the new proposed systems uses the product of the CO<sub>2</sub> capture technology as the gas generating agent. Chemical solvents are used widely for CO<sub>2</sub> capture application[28, 29]. Aqueous amines can absorb CO<sub>2</sub> and form carbamates by the following reaction [30]:



At relative high reservoir temperature condition, most CO<sub>2</sub> absorbed in carbamate solution can be dissociated. Injection of carbamate solution offers an effective route to deliver CO<sub>2</sub> to the targeted rock matrix. The aim of the new improved technique is simultaneously lowering the cost of both CO<sub>2</sub> capture and in-situ CO<sub>2</sub> generation for EOR operation.

Ammonium carbamate is selected here as the simplest representative of the solute compounds in typical CO<sub>2</sub> captured carbamate solution. Ammonium carbamate is a monovalent ammonium salt with chemical formula  $NH_2CO_2^-NH_4^+$ . Solid ammonium

carbamate decomposes at temperature above 60 °C . It has a water solubility approximately around 40 wt. % at room temperature. Ammonium carbamate in aqueous solution can largely decompose to generate CO<sub>2</sub> at 92°C [19, 31].



The formation of CO<sub>2</sub> in the system also involves a complex chemical process reported by the previous researchers[32].

Flury, Afacan, Tamiz Bakhtiari, Sjoblom and Xu [33] reported that ammonia was a suitable replacement of sodium hydroxide on bitumen extraction because ammonia had faster performance on bitumen liberation than the use of sodium hydroxide at same pH value. The liberation of bitumen from the sand grains would lead to wettability reversal from oil-wet to water-wet. Besides, Fjelde and Asen [34] also showed some evidences of more water wet surfaces generated during a CO<sub>2</sub>-WAG process in chalk rocks. Therefore, the effect of CO<sub>2</sub> generated in situ on wettability change cannot be neglected.

Southwick, van den Pol, van Rijn, van Batenburg, Boersma, Svec, Anis Mastan, Shahin and Raney [35] showed the significant cost and logistical advantages of ammonia as an alkali for alkali/surfactant/polymer (ASP) flooding. It is especially preferred in the offshore application.

The physical process within the In-Situ CO<sub>2</sub> generation system involves the mass transfer from the aqueous phase to oil phase. If there exists a driving force (concentration difference), mass transfer of CO<sub>2</sub> will naturally occur from one phase to

another. The mass transfer of CO<sub>2</sub> generated can be conveniently described by the two liquid film theory[36].

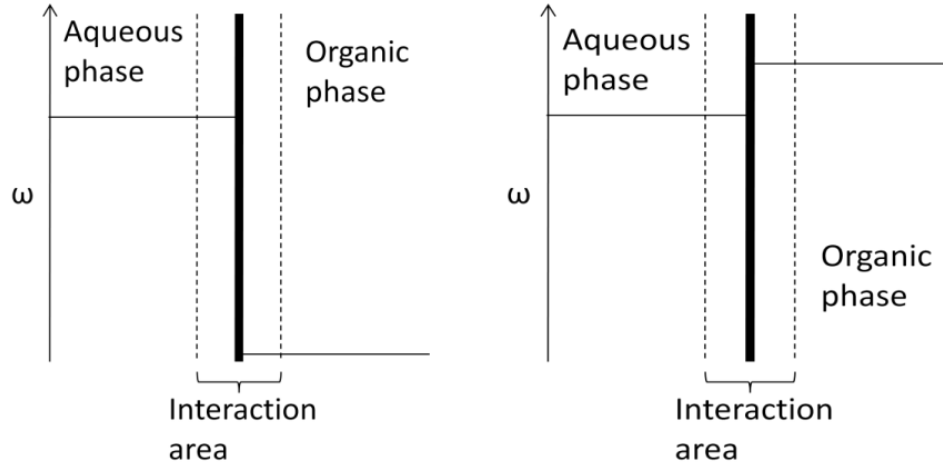


**Figure 2-1 CO<sub>2</sub> concentration as a function of distance[36].**

In Figure 2-1, plot on the left shows initial condition and right is the condition after equilibrium. In the beginning, the CO<sub>2</sub> concentration is higher in aqueous phase than in oil phase. The direction of mass transfer is from the aqueous phase to oil phase. Because of high intrinsic solubility of CO<sub>2</sub> in oil, when the equilibrium is reached, the CO<sub>2</sub> concentration in the oil phase is much higher than it in the aqueous phase. It is controlled by the partition coefficient.

$$K = \left[ \frac{\omega_{CO_2}^w}{\omega_{CO_2}^o} \right]_{P,T} \dots\dots\dots(2.3)$$

Where  $\omega_{CO_2}^w$  and  $\omega_{CO_2}^o$  are the solubility of CO<sub>2</sub> in water and oil respectively.  $\omega_{CO_2}^w$  can be calculated from the model proposed by Duan, Sun, Zhu and Chou [37] Hangx [38] summarized  $\omega_{CO_2}^w$  in aqueous phase at presence of  $K^+$ ,  $Mg^{2+}$ ,  $Ca^{2+}$  and  $SO_4^{2+}$  or DI

water condition in CWI application.  $\omega_{CO_2}^o$  can be modeled by many EOS calculations [39, 40].

For the new proposed in-situ CO<sub>2</sub> generation EOR, the effects of CO<sub>2</sub> generation involved ions,  $HCO_3^-$ ,  $NH_3$ ,  $CO_3^{2-}$ ,  $NH_4^+$  and  $H_2NCOO^-$ , on the CO<sub>2</sub> water solubility still require further investigation. Altunina and Kuvshinov [22] reported that the partition coefficient for CO<sub>2</sub> in oil/water system in the temperature range of 35-100°C and the pressure range of 10-40MPa is between 4 and 10 (i.e., dissolved mostly in oil), whereas the coefficient value for ammonia is extremely low and does not exceed  $6 \times 10^{-4}$ .

After the CO<sub>2</sub> equilibrated between aqueous and oil phase, higher CO<sub>2</sub> content results in oil swelling and viscosity reduction. The swelling factor (SF) is defined as the ratio of CO<sub>2</sub>-saturated oil volume at reservoir pressure and the temperature to original oil volume measured at reservoir temperature and atmospheric pressure [41]

$$SF = \frac{V_{CO_2-oil}(P_R, T_R)}{V_{oil}(P_{atm}, T_R)} \dots \dots \dots (2.4)$$

Where

$V_{CO_2-oil}$ , the volume of CO<sub>2</sub>-oil mixture

$V_{oil}$ , the volume of oil

When a significant amount of CO<sub>2</sub> is dissolved into crude, total oil volume will increase. This phenomenon can contribute to higher oil recovery. Increasing oil volume results in an apparent increase of oil saturation, thus allowing the discontinuous oil droplets previously trapped in the pores to merge with the mobile oil phase [42].

Assume that the residual oil saturation is the same whether the oil is carbonated or not. Then the same volume of oil will contain less pure oil if it is carbonated, due to oil swelling [43]. The dissolved CO<sub>2</sub> will cause the decrease in oil viscosity. The reduction level is mainly depending on CO<sub>2</sub> concentration in the oil. Holm [44] stated that CO<sub>2</sub> could reduce the viscosity of oil at certain reservoir condition up to 5 to 10 times because of quite high CO<sub>2</sub> solubility. If the original oil has a higher initial viscosity, a larger percentage reduction in oil viscosity will realize when it is fully saturated by subcritical CO<sub>2</sub> [45]. The reduction of CO<sub>2</sub> saturated oil viscosity is higher at lower temperatures than at high temperatures because of higher solubility of CO<sub>2</sub> occurred at lower temperature [42].

The main mechanisms of the In situ CO<sub>2</sub> generation EOR is a combination of carbonated water flooding (oil swelling and viscosity reduction) and alkali flooding (wettability reversal and in situ surfactant generation[35])

## **2.2 Materials**

### *2.2.1 Chemicals*

Ammonium carbamate (99 wt.%) was purchased from Sigma-Aldrich. NaCl (99.5 wt.%) was purchased from Sigma-Aldrich to mimic salt in reservoir brine.

Four different oils were tested as the example fluid to be displaced from the sand pack and sandstone core plugs. Pure dodecane was purchased from Sigma-Aldrich. The Earlsboro crude oil was donated by Arrow Oil and Gas (Norman, OK). Deep Star crude oil was provided by DeepStar Consortium. The oil properties are shown in Table 2-1.

**Table 2-1 Physical properties of the oils used in the experiments (at 25°C and atmospheric pressure)**

	Dodecane	Earlsboro	Deep Star
API	57.3	40	27
Viscosity, cP	1.34	4.6	22

### *2.2.2 Porous Media*

For the sand pack tests, two types of Ottawa sand from U.S. silica were tested. The size distribution of F-95 Ottawa sand was between 0.075mm and 0.3 mm with d50 at 0.145mm. The second F-75 Ottawa sand possesses size between 0.053mm and 0.6 mm and d50 of 0.15mm. The porosity of packed column was measured to be 34.5%. The permeability of the Ottawa sand pack was measured to be 4 D. The oven-dried Ottawa sand was carefully dry packed into two distinct pressure rating stainless steel columns based on the experiment objective. The total length of all sand packs was adjusted to the same 6 inches. The inside diameter of regular 3100 psi pressure rating sand pack was 0.834 inch. The inside diameter of elevated 4900 psi pressure rating sand pack was slightly larger at 1.12 inches.

Based on the geometry of the sand pack and the measured porosity of Ottawa sand, the pore volumes of the 3,100 psi rating sand pack and 4,900 psi rating sand pack were calculated as 18.95mL and 34.15mL respectively.

For the core flooding test, Berea sandstone core was used. The diameter of the core samples were drilled at 25.45mm. Length of the core plug was 148.09mm. The porosity of the core was measured as 17.13%. Pore volume was 12.91mL.

### 2.2.3 Apparatus

The effectiveness of the In-Situ CO<sub>2</sub> generation process for EOR was evaluated under elevated pressure and temperature oil displacement conditions. Figure 2-2 is a schematic of sand pack flooding apparatus. It consisted of two syringe pumps (Teledyne Isco 260D), three accumulators for different fluids, a high pressure stainless steel column as a sand pack, back pressure regulator, digital pressure gauges, heating oven and sample collector. The column was made of stainless steel and could be operated at pressures up to 4,900 psi and temperature up to 200°C. A coil of tubing was installed at the inlet of the sand pack to preheat the chemical slug. Gas evolved from effluent fluids in the process was collected in sealed burettes. Gas volume and liquid volume were recorded manually by reading the burettes level. The digital pressure gauges continuously recorded the pressure of both the inlet and the outlet of the sand pack. A digital thermometer continuously recorded the temperature of the oven.

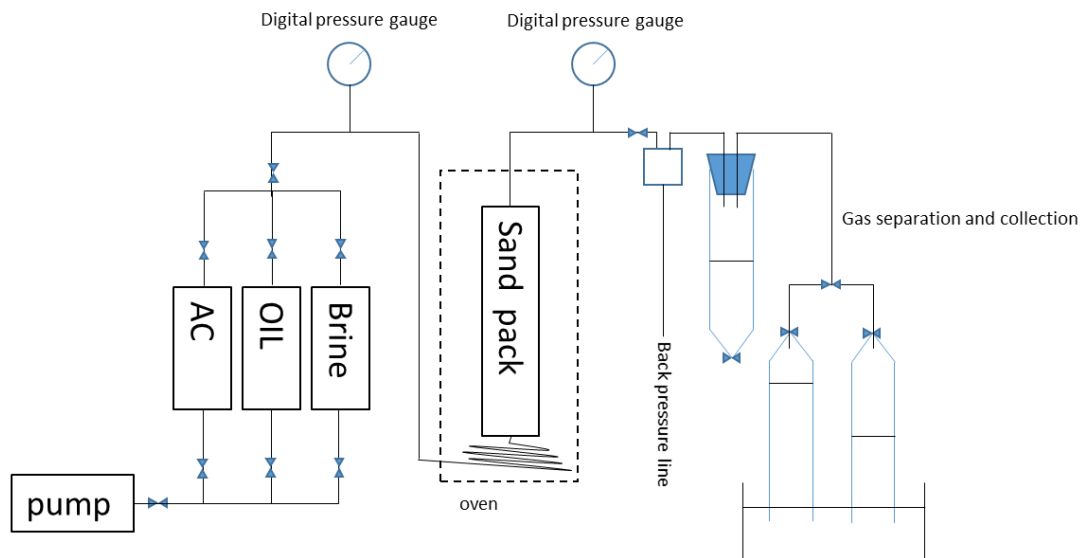


**Figure 2-2 Schematic sand pack column flooding test for in situ CO<sub>2</sub> generation EOR**

### 2.3 Experiment Procedure

Gas generating solution (5-35 wt.% ammonium carbamate prepared in 5 wt. % NaCl solution) and base brine solution (5 wt. % NaCl) were dissolved in deionized water. Density for concentrate (35 wt.%) and dilute (5 wt.%) ammonium carbamate solution were measured as 1.13 g/ml and 1.042 g/ml respectively. The density of 5 wt.% NaCl brine was measured as 1.033 g/ml.

A fixed amount of targeted oil was injected into Ottawa sand packed stainless steel column to saturate the medium. Water flooding was initiated immediately after the oil saturation process. The resulted oil saturation appeared quite low primarily due to water wetting surface of the Ottawa Sand (99.77% silica quartz[46]), thus underrated the EOR potential of proposed technique. Some modifications were made to increase initial level of oil saturation by packing sand with the spiked oil together and keeping in the oven for an extra aging step before the water flooding stage. All aged sand packs were dry packed. The dry pack was the way to prepare the sand pack. It is designed for higher residual oil recovery after the brine flooding. The normal sand packing process packed the sand with brine. Then the air was flushed by brine injection before saturating the sand pack with crude oil. During the dry pack process, no brine was injected when the sand was packed in the stainless steel column. No brine was injected before saturating the sand pack with crude oil. The crude oil injection flushed the air in the sand pack. Changing the degree of compaction could adjust the porosity of the porous media in a small range. Therefore, to get the consistent property on the sand pack column, a fixed amount of Ottawa F-75 sand was loaded in every sand pack. In this aging process, the sand packs sealed with oil were kept in an 80°C oven over one month period to



effectively reverse the wettability of the sand surface, leading to much higher residual oil saturation after the water flooding[47].

The procedure for individual sand pack column flooding test was kept identical for consistency. The residual oil saturation was initially established by injecting multiple pore volumes of brine flooding (until no further oil produced). Then a total of two pore volumes (PV) of gas generating agent were injected into the sand pack followed by 2 to 3 PVs of post brine injection to chase out the mobilized oil. In some selective tests, a shut-in cycle was added whereas after 2 PVs of ammonium carbamate injection, the flow was interrupted for approximate 24 to 48 hours downtime to allow more chemical decomposition and interphase mass transfer to proceed. The shut-in time was selected based on the ease of the experiment running. And the added shut-in cycle was designed only to see the effect of extended chemical residence time. After shut in time expired, post brine flooding was resumed. The optional shut-in cycles were conducted in the selected tests to assess any possible mass transfer limitation or the inadequate residence time of chemicals.

In this work, brine solution refers to 5 wt.% NaCl and AC solution refer to 35 wt.% Ammonium Carbamate dissolved in 5 wt.% NaCl, unless specified elsewhere. This work aims to prove the CO<sub>2</sub> EOR ability of the proposed system. Therefore, highly concentrated chemical solutions are used to deliver an excessive amount of CO<sub>2</sub>. No optimization is involved. Maintaining the identical interstitial velocity (1.46cm/hour), the flow rates were 0.03 ml/min and 0.055 ml/min in the 3100 psi-rating sand pack and 4900 psi-rating sand pack, respectively.

## 2.4 Result and Discussion

In Situ CO<sub>2</sub> generation formulation was tested as a potential tertiary recovery technique. For comparisons, the common tertiary recovery factor (Etr) was monitored and analyzed as an efficiency indicator of the newly developed process.

$$Etr = \frac{V_{In\ Situ\ CO_2\ Generation\ produced\ oil}}{V_{Dry\ packed\ oil\ volume} - V_{Brine\ flooding\ produced\ oil\ volume}} \times 100\% \dots\dots\dots (2.5)$$

The crucial operation parameters, such as sand pack inlet pressure, outlet pressure, and oven temperature, were recorded automatically per 1 minute time interval. In addition, the volume of total gas generated was quantified in ambient conditions simultaneously. The variation of the resulted oil saturation (S<sub>o</sub>) over time was plotted against the PV injected.

$$S_o = \frac{V_{Dry\ packed\ oil\ volume} - V_{Produced\ oil\ volume}}{V_{Pore\ volume}} \times 100\% \dots\dots\dots (2.6)$$

Based on the different parameters investigated, a series of total 11 tests are subdivided into five groups showed in Table 2-2. Additional details of these tests are summarized in Table 2-3 later. The resulted oil saturation values after the initial water flooding, S<sub>or</sub>, was plotted for ease comparisons.

**Table 2-2 Test groups**

	Low pressure (1 atm-80psi)	Intermedi ate pressure (1500psi)	High Pressure (4000psi)	Core floodin g	Low gas generating agent concentratio n
Earlsboro oil	Test 1-3	Test 4,5	Test 8		Test 10
DeepStar oil		Test 6	Test 9	Test 11	
Dodecane		Test 7			

### 2.4.1 Low Pressure tests (<80 psig)

This section shows the oil saturation variation during the In-Situ CO<sub>2</sub> generation EOR process executed at low pressure condition.

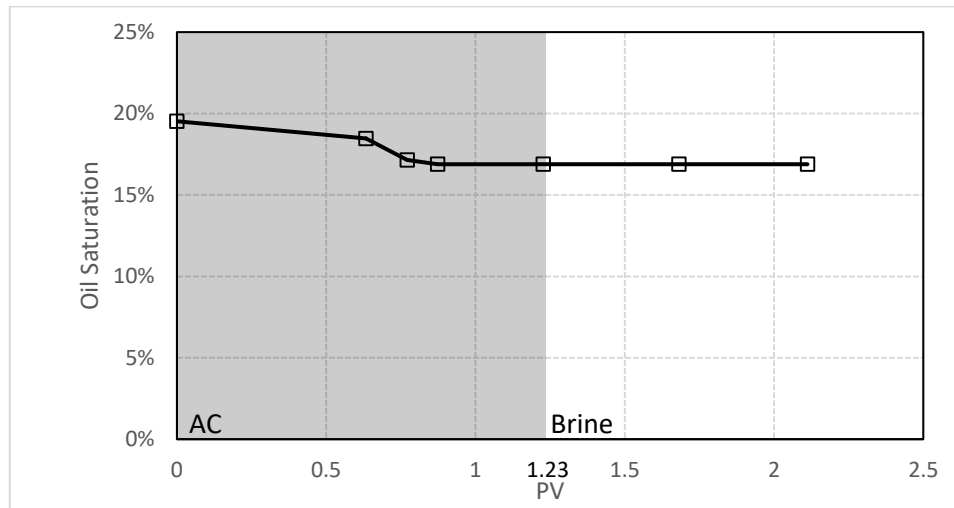


**Figure 2-3 tertiary recovery stage Oil Saturation vs. PV for tertiary recovery stages of test 1**

Test 1 was the preliminary run that showed some promising tertiary recovery with *in situ* CO<sub>2</sub> generation. It was conducted without back pressure applied. Because the column device was not pressurized, the operating temperature was limited to 96 °C, slightly below the water boiling temperature of 100 °C. The oil spiked in the sand pack of Test 1 was Earlsboro crude oil, retrieved from a site near central Oklahoma. A shorter slug of 1.23 PVs of AC slug (less than regular 2 PVs) was used followed by 0.83 PV of brine. From Figure 2-3 the residual oil saturation (Sor) after initial brine flooding was 19.50%. Following AC injection, the final oil saturation dropped to 16.87%. The estimated tertiary recovery (Etr) of the developed formulation approached 13.5%. Despite the low Sor, Test 1 indicated that this unique *in situ* CO<sub>2</sub> generation

process could potentially be applied as tertiary recovery method if the reservoir temperature met certain criteria to actively decompose the AC injected.

Based on this promising data observed at lower pressure system, further aging sand pack procedures were designed to fully capture the oil recovery potential of designed formulations. Our preliminary tests revealed that because of a combination of high porosity, high permeability, low crude viscosity and minor heterogeneity of the existing set-up, the resulted residual oil saturation after brine flooding appeared quite low: 19.5% in Test 1. This low level of residual oil saturation may not represent a common tertiary recovery situation. Thus, the procedure was modified to introduce another step of dry packing the sand medium with crude oil and aged in an 80 °C oven for equilibration to dramatically alter the wettability of the sand surface, and lead to significant increase of initial residual oil saturation after brine injection.

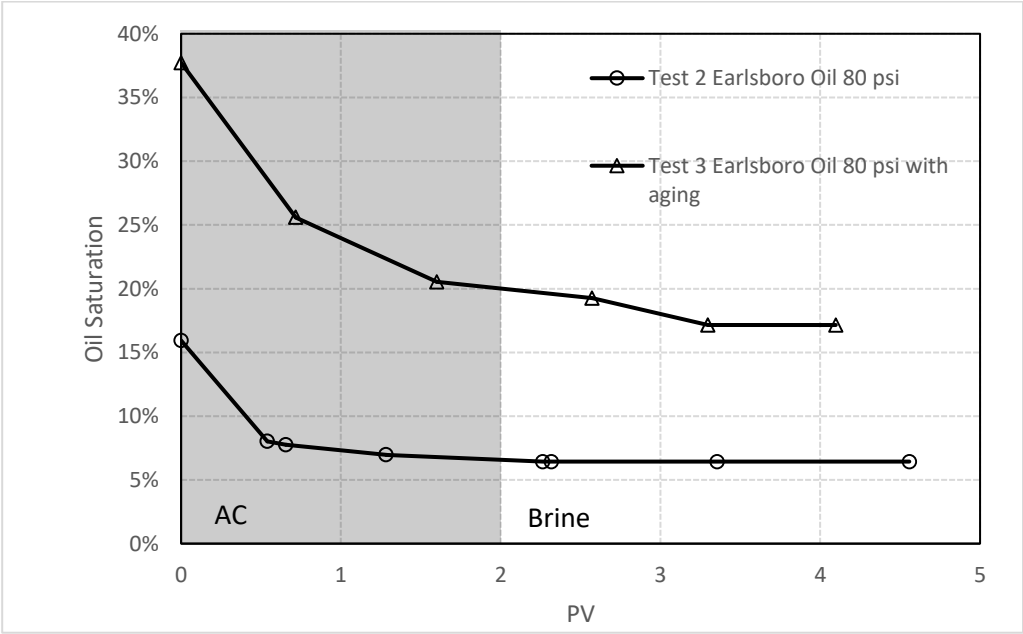


**Figure 2-4 tertiary recovery stage Oil Saturation vs. PV for tertiary recovery stages of test 2 and test 3**

Tests 2 and 3 were conducted under similar condition. By raising the reaction temperature, AC exhibits more preferred decomposition ratio and reaction rate. In these tests, the temperature was kept at 120°C, the back pressure of the system was increased to 80 psi. The same Earlsboro crude oil was used, and the only difference between tests 2 and 3 was aging step. The sand pack used in test 3 was dry packed with Earlsboro crude oil and aged at 80 °C for an extended period of 22 days.

From Figure 2-4, test 3 reached a higher Sor (37.73%) than the Sor (16.00%) of test 2 after brine injection. In test 2, the final oil saturation dropped to 6.42% after injecting 2 PVs AC, and the Etr was 59.9%. With similar AC injection, the final oil saturation of test 3 reduced to 16.62% and The Etr was 55.94%.

The aged sand pack produced a higher residual oil saturation after brine flooding than non-aged sand packs (test 1 and test 2) (see Figure 2-4). The recovery increment of test 3 was much larger than that of tests 1 and 2. Based on this, *in situ* CO<sub>2</sub> generation EOR in high residual oil saturation systems may offer better recovery performance. Note that the oil breakthrough happened within the very first PVs of AC injection.

These low-pressure tests provide initial evidence for tertiary oil recovery realized by AC injection. However, the low-pressure data may not reflect actual reservoir responses.

### 2.4.2 Intermediate Pressure Tests (1500 Psig)

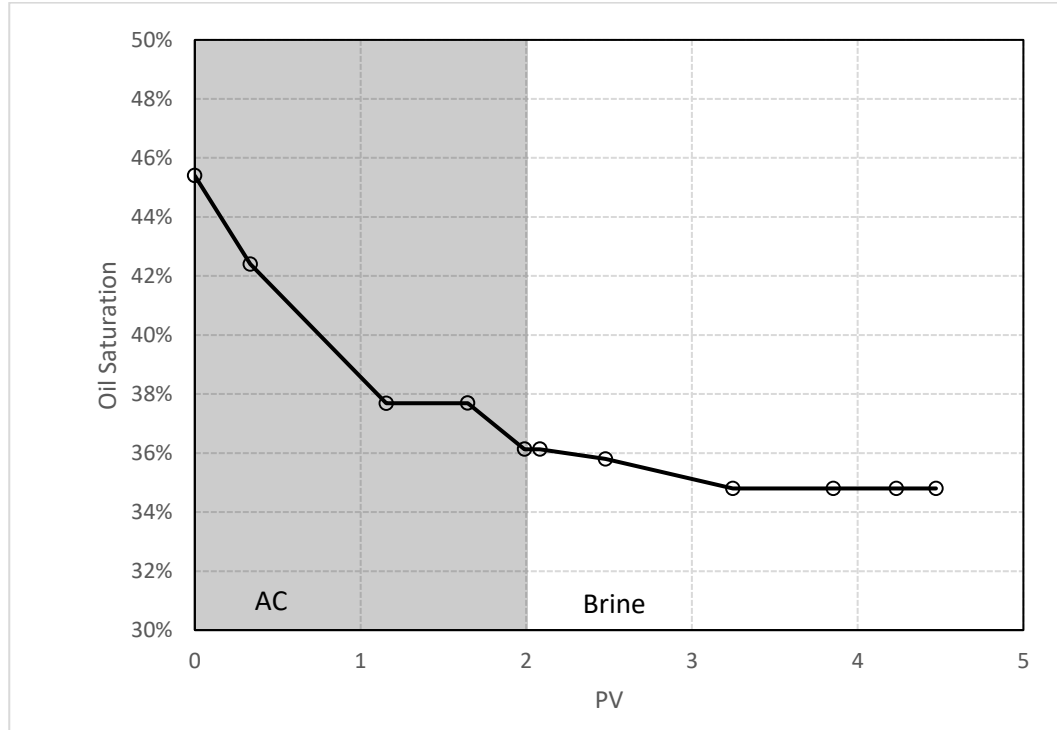


**Figure 2-5 tertiary recovery stage Oil Saturation vs Time plot of test 4**

Figure 2-5 shows the oil saturation variation during the In Situ CO<sub>2</sub> generation EOR process at intermediate pressure condition. Low pressure tests showed significant tertiary recovery in previous sections. However, low pressure injection essentially deviates from the realistic situation for oil reservoir application. Gas bubbles could be observed in the transparent line before back pressure regulator. In addition to the originally proposed recovery mechanism, forming a new free CO<sub>2</sub> phase could also provide a preferred mobility ratio during the displacement. Wassmuth, Green and Randall [48] showed that the gas and water co-injection had worse sweep efficiency than foam injection by using MRI. The CO<sub>2</sub> was generated homogeneously inside the porous media. The distribution of the generated gas was different from the injected gas.

Gas water co-injection was largely affected by the gravity segregation and large mobility contrast. And liquid lamellar was stabilized by surfactant in foam injection. The state of generated gas was between the gas and water co-injection and foam injection. Therefore, the forming of the gas phase could promote the sweep efficiency. Test 4 was designed to simulate more realistic high pressure reservoir conditions, to verify this newly developed formulation for enhancing oil recovery. In test 4, the sand pack was dry packed with Earlsboro crude oil and aged at 80 °C for 46 days. The back pressure of device was set to 1500 psig, and the temperature maintained at 120 °C.

From Figure 2-5, the Sor after brine flooding was 45.40%. Because test 4 had longer aging time than test 3, the Sor of test 4 was slightly higher. The final oil saturation decreased to 34.82%. Etr was 23.30%. At intermediate pressure condition (1500 psig), the amount of oil recovered was lower than that of low pressure tests as described previously. Under this elevated pressure, the free CO<sub>2</sub> gas phase was likely eliminated based on the observation in the transparent line right after the back pressure regulator. It was reasonable to achieve the only portion of tertiary recovery than low pressure cases.

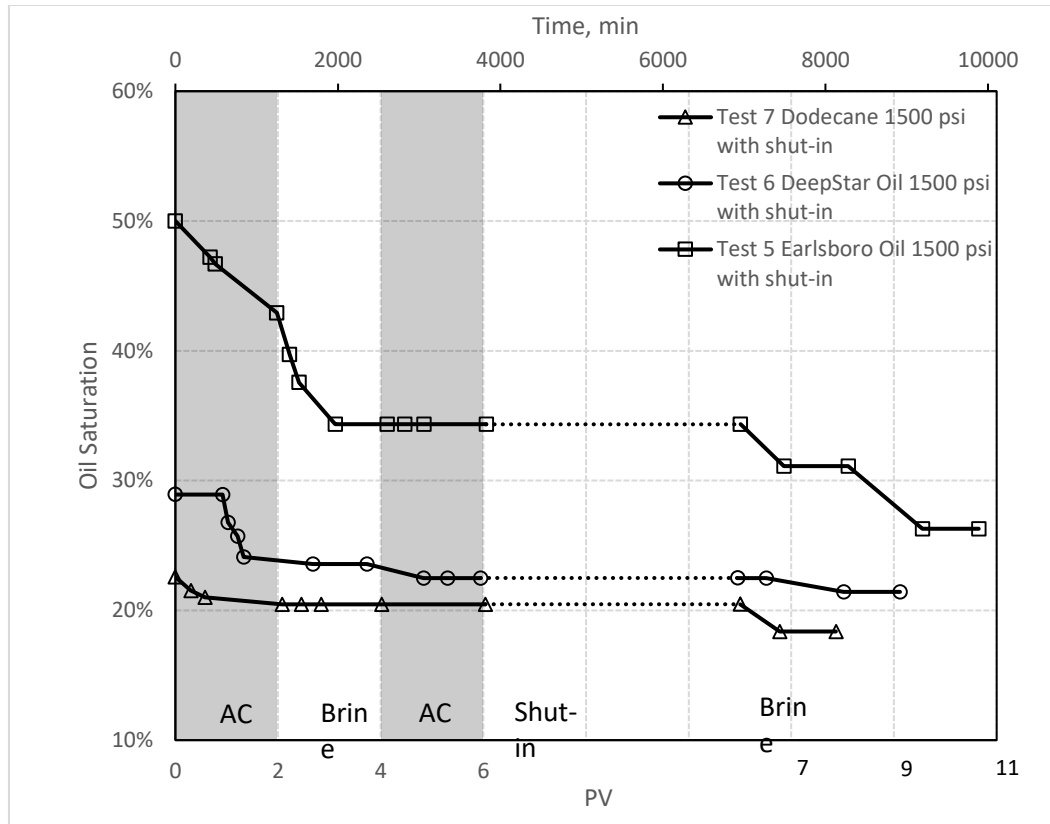


**Figure 2-6 tertiary recovery stage Oil Saturation vs. PV plot of test 5, test 6 and test 7 dash line stands for no flow stage**

Tests 5 to 7 were designed to explore how the change of oil property affect the recovery. Among these, an example light crude, heavier crude, and a single alkane were tested. Their properties were listed in Table 2-1 above. All the tested sand packs were dry packed with the selected oil and aged at 80 °C for an extended period of 50 days. Similarly, this set of experiments were run at 1500 psig and 120 °C. In the previous flow through tests, the chemical residence time was relatively short as compared to injection in actual reservoir conditions. In the previous sand pack flooding tests, the estimated AC residence time was 10 hours. We believe that the decomposition rate of AC and the mass transfer of CO<sub>2</sub> between oil and aqueous phase were both a function of time. Thus,



the extent of oil swelling and reduction of oil viscosity would approach the maximum levels after equilibrated. Whether the current system reached equilibrium within the short period of 20 hours (2 PVs injection) used required further investigation. At the meantime, a shut-in reaction cycle was introduced in some of the studies. For a shut-in effort, 3 additional stages were added. After the post-AC brine flooding, another 2 PVs of AC was delivered. Then the system was temporarily shut in at targeted pressure and temperature for 48 hours to prolong the residence time. After the shut in period, the post brine injection was resumed to chase any additional mobile oil out. Therefore, all the conditions were the same except the different oil properties used between Tests 5 - 7. Results and the comparisons between tests 5 - 7 were plotted in Figure 2-6. A secondary x-axis was added to identify the shut-in time.

In test 5, Earlsboro crude oil was tested. The Sor was 50.00%. After all the injection and CO<sub>2</sub> generation were completed, the final oil saturation dropped to 26.41%. Etr was 47.19%.

In test 6, an oil with higher API, Deep Star oil, was tested. The resulted Sor was 28.93%, and the final oil saturation dropped to 20.66%. Etr was 28.6%.

In test 7 with dodecane used, much lower Sor was detected at 22.57%. The final oil saturation was equal to 18.37%, and an Etr of 18.6% was realized. Not surprisingly, the Sor in these tests were impacted by the differences of oil property.

The shut-in process did promote additional oil collected from all three cases. It strongly indicated that the 20 hours residence time was likely inadequate for the system to reach equilibrium. Among these, Test 5 achieved the highest Etr among these 3 tests. Between Tests 5 and 6, Earlsboro crude was a lighter oil and offered a better candidate for CO<sub>2</sub>

flooding, as compared to the heavier DeepStar crude [49]. The CO<sub>2</sub> solubility in Earlsboro oil was also higher than that of DeepStar crude. Therefore, the higher CO<sub>2</sub> partition coefficient of Earlsboro oil system was more favorable than the Deep Star oil system. The resulted swelling factor of Earlsboro oil(1.46) after the dissolution of CO<sub>2</sub> should be greater than that of Deep Star oil(1.16)[50]. During the displacing process, mass transfer resistance and reaction rate were the limiting factors of the Earlsboro oil system. Apart from aforementioned factors, the Deep Star oil system is also controlled by other factors, one example was lower CO<sub>2</sub> solubility in the low API gravity oil. In general, heavier oil was quickly approaching its CO<sub>2</sub> solubility limit than lighter oil during the first AC injection period. Though additional CO<sub>2</sub> was generated during the shut-in step, it would no longer transfer to oil phase once fully saturated. Therefore, increasing the residence time appeared more effective in the Earlsboro system.

In terms of comparing test 5 and test 7, dodecane had higher API gravity leading to even larger CO<sub>2</sub> solubility, which would result in higher swelling factor. However, compared to crude oil, dodecane was a pure nonpolar alkane, which lacks complex compositions, such as polar aromatics or asphaltenes, to effectively adjust the wettability of porous media. As indicated by the low Sor observed in test 7, Ottawa sand aged with dodecane did not lead to significant wettability reversal effect. Besides, there was lack of any interfacial active substance formed between dodecane and ammonia. These two factors limited the performance enhancement.

Comparing test 5 and test 4, they were tested under similar condition. The tertiary recovery before shut-in of test 5 was quite similar to test 4 indicating good repeatability of the experiments.

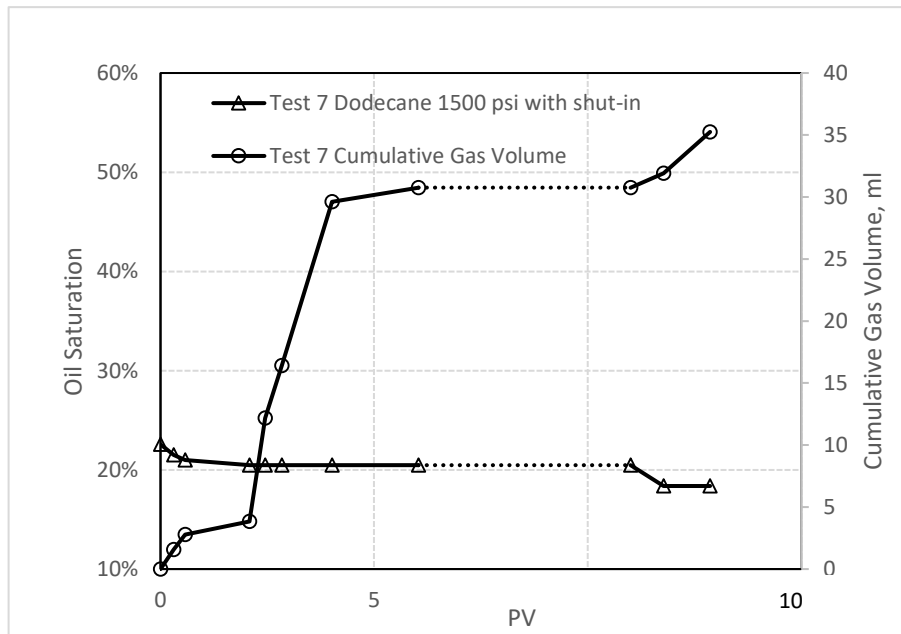
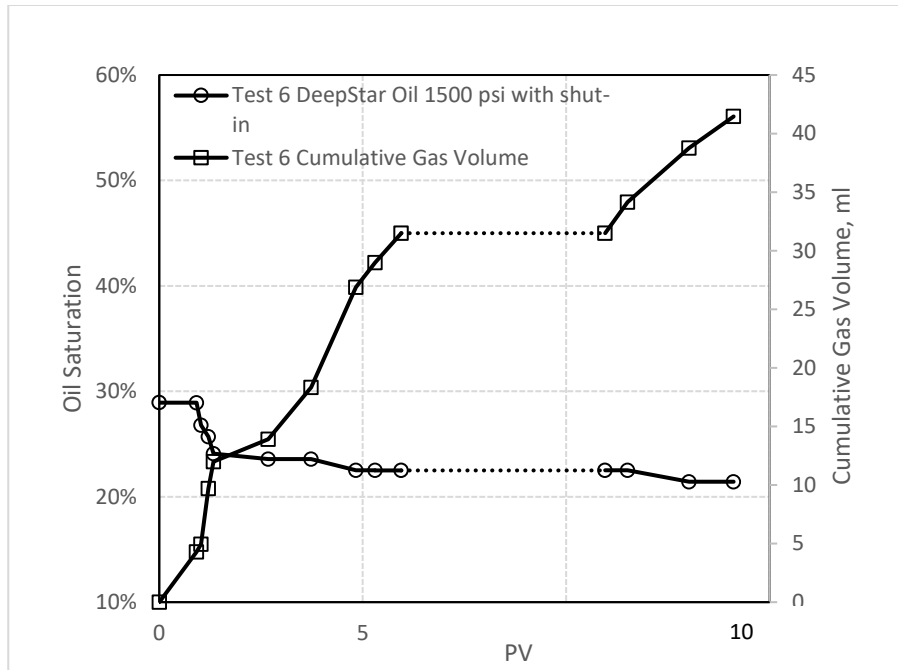


**Figure 2-7 Test 6 and Test 7 Cumulative Gas Volume and Oil saturation VS PV**  
 Figure 2-7 showed the produced gas data from tests 6 and 7. The oil breakthrough coincided with the CO<sub>2</sub> gas breakthrough point. Since decomposition of ammonium carbamate (eq. 2.2) is a reversible reaction, the collected CO<sub>2</sub> volume could not totally reflect the dissolved CO<sub>2</sub> volume present inside the highly pressurized porous media.

For example, a significant amount of ammonium carbamate could be converted to CO<sub>2</sub> and NH<sub>3</sub> at high temperature and high pressure depending on the reaction kinetics. When the effluent was cooled down, some of the produced CO<sub>2</sub> and NH<sub>3</sub> could re-associate back to some form of AC byproduct[51, 52]. The nature of this newly developed system may offer an opportunity of re-injecting/recycling the effluents for lowering the project cost.

Based on these results, it revealed that 1. longer residence time for gas generation agent can increase the tertiary recovery. 2. Better oil candidate for CO<sub>2</sub> flooding is also a favorable candidate using in situ CO<sub>2</sub> generation formulation. 3. A high acid number crude will inherit additional benefits due to wettability reversal and the alkaline produced[53-56].

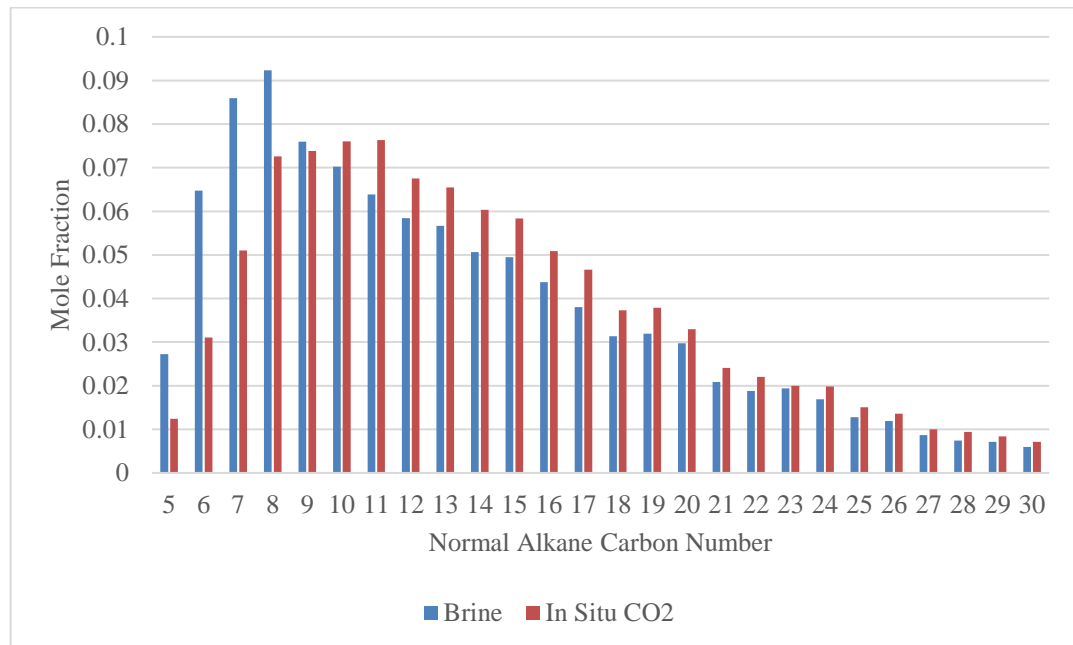


**Figure 2-8 Produced oil composition change of test 6(DeepStar oil at 1500 psi)**

Figure 2-8 was the oil compositional analysis of test 6. Only the normal alkane was plotted in the figure. The recovered oil from secondary recovery (waterflooding) and tertiary recovery (in situ CO<sub>2</sub> generation) was collected separately. Therefore, the changing of the oil composition caused by in situ CO<sub>2</sub> generation EOR could be detected by gas chromatography analysis. In water flooding produced oil sample, the mole fraction of lighter components below C<sub>9</sub> was higher than them in in situ CO<sub>2</sub> generation produced sample. Comparing to water flooding sample, in situ CO<sub>2</sub> generation produced oil sample contained more components heavier than C<sub>9</sub>.

This measurement indicated that this test did not have a multiple contact miscibility process since it could make the produced oil lighter. There was no separate gas phase in the flooding system, which was consistent with our visual observation. Asphaltene liberation caused by ammonium[33] was the reason of more heavy components in the tertiary recovered oil sample.

### 2.4.3 High Pressure Tests (4000 psig)

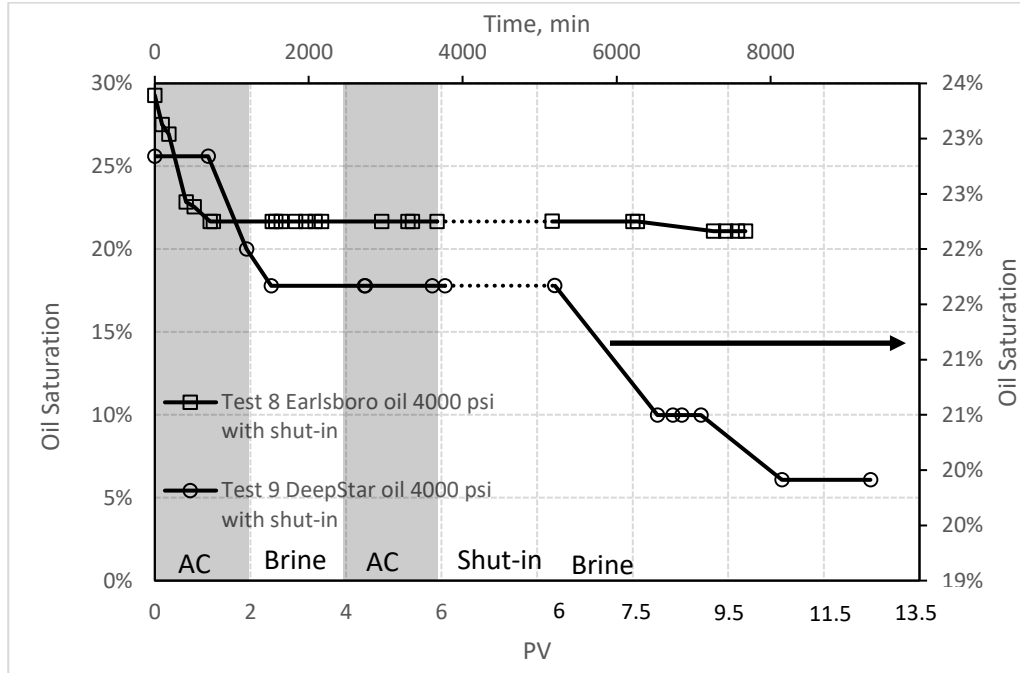


**Figure 2-9 tertiary recovery stage Oil Saturation vs PV plot of test 8 and test 9 dash line stands for no flow stage**

This set of experiments were designed to study the effect of flowthrough experiments exposed to higher pressure condition. For Eaerlsboro oil, 4000 psig was much higher than the MMP for CO<sub>2</sub>/oil mixture. For Deep Star oil, high pressure could provide greater CO<sub>2</sub> oil solubility than low pressure case. Based on the extensive studies on CO<sub>2</sub> flooding, the CO<sub>2</sub> miscible flooding could provide high tertiary recovery because of high microscopic displacement efficiency [3]. The modified high pressure rating device was used to conduct tests above the estimated Eaerlsboro oil/CO<sub>2</sub> mixture MMP. The MMP values of Eaerlsboro and DeepStar crude were estimated based on the correlations proposed by Emera and Lu [57]. The estimated MMP of Eaerlsboro oil was 3,190 psi, and MMP of DeepStar oil was equal to 10,200 psi. The modified high pressure rating

sand pack can safely operate up to 4900 psi and 275 °F. Our initial assumption was that above the MMP condition, *in situ* CO<sub>2</sub> generation EOR might offer the better performance of tertiary recovery, in analogy to conventional CO<sub>2</sub> flooding.

To operate the system above MMP of Earlsboro oil, the back pressure of the device was pre-set to 4,000 psi. The temperature of these tests was kept at 120 °C. The only difference between tests 8 and 9 was different crudes tested. In initial high pressure tests, the sand packs were not aged. Therefore, Sor of test 8 and test 9 was slightly low. The Ottawa sand used in high pressure test was F-75. Similarly, a 24 hours Shut-in chemical reaction cycle was added as most of the other tests.

Results of the oil saturation variation for different crudes under high pressure condition are depicted in Figure 2-9. For Earlsboro crude (test 8), the Sor was 29.28%, after *in situ* CO<sub>2</sub> generation processes, the final oil saturation was 21.08% and Etr was 28%. For DeepStar crude (test 9), the Sor was 22.84%, the resulted final oil saturation reached 19.69% and total Etr was equal to 13.8%.

To our surprise, while tertiary recovery of test 8 was significant, it was not much higher than that in pressure below the MMP tests. This phenomenon revealed the difference between CO<sub>2</sub> flooding and *In situ* CO<sub>2</sub> generation EOR. Firstly, unlike CO<sub>2</sub> flooding, there was no separate CO<sub>2</sub> phase involved in the *in situ* CO<sub>2</sub> generation formulation. The system pressure controlled the CO<sub>2</sub> chemical potential in CO<sub>2</sub> flooding. When the operational pressure is higher than the MMP of the CO<sub>2</sub>/reservoir crude mixture, the primary benefit of miscible flooding would be realized. In this work, *In situ* CO<sub>2</sub> generation formulation beyond the estimated MMP, the benefit of miscible flooding was not observed. The increase of pressure above the MMP would only impact the

values of CO<sub>2</sub> partition coefficient between the aqueous phase and the oil phase. Further investigation on the phase behavior of In situ CO<sub>2</sub> generation EOR system under high pressure needs to be explored.

Interestingly, for DeepStar crude (see tests 9 and 6), the tertiary recovery contribution due to adding the shut-in step was more obvious in higher pressure (test 9). This was likely indicative of increasing the CO<sub>2</sub> solubility in DeepStar crude. It is believed that increase of residence time became more effective under high pressure condition than adjusting the value in low pressure condition. Interphase mass transfer resistance thus became the controlled limitation for displacement, less depending on the CO<sub>2</sub> partition coefficient.

It can be concluded that 1. Increasing pressure above MMP did not enhance the performance of In situ CO<sub>2</sub> generation significantly. 2. High pressure could provide more favorable CO<sub>2</sub> partition coefficient, especially for heavy crude.



### 2.4.4 Core Flooding

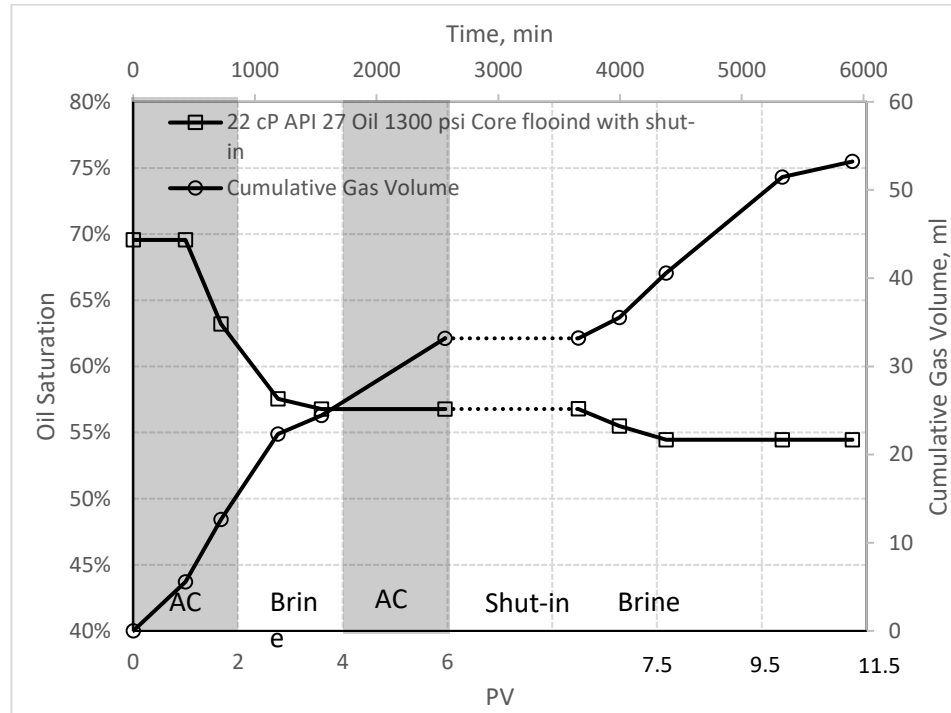


**Figure 2-10 Oil Saturation vs. Time plot of core flooding for Test 11 DeepStar Oil 1300 psi Core flooding with shut-in**

Test 11 was designed to verify that *In situ* CO<sub>2</sub> generation EOR was able to provide tertiary recovery in complex porous media at low permeability using a consolidated rock.

The core sample used in test 11 had a permeability of 127.70 mD and porosity 17.13%. It was drilled out from a Berea sandstone block. The sample length was 6 inches and diameter was 1 inch. First, the core plug was saturated by synthetic brine composed of 5 wt% NaCl to measure its pore volume. Then the brine-saturated core was loaded into core holder before applying 2000 psi confining pressure for the test. A total of 4 PVs of DeepStar oil was injected to dewater and saturate the core. The back pressure was set to 1000 psi. Then the whole core device maintained at 2000 psi confining pressure, and

1000 psi pore pressure was aged at 80°C for 25 days. After the aging step, the injection sequence was similar to the sand pack column tests. The back pressure of the system was adjusted to 1300 psi. The temperature of this run was 133 °C. A shut-in time of 24 hours was applied.

From Figure 2-10, the Sor of core test was 70.73%. After completion of in situ CO<sub>2</sub> generation injection, the final oil saturation reduced to 54.25%. The resulted Etr was 23.3%. Similarly, significant tertiary recovery for the new CO<sub>2</sub> generation formulation was realized in the core test. The trend of gas collected was quite similar to the previous gas production data observed in sand pack study. The oil breakthrough time of the tertiary recovery was slightly faster than the CO<sub>2</sub> breakthrough time in the effluent. The level of tertiary recovery was approximating the value observed from the Deep Star oil of Test 6 under intermediate pressure condition.

### 2.4.5 Dilute Concentration of Gas Generating Agent

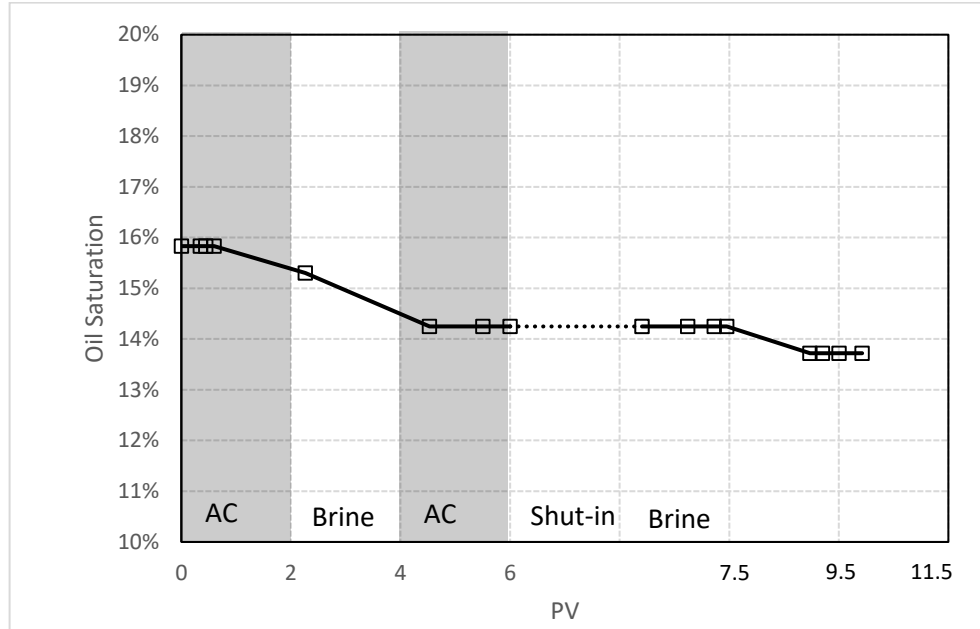


**Figure 2-11 Oil Saturation vs Time plot of Low Gas Generating Agent Concentration Test 10 Earlsboro Oil 5% gas generating agent slug 1500 psi with shut-in**

Test 10 was designed to further explore dilute AC formulation for improving the economic viability of this process. The conditions of this test involved low AC concentration, 5 wt%, back pressure of 1500 psi, temperature, 20 °C, oil used, Earlsboro crude, and no aging treatment applied.

As shown in Figure 2-11, the  $S_{or}$  was 15.9%. After all the in-situ  $CO_2$  generation injection processes, the final oil saturation dropped to 13.83%. A much lower  $E_{tr}$  of 13% was observed using dilute AC solution.

In brief, the tertiary recovery was lower than 35% AC tests. The oil breakthrough was distinctly slower than 35% AC tests.

## 2.5 Summary

Table 2-3 summarized the key findings from all the tests conducted in this work. It was quite encouraging that most tests showed significant enhancement of tertiary oil recovery. Under low pressure condition, in addition to the dominant mechanism of the In Situ CO<sub>2</sub> generation and an increase of oil swelling, the separated CO<sub>2</sub> gaseous phase provided favorable mobility ratio inside the porous medium during displacement. Although initial residual oil saturation was low, a rather high tertiary recovery was achieved.

Addition of the sand pack aging process almost sharply doubled the residual oil saturation after water flooding using Ottawa F-95 sand system. In test 8 and test 9, the Ottawa F-75 sand was used. The F-75 sample possessed similar d50 as F-95, but with a wider range of particle size distribution. Comparing F-95 and F-75 sand pack properties, the residual oil saturation of F-75 increased less dramatically after the aging process.

**Table 2-3 All Tests result summary**

	Test 1	Test 2	Test 3	Test 4	Test 5	Test 6	Test 7	Test 8	Test 9	Test 10	Test 11
Test type	os sand pack with Earlsboro	os sand pack with Earlsboro	os sand pack with Earlsboro	os sand pack with Earlsboro	os sand pack with Earlsboro	os sand pack with deep star	os sand pack with dodecane	os sand pack with Earlsboro	os sand pack with Deep Star	os sand pack with Earlsboro	100mD core with deep star
Aging time, Days	\	\	22	46	50	50	51	\	\	\	25
Porosity, %	34.5%	34.9%	35.2%	34.7%	33.9%	34.0%	34.3%	34.7%	34.4%	34.1%	17.1%
permeability, mD	4050.2	4119.3	4174.2	4071.7	3929.0	3939.2	4006.4	4079.5	4028.1	3966.5	127.7
Gas generating agent	AC	AC	AC	AC	AC	AC	AC	AC	AC	AC	AC
Gas generating agent Concentration, %	35%	35%	35%	35%	35%	35%	35%	35%	35%	5%	35%
Flow rate, ml/min	0.03	0.03	0.03	0.03	0.03	0.03	0.03	0.055	0.055	0.03	0.03
Residual oil saturation after water flooding	19.5%	16.0%	37.7%	45.4%	50.0%	28.9%	22.6%	29.3%	22.8%	15.9%	70.7%
Recovery by gas generating solution flooding	13.5%	59.9%	55.9%	23.3%	31.2%	25.0%	9.3%	26.0%	5.5%	10.0%	20.0%
Recovery by shut in reaction	\	\	\	\	16.0%	3.6%	9.3%	2.0%	8.3%	3.0%	3.3%
Temp, °C	96	120	120	120	120	120	120	120	120	120	133
Back Pressure, psi	0	80	80	1500	1500	1500	1500	4000	4000	1500	1300

The tests under intermediate pressure and high pressure largely eliminated the presence of free CO<sub>2</sub> gas phase but still exhibited satisfactory tertiary recovery, especially under high residual oil saturation conditions. Core flooding and low gas generating agent tests showed reasonable enhancements of tertiary recovery

The oil breakthrough of all the sand pack and core flooding tests occurred rapidly within the first PVs of AC slug injection in most tests. The oil breakthrough largely coincided with the CO<sub>2</sub> breakthrough in the collected effluent samples.

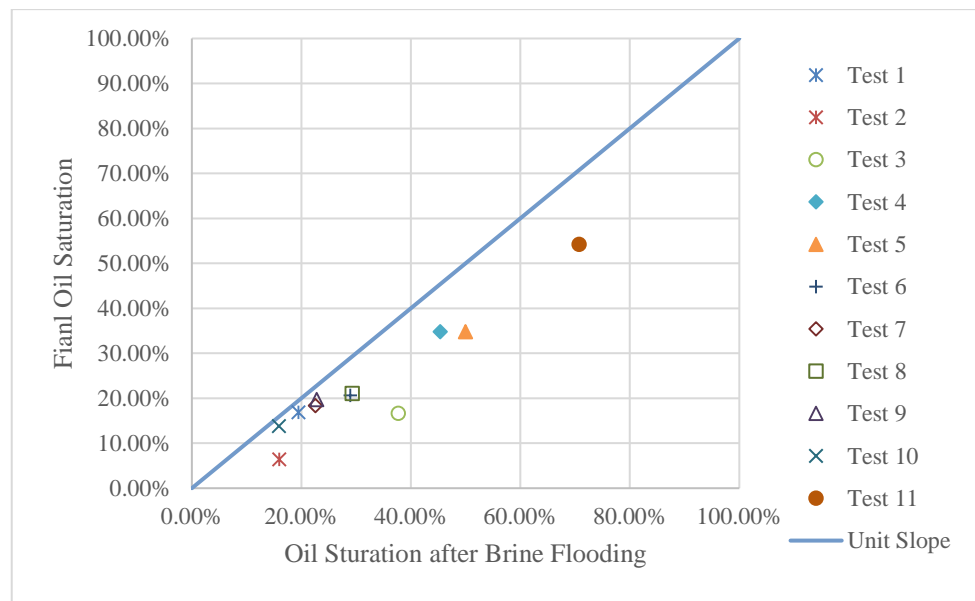


**Figure 2-12 Oil Saturation reduction plot**

To better represent the data from these multiple tests, the main EOR conclusions of the flooding tests were re-plotted into one unified curve. The individual symbol in Figure 2-12 represents the saturation data from different tests. The vertical distance between the symbols to the unit slope line represents the corresponding oil saturation reduction during the tertiary recovery. Any saturation data located on the unit slope line means lack of tertiary recovery. It is easy to recognize the resulted data in concert all deviated

from the unit slope line. In addition, the effects of tertiary recovery from *in situ* CO<sub>2</sub> generation EOR show much better improvement when initial secondary recovery levels are low (i.e., high *S*<sub>or</sub>).

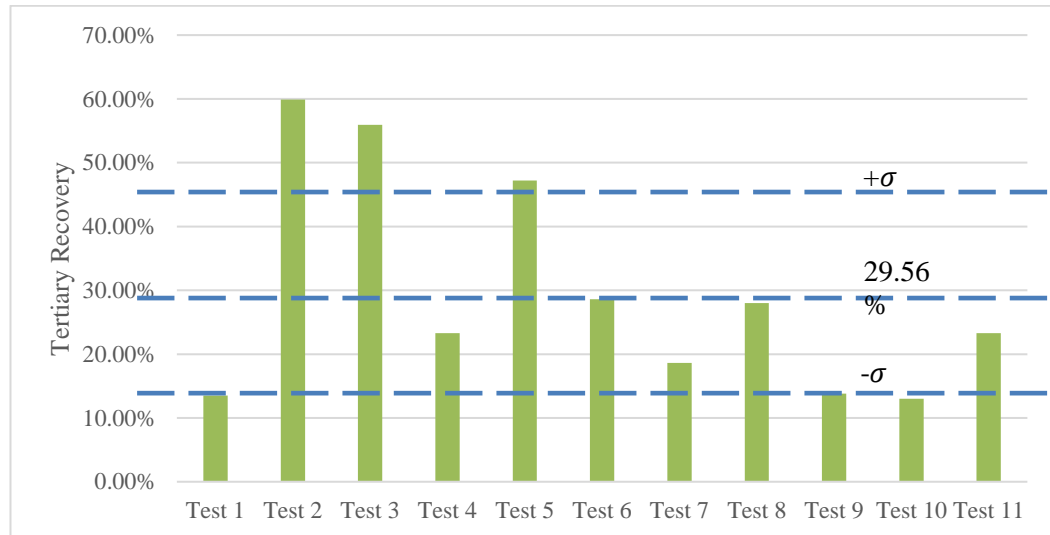


**Figure 2-13 tertiary recovery**

Tertiary recovery of all the tests was summarized in Figure 2-13. Average tertiary recovery of all the tests in this work was 29.56%. The standard deviation of these 11 tests is  $\pm 16.26\%$ .

## 2.6 Conclusion

After the investigations of novel AC formulations for In Situ CO<sub>2</sub> generation EOR, some superior advantages are revealed comparing to the earlier researches. After multiple sand pack flooding and core flooding experiments, it is proved that Ammonium Carbamate as a gas generating agent can offer significant potentials for tertiary recovery over the pressure ranges studied. The levels of tertiary recovery from this simple system are comparable with those complex system (e.g., injection of combined surfactant, polymer and alkali mixture) proposed previously by others. This

new formulation also offers better economic viability for field implementation. A 5% dilute concentration of AC slug exhibits measurable tertiary recovery. The mechanisms of In Situ CO<sub>2</sub> generation EOR involve multiple interactions such as oil swelling, viscosity reduction, wettability reversal and an increase in alkalinity. The tertiary recovery is a synergistic effect. The proposed system was an immiscible flooding process. Running In Situ CO<sub>2</sub> generation EOR experiment above MMP does not show additional miscible flooding benefits.

# **Chapter 3: In-Situ CO<sub>2</sub> Generation for EOR by Using Urea as A Gas Generation Agent**

## **3.1 Introduction**

CO<sub>2</sub> flooding is a well proven EOR technology for many mature fields and can be operated economically under reasonable oil price environment in the US [3, 58]. In recent years, applying CO<sub>2</sub> EOR in unconventional formations [59-62] and offshore reservoirs [63] attracts increasing interests. Proper CO<sub>2</sub> flooding could have high microscopic displacement efficiency but sometimes suffers poor macroscopic displacement efficiency. This drawback is mainly due to the large density and viscosity contrast between the injected CO<sub>2</sub> and crude oil; the reservoir will exhibit gravity segregation problems as a result of unfavorable mobility ratio during the CO<sub>2</sub> injection. Water Alternating Gas (WAG) was introduced to alleviate these phenomena during CO<sub>2</sub> flooding [7, 8, 64].

In some cases, WAG is still hard to become economically feasible especially inside a thick formation [5]. Many efforts were required for optimization of WAG ratio and slug sizes to get a good sweep efficiency[7]. The optimized WAG parameters were changing cycle by cycle because of the rock-fluid system interaction[9]. To address excessive conformance control issues and maximize the recovery, Carbonated Water Injection (CWI), i.e., injecting water with dissolved CO<sub>2</sub>, was proposed as an alternative approach. To date, quite a few field scale [13-15] and laboratory scale [10-12, 26, 27, 65-67] tests were reported. Unlike installing a new CO<sub>2</sub> flooding unit, the existing water flooding system is ready to implement CWI with only minor modifications. For



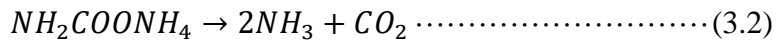
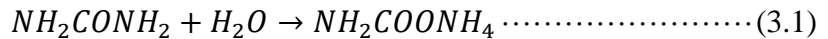
example, installation of a pressurized mixing tank allowing rapid CO<sub>2</sub> dissolution in water at the surface can easily incorporate the CWI into the water flooding practice.

However, delivery of enough CO<sub>2</sub> volume is often constrained by the CO<sub>2</sub> water solubility in CWI [16, 17]. Previously, Shu [16] developed a patented process to add chemical promoters (10 to 30 weight % of a base) in CWI to overcome the limitation of the gas water ratios of CWI. In some cases, adding the required chemical promoter significantly increases the project costs and also the complexity of the system operations. Therefore, in-situ CO<sub>2</sub> generation for EOR was considered in the past few years as an alternative to address some of the issues as described above. In situ CO<sub>2</sub> EOR was a single aqueous phase injection. The sweep efficiency was better than water flooding when the oil viscosity was reduced. Move over, it had many flexibilities on mobility control method like water flooding. Example formulations involved aluminum salt-carbamide-surfactant, ammonium carbamate-surfactant, sodium carbonate-acid-surfactant and ammonium bicarbonate-surfactant-polymer were developed [18-25]. Li et al. Li, Ma, Liu, Zhang, Jia and Liu [25] reported a pilot test of in-situ CO<sub>2</sub> generation for the offshore reservoir. Among these efforts, quite a few rather complex formulations were used to achieve reasonable oil recovery, involving a combination of elevated concentrations of surfactant, polymer, plus additives like alkali or acids.

The Economic viability of any EOR project is affected by the complexity of the systems installed. Therefore, the aim of this work is especially targeting on eliminating the shortcomings of prior in situ CO<sub>2</sub> generation system. The potential benefits of this improved formulation may include:

- i. Not relying on the natural CO<sub>2</sub> sources and installation of CO<sub>2</sub> transportation pipeline.
- ii. Better sweep efficiency than CO<sub>2</sub> WAG process.
- iii. Several folds increase of GWR comparing to GWR limitation of CWI.
- iv. Simple and cheap.
- v. Desirable tertiary recovery performance at both above and below minimum miscibility pressure conditions.
- vi. Exceptional hardness tolerance of reservoir brine.

Based on our recent work[31], the modified in situ CO<sub>2</sub> generation system uses the urea (NH<sub>2</sub>CONH<sub>2</sub>) as another potential gas generating agent. For decades, urea has been commercially available and manufactured in massive quantities worldwide. It exhibits very high water solubility (1,080g/L at 20 °C [68]) and can be safely transported as a solid form or in concentrate solution with minimum hazard to human and environment. At relatively high-temperature condition (in the deep reservoir), urea will be hydrolyzed in aqueous solution thus release ammonia and carbon dioxide. The basic chemistry of urea hydrolysis contains two steps:



Eq. 3.1 is a mild exothermic reaction and eq. 3.2 is a strongly endothermic reaction. The hydrolysis of urea is commonly discussed in wastewater treatment processes and some selective catalytic reductions of NO<sub>x</sub> inside automotive device [69-72]. The kinetics of

urea hydrolysis were studied extensively [73-78]. Several studies on catalyzed urea hydrolysis were reported previously in literatures [79-81] and patents [82].

It is anticipated that release of  $\text{CO}_2$  and  $\text{NH}_3$  from urea hydrolysis would result in positive effects on oil recovery. The tertiary recovery based on this in situ  $\text{CO}_2$  generation EOR process is mainly a synergistic effect involving wettability alteration, oil swelling and viscosity reduction as documented previously[31].

Recently, ammonia was applied as an alkali for alkali/surfactant/polymer (ASP) flooding [35]. They reported a successful ultralow interfacial tension ASP system been developed with ammonia. Significant cost (saving) and logistical advantages of applying ammonia were pointed out for offshore application.

Flury, Afacan, Tamiz Bakhtiari, Sjoblom and Xu [33] reported that addition of ammonia had similar but faster performance on bitumen liberation than the use of sodium hydroxide at same pH level. Ammonia could replace sodium hydroxide on bitumen extraction. Upon bitumen extraction, sandstone wettability reversal would be realized due to ammonia used. Evidence of more water wet surface during the  $\text{CO}_2$ -WAG process in chalk rocks was observed by Fjelde and Asen [34].

Aqueous urea solution generated a significant volume of  $\text{CO}_2$  at elevated temperature. Once formed, there would be a net  $\text{CO}_2$  mass transfer between the aqueous phase and oil phase in the reservoir. The partition coefficient can describe the partitioning of  $\text{CO}_2$  between the oil and aqueous phase.

Altunina and Kuvshinov [22] reported that the partition coefficient values for CO<sub>2</sub> in water-oil system in the temperature range of 35-100°C and the pressure range of 10-40MPa are between 4 and 10, whereas this coefficient for ammonia rarely exceed  $6 \times 10^{-4}$ .

After the CO<sub>2</sub> equilibrated between aqueous and oil phase, the oil-solubilized CO<sub>2</sub> leads to oil swelling. The SF (swelling factor) is defined as the ratio of CO<sub>2</sub> saturated oil volume at reservoir pressure and temperature divided by the oil-only volume measured at the same temperature and atmospheric pressure [41]

$$SF = \frac{V_{CO_2-Oil}(P_R, T_R)}{V_{Oil}(P_{atm}, T_R)} \dots\dots\dots (3.3)$$

Where

$V_{CO_2-oil}$ , the volume of CO<sub>2</sub>-oil mixture

$V_{oil}$ , the volume of oil

Increasing oil saturation caused by oil swelling allows the discontinuous oil droplets previously trapped in the pores to gradually merge with the flowing oil phase[42].

Assume that the residual oil saturation is the same whether the oil is carbonated or not.

Then the same amount of oil volume will contain less pure oil if it is carbonated, due to oil swelling [43].

The dissolved CO<sub>2</sub> will also tend to cause a decrease of oil viscosity. The level of reduction mainly depends on the dissolved CO<sub>2</sub> concentration in oil. Holm [44] stated that CO<sub>2</sub> could reduce oil viscosity under certain reservoir conditions by 5 to 10 folds because of the high CO<sub>2</sub> solubility. If the crude has a higher initial viscosity, a significant reduction of oil viscosity will occur after it is saturated by subcritical CO<sub>2</sub>

[45]. The CO<sub>2</sub>-led viscosity reduction is larger at lower temperatures than at high temperatures because of higher CO<sub>2</sub> solubility in crude at lower temperature [42]. To show the potential of this newly proposed formulation, data from prior studies on tertiary recovery using CWI and in situ CO<sub>2</sub> generation approaches were briefly summarized in Table 3-1.

**Table 3-1 literature reported CWI and in situ CO<sub>2</sub> generation tests**

Author	Mayer, Earlougher Sr, Spivak and Costa [83] Initial	Mayer, Earlougher Sr, Spivak and Costa [83] Second	Mosavat and Torabi [27]	Steffens [36]	Kechut, Jamiolahmady and Sohrabi [12]	Fathollahi and Rostami [84]	Wang, Hou and Tang [24]
Oil density, API	13.5	12.3	45.4	Hexadecane	36.15	Decane	MW C11+ 240
Oil Viscosity, cP	475	406	2.76	Hexadecane	158	Decane	10.92@80 °C
Pore Pressure	850	100	594 to 1494	362.6	2500	2000 or 3500	870
Temp, F	125	125	77 to 104	ambient	100	84	176
So after water flooding	49.9%	57.8%	26.4% to 27.4%	27	32.45%	32.3% or 33.4%	33.89% to 38.77%
Incremental	17.0%	19.4%	6.7% to 12.5%	\	9%	0.79% or 2%	5.4% to 10%
Etr	34.1%	33.6%	16.5% to 33.5%	24.0%	28.4%	2.4% or 13.6%	11.12% to 18.84%
Carbonated water injected	CO <sub>2</sub> , CWI till no oil produced	84CO <sub>2</sub> /16N <sub>2</sub> mol%, CWI till no oil produced	6 PV	23 PV	5.36 PV	1 PV	10%-20% gas generating agent with 0.3wt% surfactant and 0.05% polymer, 0.8PV to 2PV
Permeability, mD	172	184	4037 to 7184	1200	4580	57	375.1 to 213.0
Porosity,%	23	26.9	26.92% to 28.15%	26	35	18	35.3 to 38.9

### 3.2 Materials

#### 3.2.1 Chemicals

High purity urea (99 wt.%) and Calcium chloride dihydrate were purchased from ACROS ORGANICS. Sodium chloride (99.5 wt.%), Potassium chloride (99%),

Magnesium chloride(98%) and Magnesium sulfate(99%) were purchased from Sigma-Aldrich.

Three different oils were tested: Pure dodecane and two site crudes, Earlsboro crude and Deep Star crude, and their properties are shown in Table 3-2.

**Table 3-2 Physical properties of the oils used in the experiments (at 25°C and atmospheric pressure)**

	Dodecane	Earlsboro	Deep Star
API	57.3	40	27
Viscosity, cP	1.34	4.6	22

### 3.2.2 Porous Media & Apparatus

A selected Ottawa sand (F-75) from U.S. silica was used as the porous media in the sand pack studies. The size distribution of F-75 Ottawa sand was between 0.053mm and 0.6 mm with d50 at 0.15mm. The sand pack tests were conducted at two different pressure levels: 1500 psi and 4000 psi. For these flowthrough tests, similar set-up of the sand pack device and procedures were installed and largely adopted from our previous study[31].

## 3.3 Experiment Procedure

Urea solutions (5-35 wt.%) were pre-dissolved at two sets of conditions: 5 wt. % NaCl or artificial seawater. The recipe with high divalent concentration was adjusted to mimic the harsh condition of seawater (see Table 3-3).

**Table 3-3 Composition of Artificial Seawater**

Chemical	Concentration, wt. %
NaCl	2.629
KCl	0.074
CaCl <sub>2</sub>	0.099
MgCl <sub>2</sub>	0.609
MgSO <sub>4</sub>	0.394
Total	3.805

A known amount of targeted oil (dodecane or crude) was first injected into Ottawa sand packed stainless-steel column to saturate the medium. Water flooding was initiated immediately after the oil saturation process. During the sand pack aging process, the oil-loaded sand pack was kept in an 80°C oven beyond one month period to gradually reverse the wettability of the sand, leading to much higher residual oil saturation after treatment[47].

The process of sand pack flooding was standardized for consistency and allowed to compare with other gas produced agent from our prior study. First, the residual oil saturation was established by the adequate amount of brine flooding (till no more oil produced). Then a total of 2 pore volumes (PVs) of urea solution were injected into the sand pack followed by 2 to 3 PVs of post brine injection to drive out the mobilized oil. In this work, one pore volume was equal to 18.95 mL for low pressure (between 1,500 - 3,100 psi) system, and 34.15 mL for high pressure (up to 4,900 psi) system, respectively. The net (tertiary) oil recovered after the water flooding through in situ CO<sub>2</sub> generation and the volume of CO<sub>2</sub> collected in the effluent were recorded for performance analyses. In several tests, a shut-in cycle was added where 2 PVs urea solution was injected, and then the flow was interrupted for approximately 24 hours to allow a more complete chemical decomposition and interphase mass transfer to occur with longer residence time. After shut in, post brine flooding was resumed. These shut-in cycles were executed in some tests to account for possible mass transfer limitation resulted from insufficient chemical residence time.



Among the critical process parameters, different brine compositions, varying gas generating agent concentration, oil properties, injecting pressures and flow rate were evaluated.

Besides the sand pack flooding test, the PVT study was performed to understand the phase behavior after the CO<sub>2</sub> is formed under reservoir condition. In the urea solution PVT study, the experiment was designed to mimic the reservoir condition with constant pressure and temperature. A 5 wt.% NaCl-only and 5 wt.% NaCl plus 10 wt.% urea solutions were prepared with DI respectively. The experiment setup was depicted in Figure 2-2. It consisted of one piston cell, one Teledyne Isco 260D syringe pump, and an oven. One side of the piston cell was filled with testing solution. The other side was filled with mineral oil and connected with syringe pump to control the pressure during the experiment. A 50-mL of the targeted solution was pre-loaded to one side of the piston cell carefully. Then the residual air was displaced out without losing solution by injecting a mineral oil to the other side of the piston cell. Before heating, the system was sealed and pressurized to 1500 psi at room temperature for 24 hours. Once no volume change of the system was observed, the piston cell was heated to a targeted temperature of 250°F for a pre-determined period. At the end of the test, the system was slowly cooled down to ambient temperature. The syringe pump was held at a constant pressure of 1500 psi during the whole experiment process. The system volume change caused by temperature changes at constant pressure was recorded for interpretation.

### 3.4 Results and Discussion

In this work, urea-based CO<sub>2</sub> generation EOR was studied as alternative tertiary recovery approach. The tertiary recovery factor (E<sub>tr</sub>) was collected and analyzed as an efficiency indicator of this new in-situ system. Oil saturation over time, S<sub>o</sub>, was plotted for analysis.

In this work, eight sand pack flooding tests were designed to provide the proof of concept for using urea as gas generating agent for enhancing oil recovery. The resulted changes of sand pack oil saturation (S<sub>o</sub>) during the tertiary recovery stage were plotted against PVs injection. Tertiary recovery gauged immediately after the oil cut reaching 0 in the effluent (S<sub>or</sub> established). The column test conditions were summarized in Table 3-4.

**Table 3-4 Column test conditions**

Test number	1	2	3	4	5	6	7	8
Oil phase	Earlsboro Oil	Earlsboro Oil	Earlsboro Oil	Dodecane	Deep Star Oil	Earlsboro Oil	Earlsboro Oil	Earlsboro Oil
Porosity, %	34.49%	34.46%	33.83%	34.37%	34.32%	34.96%	35.85%	35.77%
Permeability, mD	4039	4033	3909	4015	4006	4132	4315	4298
Aging time, days	46	46	46	60	60	60	60	60
Brine	5%NaCl	5%NaCl	5%NaCl	5%NaCl	5%NaCl	5%NaCl	Seawater	5%NaCl
Gas generating agent Concentration, %	35.00%	35.00%	35.00%	10.00%	10.00%	10.00%	10.00%	5.00%
Temp, °C	120	120	120	120	120	120	120	120
Back Pressure, psi	1500	1500	4000	1500	1500	1500	1500	1500
Flow rate, ml/min	0.03	0.08	0.055	0.03	0.03	0.03	0.03	0.03
S <sub>or</sub>	28.04%	30.70%	29.57%	17.42%	33.24%	32.72%	25.32%	22.70%

### 3.4.1 Effect of Injection Flow Rate

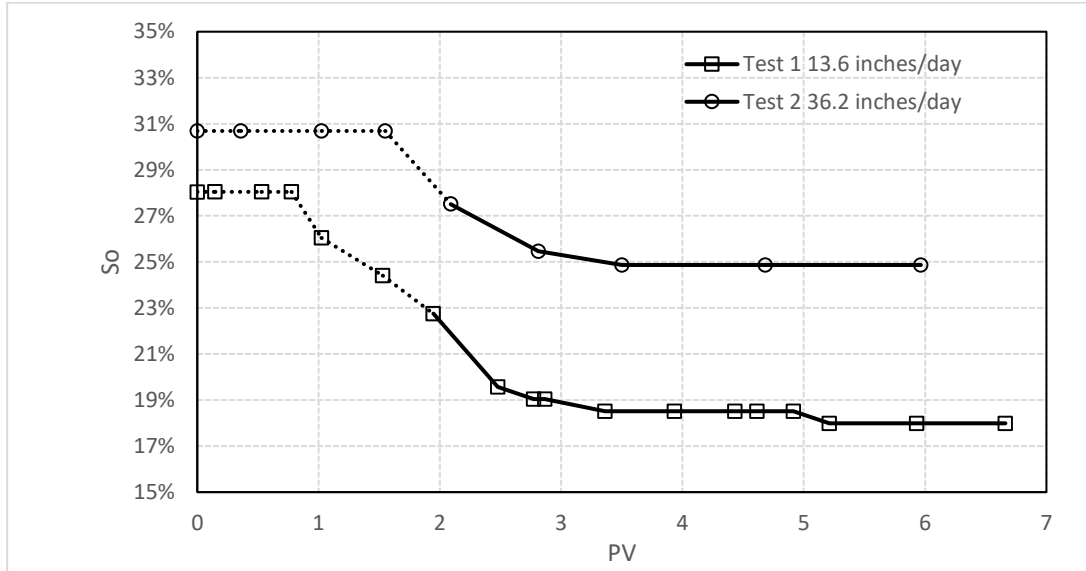


**Figure 3-1 Oil Saturation vs. PV for tertiary recovery stages, operating at different flow rate, NaCl 5% Brine, 1500 psi and 120 °C with Earlsboro oil**

Figure 3-1 shows the flow rate effect on the tertiary recovery at 1500 psi back pressure and 120 °C with same oil and brine. The dashed line showed the chemical (urea) slug injection and the solid line showed the (post) brine flooding. The chemical slug contained 35% Urea and 5% NaCl solution. The concentrated urea solution was applied to provide preliminary evidence for tertiary recovery potential using this approach. A 5% NaCl solution was used as reservoir brine in pre- and post brine flooding. Two different flow rates (0.03, 0.08 mL/min, equal to the interstitial velocity of 13.6, and 36.2 inches/day, respectively) were tested. Two PVs of the gas generating urea solution was injected and followed by continuous post brine flooding until no more oil eluted. From Figure 3-1, two sand packs had minor different  $S_{or}$  initially after pre-brine flooding. However, at the end of the in-situ CO<sub>2</sub> generation EOR process, low flow rate

test showed superior oil recovery performance. Urea injection at a lower flow rate (0.03 mL/min) achieved 35.85% of tertiary recovery compared to 18.97% when injecting at a high flow rate (0.08 mL/min). For lower injection rate, the better EOR observed was attributed to the longer chemical residence time (631 min for lower flow rate and 237 min for higher flow rate) in the porous medium. It is believed that either urea hydrolysis rate or the mass transfer of CO<sub>2</sub> generated from aqueous phase to oil phase rendered large amount oil recovery. Based on the kinetic data of urea hydrolysis available [76], the predicted half-life of urea in gas generating solution at 120°C (1437 min) was much longer than the chemical residence times tested in this study. It revealed that longer residence time could offer better oil recovery based on in situ CO<sub>2</sub> generation system. By increasing chemical conversion factor of same urea injected concentration, more of CO<sub>2</sub> and NH<sub>3</sub> were generated enabling to release the trapped oil.

#### *3.4.2 Effect of Injection Pressure*

Numerous studies showed that a CO<sub>2</sub> miscible flooding gave better recovery than immiscible flooding [3, 6, 85]. To investigate the minimum miscible pressure (MMP) effect on the tertiary recovery of in situ CO<sub>2</sub> generation EOR, operating pressure below and beyond MMP was compared for same crudes used, Earlsboro oil.

The MMP of Earlsboro oil was first estimated close to 3,190 psi based on the correlation proposed by Emera and Lu [57].

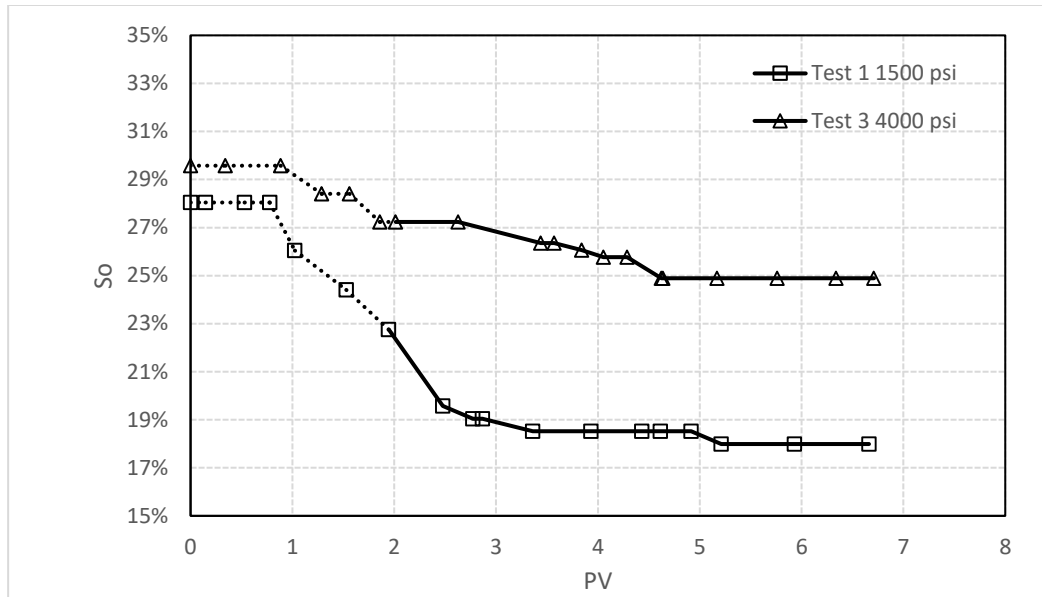


**Figure 3-2 Oil Saturation vs. PV for tertiary recovery stages, operating at different pressure, NaCl 5% Brine, velocity of 13.6 inches/day and 120°C with Earlsboro oil**

The operational conditions of Test 3 were similar to Test 1. There were two main differences between Tests 3 and 1. For supra-MMP condition, 4,000-psi back pressure was applied in Test 3 vs. sub-MMP of Test 1 (1,500 psi). Secondly, the PVs of Test 3 (34.15 mL) was larger than that of Test 1 (18.95 mL) due to the larger diameter of high-pressure rating sand pack device. For better comparison, the injection flow rates were adjusted to have similar interstitial (seepage) velocity accounting for different sizes of diameter. From Figure 3-2, the resulted  $S_{or}$  of both tests after pre-brine flooding were quite similar. To our surprise, at the end of the runs, better EOR performance was observed in the low-pressure (sub-MMP, 1,500 psi) system. Test 1 had higher Etr as 35.85% in comparison of 15.80% Etr of test 3. This revealed that there was no separate  $CO_2$  phase occurrence during the urea flooding (otherwise Etr of test 3 would be much higher than test 1). The benefits of  $CO_2$  miscible flooding beyond the MMP did not

exist in this immiscible process via CO<sub>2</sub> generated in situ. In this work, most CO<sub>2</sub> generated was completely dissolved in the aqueous brine. The amount of CO<sub>2</sub> produced fully distributed between the trapped oil and aqueous phase in the porous medium. Reduction of tertiary recovery in the high-pressure system could be attributed to multiple reasons, such as the decrease of the CO<sub>2</sub> partition coefficient (i.e., increasing partitioning in brine at higher P), the impact of extraction pressure on the swelling factor. The relationships between these phenomena and extraction pressure need additional investigation and are beyond the scope of this work.

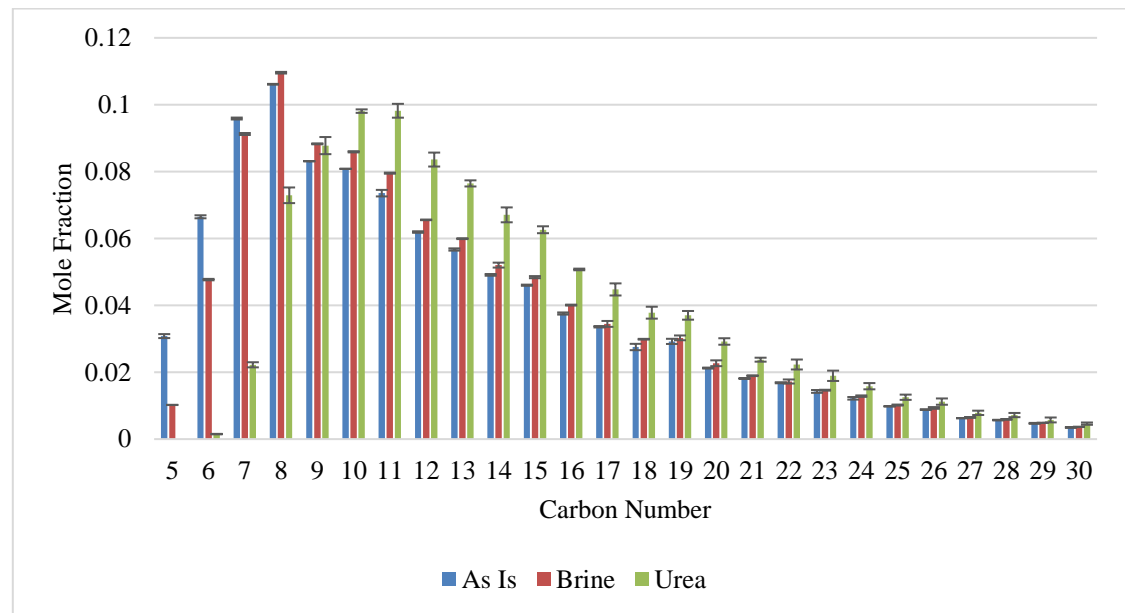
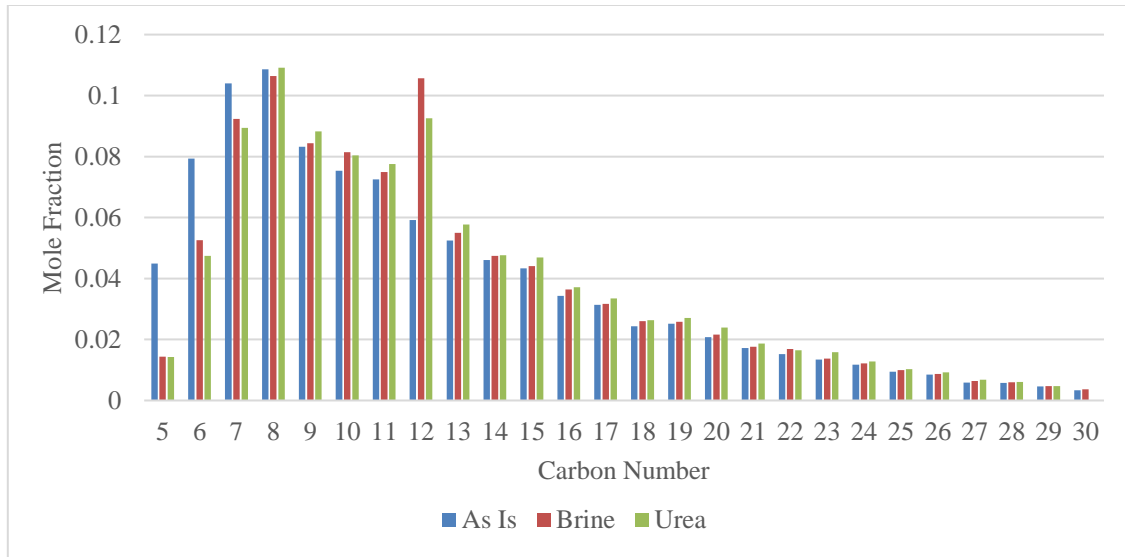


**Figure 3-3 Normal alkane composition changing in test 1(top) and test 3(bottom). The analyses for high pressure test (4,000 psi, Test 3) were carried out in triplicates for the individual sample to generate standard deviations in the curves.**

The crude oil samples from Tests 3 and 1 were both collected at sand pack effluent for further compositional analysis. For this effort, the original oil sample, the eluted oils collected from the effluents of pre-brine flooding and after in situ CO<sub>2</sub> generation

process were analyzed using a Gas Chromatography method as whole oil sample. Only normal alkane concentration distributions in the crude oil were studied in this work. Data from the compositional analyses of Tests 1 and 3 were shown in Figure 3-3. All the observed concentration changes were beyond the QA/QC error of the GC equipment. First, between original crude (As Is sample) and brine flooding samples, the concentrations of lighter components (<C8) in original crude were distinctly greater than those in brine flooding samples, a similar trend found in Tests 1 and 3. The decrease of n-alkane compositions in most brine flooded samples was likely caused by evaporation of light component during the aging processes. In Test 1 and test 3, both sand packs were first dry packed with Earlsboro oil and aged at 80 °C for an extended period. The aging treatment was beneficial to build up a desirable high  $S_{or}$  after brine flooding, whereas some lighter alkanes inevitably evaporated from the spiked crude oil in the sand pack during the aging period. The original sample composition difference between test 1 and test 3 is caused by the evaporation of the lighter components during the crude oil storage at 1.6°C.

Comparing oil samples obtained in brine flooding and after urea injection, a notable reduction in light and medium components in tertiary recovered oil samples was observed in both sub-MMP (Test 1) and supra-MMP system (Test 3). To our surprise, the concentrations of C8 plus components were increasing while lighter components (< C8) concentrations decreased. In other words, oil with more heavier components was eluted by in situ CO<sub>2</sub> generation. In a regular multi-contact miscible (MCM) CO<sub>2</sub> flooding system, the light and probably medium components could be produced more



and heavier components instead would be left behind in the porous media because of dynamic composition changing over the course of the MCM process between the CO<sub>2</sub> front and the contacted crude oil. Not surprisingly, lighter components tend to be easily extracted by the CO<sub>2</sub> flood front thus dominated the recovered oil composition. Interestingly, applying in-situ CO<sub>2</sub> generation EOR, the opposite phenomena were observed; that is, the concentration of heavy components in the eluted oil increased. Comparing 1500 psi (test 1) and 4000 psi (test 3), the level of heavier components concentration was more obvious in the high-pressure system.

The explanation for the observed behaviors was that there appeared no separate gas phase CO<sub>2</sub> presence in urea injection. The generated CO<sub>2</sub> first formed in the aqueous phase by urea decomposition. Then because of apparent high CO<sub>2</sub> solubility in crude oil, the dissolved CO<sub>2</sub> in brine would migrate to the oil phase. Once the CO<sub>2</sub> levels depleted in the aqueous phase, the decomposition reactions could shift further to the product CO<sub>2</sub> and NH<sub>3</sub> side and lead to more complete hydrolysis of urea. MCM process in a common CO<sub>2</sub> miscible flooding was not occurring. Therefore, the extraction (concentration) of light and medium components in the oil recovered was not detected.

The concentration of heavier components in the produced oil could be attributed to the increasing concentration of NH<sub>3</sub> effect in the in-situ CO<sub>2</sub> generation system. Asphaltenes adsorption on the sand surface would effectively reverse the wettability during the aging process. Adsorption of heavier n-alkanes would be greater than light and medium components on the sand surface. During brine flooding stage, the injected brine could not liberate the asphaltenes sorbed on the sand surface. However, during urea injection stage, the produced NH<sub>3</sub> have the ability to release the adsorbed

asphaltene from the sand surfaces significantly and shift the surface becoming more water-wet. Thus, more heavier n-alkanes was able to produce along with some liberated asphaltenes by in situ generation of CO<sub>2</sub> treatment.

3.4.3 Effect of Oil with Different Properties

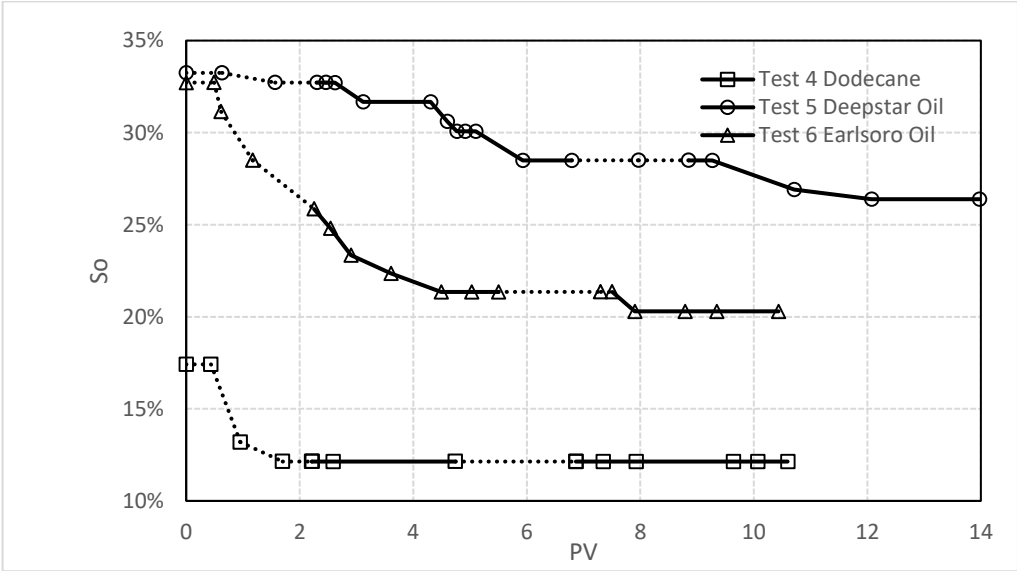


**Figure 3-4 Oil Saturation vs. PV for tertiary recovery stages, operating with different oils at 1500 psi, NaCl 5% Brine, 13.6 inches/day and 120°C**

Figure 3-4 shows the oil saturation variations during the In-Situ CO<sub>2</sub> generation EOR process tested with the selected three different oils. All three sand packs were first aged before initiating the flooding step. This series of tests were conducted using lower urea concentration of 10% in 5% NaCl solution as the gas generating slug to assess CO<sub>2</sub> generation EOR capacity. Similarly, pre- and post-brines were kept at the same level of 5% NaCl solution, and the rest of the operating conditions were kept as identical as previous tests. Note that in this series of tests, an extra chemical shut-in step was added. After a complete cycle of in situ CO<sub>2</sub> generation EOR process (pre-brine, chemical slug,

post-brine), a second two PVs chemical slug was immediately injected and followed by a 24-hour shut-in step to provide longer CO<sub>2</sub> mass transfer time and to offer better chemical utilization ratios with longer chemical hydrolysis period.

As shown in Figure 3-4, both Deepstar oil and Earlsboro oil exhibited similar S<sub>or</sub> after brine flooding. Moreover, after longer aging process treatment (60 d, Table 3-4), the S<sub>or</sub> of the Earlsboro Oil sand pack (Test 6) had a higher S<sub>or</sub> (32.7%) than that of Earlsboro sand packs with shorter aging time (28% S<sub>or</sub> of Test 1). The dodecane-spiked sand pack showed much lower S<sub>or</sub> (17.4%) with the same amount of aging time. It was mainly because that Dodecane was a pure n-alkane. There were no other polar components can effectively reverse the sand wettability during the aging treatment. In the meantime, the viscosity of dodecane was close to the displacing phase. Therefore, during the brine flooding, the dodecane-spiked sand pack had a much more preferred mobility ratio than crude oil cases.

Before the extra shut-in reaction step, during the first 2 PVs chemical slug injection, a 10% urea solution could significantly improve oil recovery in all three oils tested. The result of Earlsboro oil sand pack showed the highest oil saturation reduction of 12.42%. The amounts of oil saturation reduction in Deepstar and Dodecane runs were 6.86% and 5.29%, respectively. However, the initial S<sub>or</sub> of Dodecane test was much lower. The net E<sub>tr</sub> might be a better performance indicator than the levels of oil saturation reduction. The measured E<sub>tr</sub> of Earlsboro oil, Deepstar oil, and Dodecane were 34.29%, 14.29%, and 30.3%. Since the initial S<sub>or</sub> of Dodecane case might be on the lower end to perform an ideal scenario of tertiary recovery, the collected data did indicate that urea-based CO<sub>2</sub> generation could achieve better performance with low-density oil. Thus, dodecane

run could be considered as the best contender among these three oil tested. Its superior outcome could be attributed to increasing partition coefficient in dodecane case because of higher CO<sub>2</sub> solubility in low-density oil. Also, low-density oil was less viscous among the oils tested; the mass transfer resistance was quite smaller in lower density oil tests.

During the sequent (2<sup>nd</sup>) 2 PVs gas generating agent injection and shut-in period, the amount of oil produced was significantly less than the first injection cycle, except Deepstar oil run. In the Dodecane test, there was negligible oil produced after the second run of chemical injection. In Deepstar and Earlsboro oil cases, a notable 30.76% and much less 8.58% of the total tertiary recovery were recovered, respectively, after the second injection cycle. There were two possible reasons. As previously described, the resulted  $S_{or}$  after pre-brine flooding was much lower in dodecane test. Not surprisingly, the amount of CO<sub>2</sub> generated at the first gas generating agent injection stage was adequate to produce most Dodecane that could be recovered through the mechanisms controlled by in situ CO<sub>2</sub> generation EOR. The required CO<sub>2</sub> volume was much smaller in Dodecane than Crude oil, as large portion of oil been removed by the brine flooding. Secondly, both crude oils studied were more viscous than pure n-alkane. The mass transfer resistance was much higher in crude oil runs. Therefore, the extra residence time during shut-in step provided a beneficial longer period for the system to compensate the mass transfer limitations of CO<sub>2</sub> in the crude oil system. The viscosity of Deepstar oil (22 cp) was larger than Earlsboro oil (4.6 cp). In the Deepstar oil test, cumulative oil recovered over the shut-in period hold a greater portion of total recovery

than Earlsboro oil under similar conditions. This observation also aligned with the effects of viscosity difference explanation mentioned above.

3.4.4 Presence of Divalent Ions

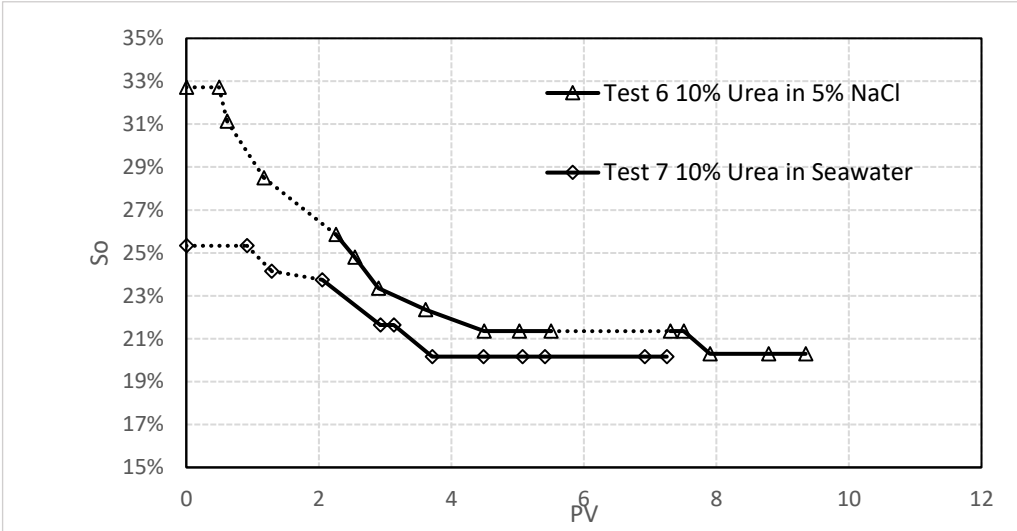


**Figure 3-5 Oil Saturation vs. PV for tertiary recovery stages, operating with seawater/NaCl,1500 psi, 13.6 inches/day and 120°C with Earlsboro oil**

Elevated concentrations of common divalent ions like calcium and magnesium in reservoir brine tend to form carbonate precipitates with  $CO_3^{2-}$  in  $CO_2$  based miscible or immiscible flooding processes [86]. Excessive formation of precipitates in porous media could lead to severe formation damage whereas precipitation occurred in wellbore could cause scaling and blockage in the perforated zone. If too much  $CO_2$  was consumed in carbonate precipitates, the rest of  $CO_2$  available may not be enough to sustain a desirable tertiary recovery. Therefore, it is important to assess the new proposed formulation under different divalent ions concentrations. Various gas generating agent concentrations ranging from 1% to 40% of urea in synthetic seawater were prepared and monitored at room temperature for 20 days before proceeding any

flooding test. Among 20 days equilibration, no apparent precipitates were detected in any of the prepared samples.

From Figure 3-5, similar oil recovery behaviors in seawater run as compared to NaCl brine test were observed. The first sign of oil breakthrough happened during the gas generating agent injection stage. The only difference was in seawater run oil breakthrough was slightly retard. The  $S_{or}$  after brine flooding (25.3%) was slightly lower than previous Earlsboro oil tests (28% to 32.7 %). The tertiary recovery in this test 7 was 20.41%. Because of low  $S_{or}$ , the oil volume left for tertiary recovery in test 7 was smaller than test 6. Despite the shut-in reaction stage included in test 6, the final oil saturation was about the same in these two trials. It indicated that the amount of  $CO_2$  consumed by divalent ions in test 7 did not dramatically affect the oil production.

From the collected effluent, no large carbonate crystals were observed. A small amount of clayey like precipitates were dispersed in the eluted brine. The formation of colloidal carbonate precipitates on the sand surface and in the bulk brine did not build up the capacity to block the highly permeable sand pack since the sand pack permeability was close to 4 D in this work. Potential formation damage in lower permeability cores still needs further investigation in the future.

### 3.4.5 Effect of Gas Generating Agent Concentration

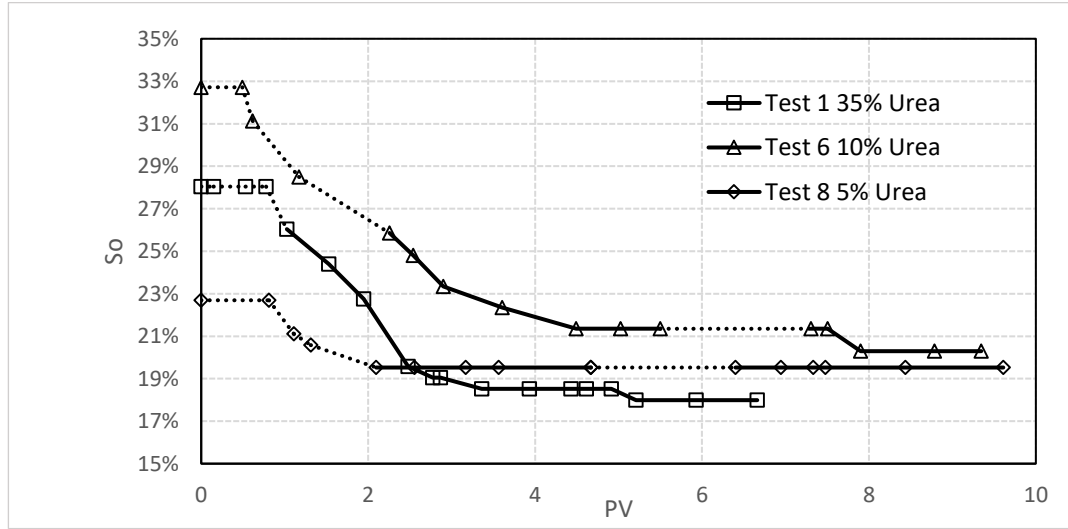


**Figure 3-6 Oil Saturation vs. PV for tertiary recovery stages, operating with different Urea concentration, NaCl 5% Brine, 1500 psi, 13.6 inches/day and 120°C with Earlsboro oil**

One low gas generating agent concentration (5% urea) test was done to assess the better economic feasibility and optimization potential of this new proposed in situ CO<sub>2</sub> EOR system. From Figure 3-6, the extra step of the second gas generating agent injection and the 24-hour shut-in reaction of test 8 were not beneficial for improving tertiary recovery. After the first chemical injection stage, 5% urea with 5% NaCl could produce the majority of the tertiary oil recovery. Among these, 35% urea test had the highest tertiary recovery and 5% test had the lowest tertiary recovery. However, the tertiary recovery did not increase proportionally with the increase of urea concentrations. The chemical concentration and injected pore volume are well enough than the system required. Based on these limited data, additional optimizations should be further explored.

### 3.4.6 Urea Solution PVT Test

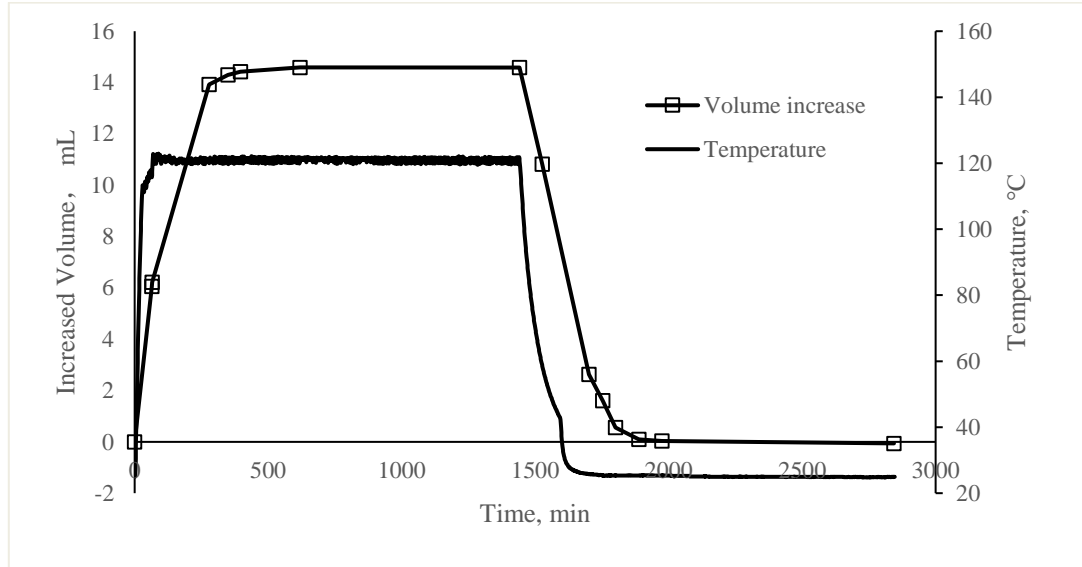


**Figure 3-7 The 5 wt. % NaCl solution base case**

Figure 3-7 was the base case (5 wt.% NaCl-only) test. The readings of the system pre-equilibrium stage before the heating were not included in this plot for clarity. At constant pressure (1500 psi) condition, when temperature is approaching 250°F (120 °C), the fluid volume significantly increased. The volume increase could be quantified by recording the pump volume change. The thermal expansion of the fluid in the piston cell was 14.58 mL. Once the system reached equilibrium at 250 °F, it was cooled down to room temperature again. After the system reached a new equilibrium at 1500 psi and room temperature, the recorded volume change was -0.06 mL.



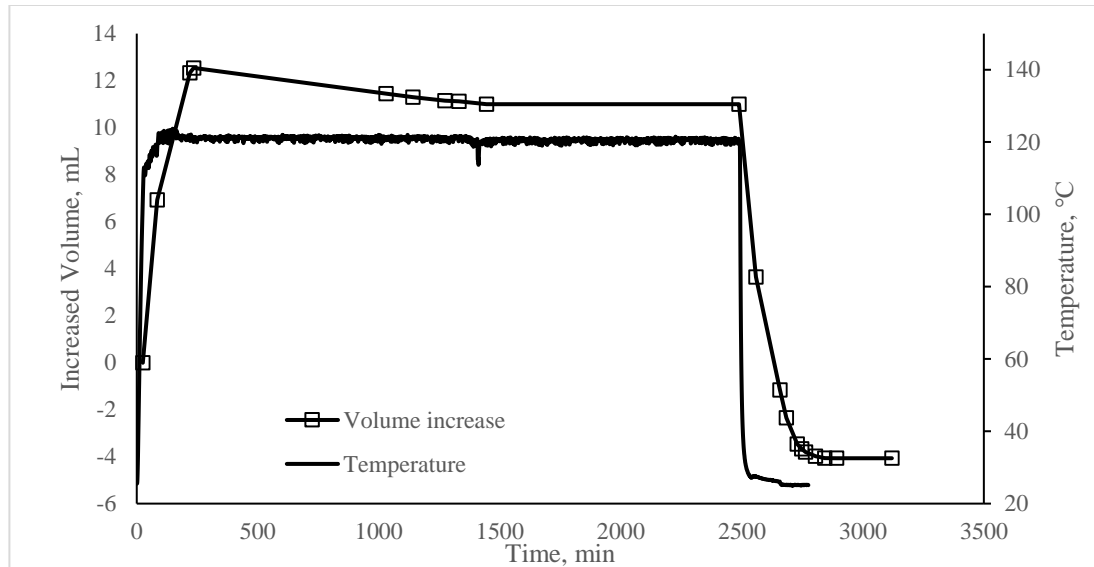


**Figure 3-8 The 5 wt.% NaCl and 10 wt.% urea solution tested case**

Figure 3-8 was the PVT study for the 5 wt.% NaCl plus 10 wt.% urea solution. After the heating, the fluid volume in the piston cell increased by 12.54 mL initially. Unlike the brine base case, the fluid volume started to decrease when the system was approaching equilibrium (> 1000 mins). The net fluid volume increase was stabilized at 11 mL. The difference between the brine and urea brine solution indicated that urea hydrolysis was a much slower process comparing to the aqueous phase thermal expansion. Therefore, the 12.54 mL volume increase was dominant by the thermal expansion. Then the net effect of the water consumption (depletion) of the urea hydrolysis was realized later when the notable amount of water molecules was reacted with urea. After the gas generating solution reached equilibrium, the piston cell was cooled to room temperature while maintaining at constant P. The final volume change was a negative value of -4.07 mL which means that urea hydrolysis consumed 4.07 mL water of original solution. The volume increase in the base case caused by heating was more significant than the

gas generating case. Therefore, no free gas phase was forming with 10 wt.% gas generating agent solution at 250°F and 1500 psi.

### 3.5 Summary

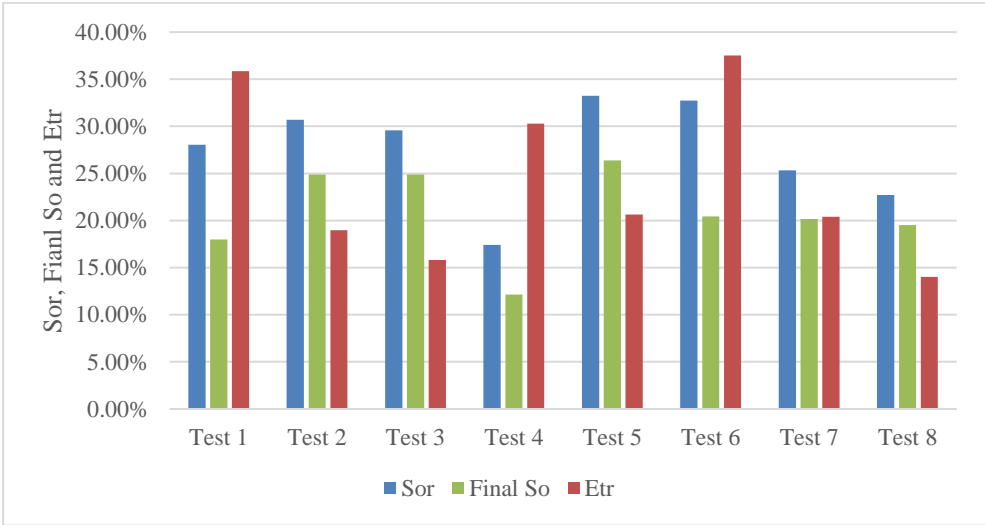


**Figure 3-9 Oil saturation change and tertiary recovery for all the tests**

Figure 3-9 is a detailed summary of the tests of urea based in situ CO<sub>2</sub> generation approach. Because of the unique pore throat structure of each sand pack, the residual oil recovery was not fully controllable[27, 84]. Variation of the residual oil saturation after water flooding was noticeable. Despite variations in residence times, operating pressures, types of oil used, levels of divalent ions and gas generating agent concentrations, the majority of the tests in this work showed a significant tertiary recovery. Mechanisms of swelling and viscosity reduction were showed separately in pure alkane test. For all the simple homogenous sand pack experiments, the dominant tertiary recovery mechanism is oil swelling. Effect of wettability reversal was observed

in the compositional analysis of collected oil samples. Presence of divalent ions did not cause adverse effects in the tests.

Even including several tests with extremely low original  $S_{or}$ , overall the average tertiary recovery was calculated close to 24.19%. In comparing with the Table 3-1, this recovery was achieved by a cheaper and less complex system (Urea Price: \$345/TON) that required no more facilities other than basic water injection, and similar to the results from our recent study [31]. The tertiary recovery was higher than most of the published data. Though, this work was still at the very first stage of development to prove the validity of this newly proposed technique. It appears that the potential for the optimization of this technique was quite large based on some promising data documented here.

### **3.6 Conclusion**

After the study of the new proposed simple chemical system for In Situ  $CO_2$  generation EOR, its advantages are revealed comparing to the earlier researches.

1. Urea as a gas generating agent can provide significant tertiary recovery under the tested conditions.
2. The tertiary recovery of the newly proposed simple chemical system is comparable to the complex system (combined surfactant, polymer, and alkali) proposed by earlier In situ  $CO_2$  generation types of research. This fact allows outstanding economic feasibility.
3. The mechanisms of In Situ  $CO_2$  generation EOR are oil swelling, viscosity reduction, and wettability reversal.

4. Running In Situ CO<sub>2</sub> generation EOR experiment above MMP does not show miscible flooding benefits.
5. Urea is a better gas generating agent than other carbamates or carbonates because of its outstanding divalent cations resistance.

## **Chapter 4: In-Situ CO<sub>2</sub> Enhanced Oil Recovery: Parameters**

### **Affecting Reaction Kinetics and Recovery Performance**

#### **4.1 Introduction**

CO<sub>2</sub> injection as a dominant enhanced oil recovery (EOR) method is applied successfully in the US for over 40 years[87]. It is estimated that approximately 5% of US oil production was coming from CO<sub>2</sub> EOR[88]. There were 152 CO<sub>2</sub> EOR projects active in 2014[89]. From another perspective, CO<sub>2</sub> capture and storage (CCS) is proposed and practiced for years to address global climate change[90]. Expanding the use of captured CO<sub>2</sub> for EOR operations offers one of the best options to reduce the CO<sub>2</sub> emission. In the last decade, many US major CO<sub>2</sub> EOR operators have economically operated in mature oil fields, and more recently some even explored the potential in unconventional reservoirs[91]. In post-2014 low oil price environment, the CO<sub>2</sub> flooding remains a promising EOR technique for major offshore reservoirs[63, 92]. However, behind the optimistic data of the CO<sub>2</sub> EOR projects, some common issues are still limiting its full potential, e.g., mobility control, CO<sub>2</sub> availability, CO<sub>2</sub> transportation, and infrastructure requirements.

Under idealized laboratory conditions, most supercritical CO<sub>2</sub> testing shows exceptional tertiary recovery because in essence, it is miscible flooding [3]. However, when CO<sub>2</sub> moves to actual field tests, the large contrast of viscosity and density between the displacing phase of injected CO<sub>2</sub> and the displaced phase inevitably leads to less desirable mobility ratios. While the microscopic displacement efficiency may be quite high, the actual sweep efficiency is drastically reduced resulting in less robust tertiary

recovery. To address the mobility control issue, the Water Alternating Gas (WAG) method is proposed[7, 8, 64]. In cases like that of a thick formation, WAG is still hard to operate properly within economic constraints[5]. Because the optimal WAG ratio and slug sizes are constantly changing between individual cycle, site optimization procedures require extensive efforts and monitoring [9]. Others have proposed Carbonated Water Injection(CWI), i.e., injecting water with dissolved CO<sub>2</sub>, to eliminate the mobility control issue associated with injecting gaseous CO<sub>2</sub> and have demonstrated these in both field scale[13-15] and laboratory scale[10-12, 26, 27, 65-67] tests. Regarding the field practice, CWI requires no surface facilities beyond the basic water flooding system except the pressurized mixing tank for the CO<sub>2</sub> dissolution step. In many cases, it offers a low-capital alternative versus the WAG method and achieves similar sweep efficiency as water flooding. Nonetheless, the CO<sub>2</sub> delivery ability of CWI is limited by CO<sub>2</sub> water solubility at the reservoir conditions [16, 17]. More recently, injection of CO<sub>2</sub> foam, or various CO<sub>2</sub> thickeners and gels were also extensively investigated for their potential in improving mobility control of EOR [88]. To date, quite a few of these new approaches remain at lab stage. Before full scale implementation, evidences of their affordability must be first demonstrated based on field pilot tests.

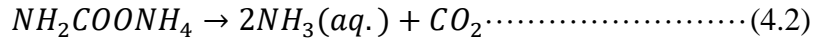
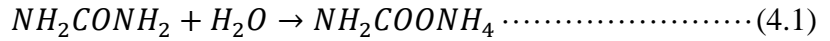
A few decades ago, Shell Oil Co proposed one of the very first ICE systems by applying sodium carbonate-sodium bisulfite, sodium bicarbonate-sodium bisulfite and sodium carbonate-hydrochloric acid/sulfuric acid to generate CO<sub>2</sub> in situ[93]. A variety of chemical CO<sub>2</sub> generating agents and formulations were offered subsequently.

Regarding gas generating efficiency, most documented candidates to date could be categorized into two groups, single fluid system, i.e., self CO<sub>2</sub> generating ability with single chemical slug injection, and dual fluid system, i.e., basic salt slug followed by secondary acid slug injection to initiate various CO<sub>2</sub> generating mechanisms. The single fluid systems include surfactant-carbamide-ammonium salts[23], carbamide-surfactant[22], ammonium bicarbonate-surfactant-polymer[24], urea-steam[94, 95], aluminum salt- carbamide-surfactants[21], ammonium carbamate-surfactant-polymer[19], low pH HEDTA-EDTA-carbonate reservoir[96, 97] and citric acid-carbonate reservoir[98] systems. Examples of the dual fluid systems involve sodium bicarbonate-citric acid[99], sodium carbonate-acid[20, 25, 100] and carbonate salt-acid-surfactant[18, 101]. One common scheme of these advanced approaches is, either field operations are difficult to control, e.g., multiple fluid slugs with different pH during sequential injection, or adjusting multiple components in solution are challenging, e.g., surfactant, polymer, alkali, acid involved. Increasing system complexity significantly hampers the project economic viability. Therefore, work done by this group focused on single fluid systems eliminating the use of functional additives (surfactant, polymer, acid, alkali). By taking the advantages of the self-initiating chemical hydrolysis of urea and the reasonable level of tertiary recovery potential, the newly developed approach allowed a simple and cheap ICE process[31, 102].

In this work, our previous studies with urea as the gas generating agent were expanded because of its easy access, reasonable price, and superior water solubility for EOR field operations. Additionally, the raw material can be safely handled as bulk solid or

concentrated solution with minimum hazardous concerns to human and environment[102].

Urea hydrolyzes at elevated temperature to release ammonia and carbon dioxide:



The urea hydrolysis is studied across various research areas (waste water treatment, automotive selective catalytic reduction[69-77], etc). With proper conditions and control, the produced CO<sub>2</sub> and NH<sub>3</sub> from urea hydrolysis offer great potential to improve tertiary oil recovery. Recently, injection of NH<sub>3</sub> aqueous solution only has shown advantages in alkali/surfactant/polymer(ASP) flooding comparing to Na<sub>2</sub>CO<sub>3</sub>[35, 55] and exhibited a positive effect on wettability reversal on the silica sand surface[33]. Additionally, the majority of the CO<sub>2</sub> produced in aqueous phase migrated to the entrapped oil phase due to its high partition coefficient between oil and aqueous phases. After significant CO<sub>2</sub> dissolution in oil, the oil saturation moves higher as a result of oil swelling[41-43] and decreasing oil viscosity [44, 45, 50, 103] leading to significant residual oil mobilization and better recovery.

As research related to ICE mechanisms go forward, more questions are arising than are being answered. Among these concerns is that elevated divalent cations in brine might cause formation damage during the CO<sub>2</sub> flooding process[86] through calcium carbonate precipitation. Many earlier works were executed at no to trace divalent ion concentrations. However, site-specific reservoir brine conditions vary case by case[31].



Second, in our previous effort, the reservoir temperature was kept at 120 °C. It is logical to further explore the operational envelope of the proposed ICE process since not all the reservoirs suitable for CO<sub>2</sub> flooding are within such a high temperature range. Third, in our earlier studies highly concentrated reagent solutions were used to prove the validity of this new approach. Therefore, additional studies to optimize formulation design is required to provide a realistic cost estimate for any field trial. Last but not the least, the urea hydrolysis reaction rate and mass balance were estimated previously based on the kinetic data derived from the literatures focused on wastewater treatment studies. Thus, the calculated data might not be truly representative of reservoir conditions, which are rather complicated and extreme as compared in the case of conventional wastewater treatment facilities. Monitoring the actual urea hydrolyzes and the residual mass at site-specific reservoir conditions can offer a better picture of the newly developed ICE system.

## **4.2 Materials**

### *4.2.1 Chemicals*

High purity urea (99 wt.%) and calcium chloride dihydrate were purchased from Acros Organics. Sodium chloride (99.5 wt.%), potassium chloride (99%), magnesium chloride(98%) and magnesium sulfate(99%) were purchased from Sigma-Aldrich. The special 5 mL-microwave reactors with 300 psi pressure rating were purchased from Chemglass. Vanadium pentoxide (99.6%) was purchased from Acros Organics. Sodium orthovanadate (99.98%), sodium hydroxide (97+%), acetonitrile (HPLC grade, ≥ 99.93%) and water (HPLC Plus) were purchased from Sigma-Aldrich.

Earlsboro crude was the targeted oil for the optimization. It was a 40 API crude with a room temperature viscosity of 4.6 cP. The MMP of CO<sub>2</sub> for this oil was estimated as 3190 psi[57].

#### *4.2.2 Porous Media & Apparatus*

For the sand pack tests, Ottawa sand F-75 from U.S. Silica was selected for most tests. The F-75 Ottawa sand pore sizes were from 0.053 to 0.6 mm with d50 of 0.15 mm. The sand was air-dried in an 80 °C oven overnight before being packed into the stainless-steel (316 stainless steel) column. For better comparison, the total length of each sand pack was adjusted to be identical at 6 inches. The inside diameter (ID) of a regular 3100 psi pressure rating sand pack was 0.834 inch. The average pore volume of the packed columns was 18.95 mL +/-0.18 mL.

For the flow-through tests, similar apparatus setup was used as described in our previous work[31].

### **4.3 Experimental**

#### *4.3.1 Urea Hydrolysis and Catalytic Reactions*

A series of urea hydrolysis tests were carried out to monitor the kinetics of the urea hydrolysis reactions and any modifications of reaction rates by catalysts to provide additional critical parameters (i.e., the reaction constant) for a future field scale pilot test and reservoir simulations.

Urea solutions were analyzed by HPLC (High-Performance Liquid Chromatography) installed with a UV/Vis detector. The UV/Vis detector was set at 200 nm. A reverse phase C18 column was used to separate the urea peak. An acetonitrile and water (50/50)

solution was used as the mobile phase. The HPLC pumping rate was 0.7 mL/min. The C18 column temperature was kept at 30 °C.

The microwave reaction vials were set up as the urea hydrolysis reactor. The reactor could be operated safely up to 400 psi and 300 °C to withstand the pressure increase as a result of generating CO<sub>2</sub> and heating over the course of hydrolysis. A series of 10 wt.% urea-only and urea solutions with catalyst (1wt.% NaOH) were prepared in deionized water. For one group of measurements, individual vials were first loaded with 5 mL of the stock solution. Six replicate reactors were involved and sealed with the same targeted solution. Then the whole set of reactors were simultaneously heated to the targeted temperature while the reaction times were recorded. At each designed time interval, one of the reactors was removed from the oven and immediately cooled in a room temperature water bath to quench further reaction. After the cooling of last (6th) reactor was finished, all post-hydrolysis sample solutions were retrieved and further diluted before the HPLC analyses. The change of urea concentration against different reaction periods could then be plotted to quantify the reaction constant at any particular temperature.

#### *4.3.2 Sand pack flooding with the presence of divalent ions*

Ottawa F-75 sand was evenly packed in the stainless-steel column with diameter 0.834 inch and length 6 inches. A fixed amount (90 g) of Ottawa sand was loaded to the column for each test. Similar compaction was applied to the filled materials. Porous media properties like porosity and permeability were highly consistent between runs, as is summarized at Table 4-2. A known amount of Earlsboro crude oil was injected into the dry sand pack to develop a full oil saturated sand pack. After the oil saturation step,

all sand packs were aged with the crude oil for 60 days at 80°C[47]. Once ready, the aged sand pack was flooded according to different strategies. In this study the in situ CO<sub>2</sub> generation EOR was applied as a tertiary recovery method, so the first stage involved a water flooding to establish a residual oil saturation. A total of 8 to 10 pore volumes (PVs) of either mimic sea water or API brine would be injected before applying additional stages after the oil cut approached zero. Table 4-1 showed the brine ingredients used in this work.

**Table 4-1 The brine composition**

Chemical	Seawater Salt Concentration, wt. %	API Brine Salt Concentration, wt. %
NaCl	2.629	8.000
KCl	0.074	\
CaCl <sub>2</sub>	0.099	2.000
MgCl <sub>2</sub>	0.609	\
MgSO <sub>4</sub>	0.394	\
Total	3.805	10.000

Once the residual oil saturation was established, injection of urea was initiated. The gas generating urea solutions were prepared in mimic seawater or API brine. Urea concentrations used in this work were ranging from 1 wt.% to 35 wt.%. For consistency and better comparison, the injected gas generating agent solution volume was kept at 2 PVs for all the tests, which means that the total amount of urea varied from test to test, just as the amount of CO<sub>2</sub> and ammonia generated was allowed to vary from test to test. After completion of the gas generating agent injection, post urea water flooding immediately followed until the oil cut again reached zero. In addition to the continuous flow tests, several shut-in cycles were included as part of the tests to allow additional time for the urea to decompose and for the CO<sub>2</sub> generated in solution to diffuse into the residual oil phase, as well as for the ammonia generated to react with the surface of the

sand in the aged sand pack. For tests involving a shut-in reaction cycle, after the chemical injection, a 72-hour flow stoppage (interruption) was added while the pressure and temperature were kept at the test conditions. To compare high and low injection rates, 0.3 mL/min and 0.03 mL/min flow rate were tested. The changing of the injection rate was also to observe the effect of the chemical residence time on the oil recovery. Among the standard injection strategies, after 1 PV reactive chemical injection, with or without shut-in reaction cycle, there followed adequate pore volumes of water flooding to achieve zero oil cut before either switching to the next chemical slug injection or concluding the experiment.

The depth of the Red Fork formation that produced the Earlsboro crude oil was from 3000 ft to 4500 ft[104]. Therefore, the test pressure was set to 1500 psi to represent the formation reservoir pore pressure. At the same pressure, different temperatures were used to evaluate the effect of the urea hydrolysis reaction kinetics.

The effluent of the sand pack flooding was collected and analyzed to determine the urea mass balance and the amount of unreacted urea eluted from the column. All the effluent collected from a specific test was gathered in a large container. The sample for HPLC analysis was taken from the container after the effluent been well mixed. The conversion factor could be calculated once the urea concentration of the effluent was determined.

$$conversion\ factor = \frac{V_{effluent} \times C_{urea\ in\ effluent}}{V_{injected} \times C_{urea\ prepared}} \dots\dots\dots (4.3)$$

Where:

$V_{effluent}$ : Total volume of the collected effluent

$C_{urea\ in\ effluent}$ : Urea concentration in the effluent

$V_{injected}$ : Total volume of the injected urea slug

$C_{urea\ prepared}$ : The original urea concentration before the injection

## 4.4 Results and Discussion

### 4.4.1 Urea Hydrolysis Kinetics

The urea hydrolysis reaction was reported previously to be a first order reaction[105], for which the reaction rate can be expressed as,

$$\frac{dC}{dt} = kC \dots\dots\dots(4.4)$$

Where,

C, the urea concentration, M

t, reaction time, min

k, the reaction rate constant,  $\text{min}^{-1}$

After integration

$$kt = \ln(C_0) - \ln(C_t) \dots\dots\dots(4.5)$$

Therefore, from results of HPLC analysis of post reacted samples, net urea concentration change over time at fixed temperature could be used to calculate the corresponding reaction rate constant by plotting  $\ln(C_t)$  versus time, t. Additional reaction rate constants were determined at various temperatures. Based on the

Arrhenius theory, the temperature dependence of the rate constant can be simply described as,

$$k = Ae^{E_a/(RT)} \dots\dots\dots(4.6)$$

Where

T, the absolute temperature, K

A, the pre-exponential factor, min<sup>-1</sup>

E<sub>a</sub>, the activation energy for the reaction, kJ/mol

R, the universal gas constant, kJ/mol • K

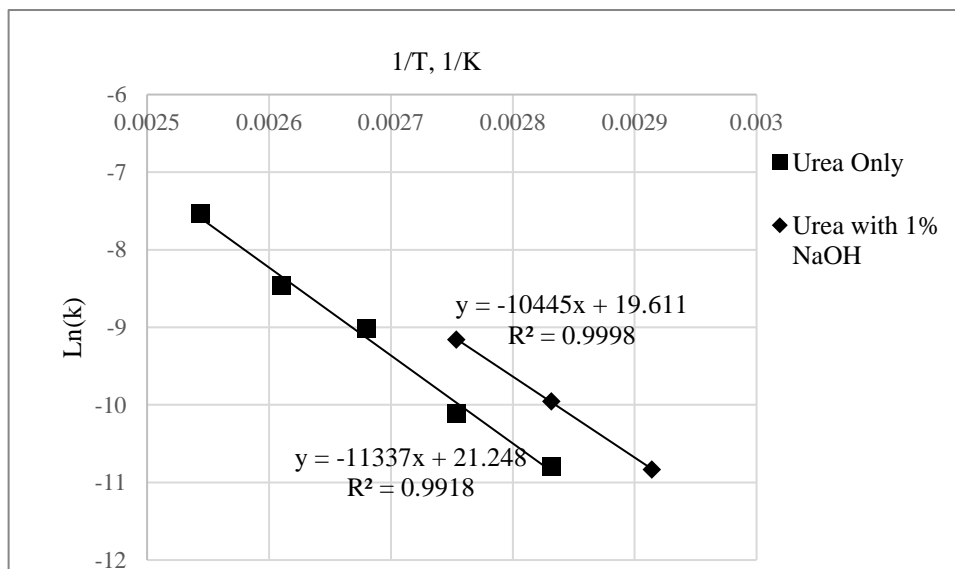


**Figure 4-1 Temperature dependence of the rate constant for Urea hydrolysis**

Figure 4-1 shows the reaction rate constant temperature dependence for urea hydrolysis in both the absence and the presence of the NaOH catalyst. Urea was hydrolyzed without catalyst at temperatures from 80 to 120 °C and with 1 wt. % NaOH (catalyst) at temperatures from 70 to 90 °C. For urea hydrolysis without catalyst, the pre-exponential

factor and the activation energy for the reaction were calculated to be  $94.26 \text{ kJ/mol}$  and  $1.7 \times 10^9 \text{ min}^{-1}$  graphically. When 1 wt. % NaOH was added, the pre-exponential factor and the activation energy for the reaction of the hydrolysis were  $86.84 \text{ kJ/mol}$  and  $3.3 \times 10^8 \text{ min}^{-1}$ , respectively. Therefore, these reveal that 1: hydrolysis of urea could proceed in several hours to few days at temperature  $> 70 \text{ }^\circ\text{C}$  2: Addition of basic solution (1 wt.% NaOH) could drastically enhance the urea decomposition rate. Previous researchers[70, 72, 74, 75, 77, 80, 81, 105, 106] drew similar conclusions on the efficacy of NaOH.

#### 4.4.2 Flow through Tests Data Interpretation and Conditions

Properties of in situ  $\text{CO}_2$  generation formulations were further evaluated for their potential in field implementation of tertiary recovery. The regular tertiary recovery factor ( $E_{tr}$ ) was monitored and applied as an efficiency indicator for the process.

$$E_{tr} = \frac{V_{In\text{ Situ } CO_2\text{ Generation produced oil}}}{V_{Dry\text{ packed oil volume}} - V_{Brine\text{ flooding produced oil volume}}} \times 100\% \dots \dots \dots (4.7)$$

During the flow through experiments, the most crucial operation parameters, such as sand pack inlet pressure, outlet pressure, and oven temperature, were recorded automatically per 1-minute time interval. In addition, the volume of total gas generated was simultaneously quantified, with an in-house built gas collector near the column outlet, operated at ambient conditions. The varying oil saturation ( $S_o$ ) during flooding was plotted against the PV injected.

$$S_o = \frac{V_{Dry\text{ packed oil volume}} - V_{Produced\text{ oil volume}}}{V_{Pore\text{ volume}}} \times 100\% \dots \dots \dots (4.8)$$



A total of 11 sand pack flooding tests were conducted. The detailed experiment conditions are summarized in Table 4-2. Different variations of tests were aimed to address the impacts of injection strategy, flow rate, urea concentrations and elevated divalent ion concentration. The main goal was to assess the key parameters affecting the economic and physical feasibility of this in situ CO<sub>2</sub> generation EOR system for field implementation. Oil saturation versus injected pore volume plots were used to analyze the performance of individual experiments. Variations of injection strategies introduced different Damköhler numbers for each experiment. The following equation could calculate the Damköhler numbers:

$$Da = kC_0^{n-1}\tau \dots\dots\dots(4.9)$$

Where:

k, the reaction rate constant, min<sup>-1</sup>

C<sub>0</sub>, the initial urea concentration, M

n, the reaction order

τ, the mean residence time, min

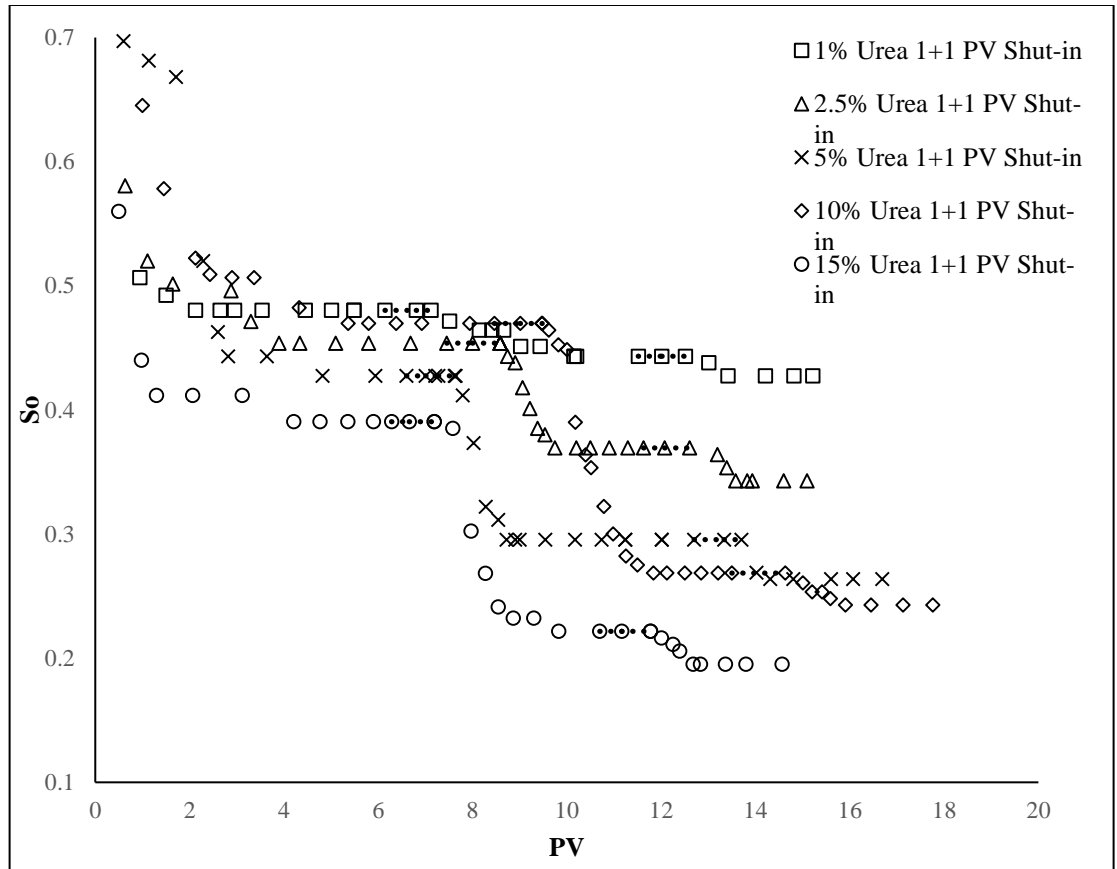
**Table 4-2 Experiment Conditions**

	Gas generating agent Concentrati on, %	Flow rate, mL/mi n	Residual oil saturatio n after water flooding	Porosity, %	Permeability , mD	Injection strategy	Damköhl er numbers
Test 1	Urea 1 wt.%sea water	0.3	48.0%	33.9%	3876.9	1+1 PV Shut-in	2.35
Test 2	Urea 2.5 wt.%sea water	0.3	45.4%	33.7%	3846.8	1+1 PV Shut-in	2.35
Test 3	Urea 5 wt.%sea water	0.3	42.7%	34.2%	3938.8	1+1 PV Shut-in	2.35
Test 4	Urea 10 wt.%sea water	0.3	47.0%	33.7%	3841.6	1+1 PV Shut-in	2.35
Test 5	Urea 15 wt.%sea water	0.3	39.1%	33.6%	3824.9	1+1 PV Shut-in	2.35
Test 6	Urea 5 wt.%sea water	0.03	43.7%	34.1%	3921.1	1 PV flow through 1 PV Shut -in	1.34
Test 7	Urea 5 wt.%sea water	0.03	44.3%	33.8%	3853.2	2 PV Flow Through 1 PV flow	0.32
Test 8	Urea 10 wt.%sea water	0.03	42.7%	34.3%	3962.5	through 1 PV Shut -in	1.34
Test 9	Urea 10 wt.%sea water	0.03	50.1%	34.0%	3907.5	2 PV Flow Through	0.32
Test 10	Urea 10 wt.% API Brine	0.3	44.9%	33.3%	3764.2	1+1 PV Shut-in	2.35
Test 11	Urea 35 wt.%sea water	0.3	43.1%	34.5%	3995.2	1+1 PV Shut-in	0.09

\*Note: In all tests, aging time was 60-days, back pressure was 1500 psi, temperature was, 120 °C except Test 11 (80 °C)

#### *4.4.3 The Suitable Chemical Concentrations*

The injection strategy in this section was designed to find the appropriate chemical residence time. After waterflooding to residual oil saturation, 1 PV of urea solution was injected into the sand pack. Then the flow was stopped for 72 hours, immediately after completing the required chemical injection. Based on the observed urea hydrolysis kinetic data discussed above, the half-life of urea at 120 °C was equal to 1,290 minutes. Thus, a 72-hour hydrolysis time during the shut-in should guarantee that 90% of the reactant would have been converted to CO<sub>2</sub> and NH<sub>3</sub> (aq.). The actual reaction rate was not the only limitation to the oil recovery, however; instead it was also controlled by the mass transfer resistance of CO<sub>2</sub> between different phases. This process was similar to a CWI process with an extremely high carbonation level[5] plus some assistance from the produced ammonia.



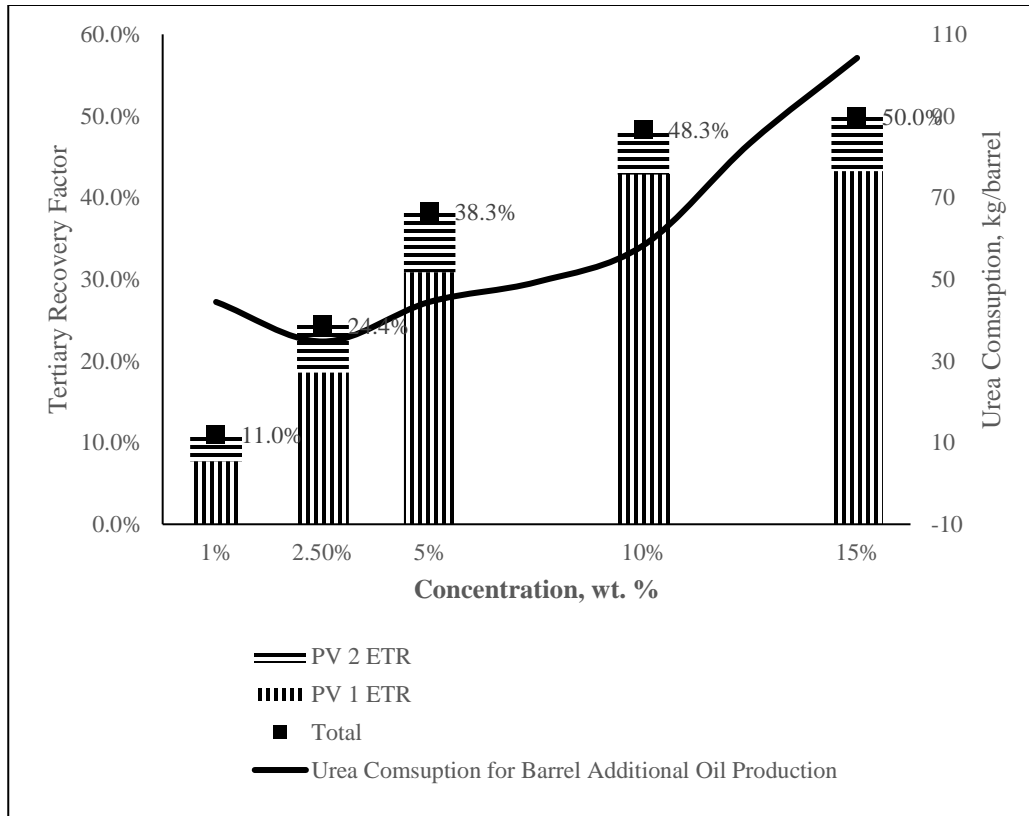
**Figure 4-2 Oil saturation VS time for different urea concentration injection (Test1-5) The dashed lines between the dots indicate the injection of the gas generating agent slug.**

Figure 4-2 shows the concentration effect on the tertiary recovery. Beside concentration variations, these five tests were performed similarly at 1500 psi back pressure and 120 °C with Earlsboro oil, seawater, and identical injection strategy. The purpose of these tests is to determine the optimum range of urea concentrations of in-situ CO<sub>2</sub> generation formulations using this one particular injection strategy.

From Figure 4-2, there was no apparent oil produced during the injection periods of the first or second chemical slugs and or even during the shut-in stages. It is believed that since the injection flow rate for these tests was kept at 0.3 mL/min, the active oil

production stage was mostly completed in less than one hour. For these tests the chemical residence time was much shorter (60-minutes vs. 1290-minutes) than the half-life at this temperature. Based on the reaction rate, only 3.2% of the urea reacted during these test. Under these conditions, simply injecting urea-seawater solutions could not promote detectable tertiary recovery due to lack of adequate urea conversion to CO<sub>2</sub> and NH<sub>3</sub>.

In contrast, once the post brine flooding resumed after the 72-hour shut-in period, distinct oil elution was observed within 0.2 PV seawater injection. The expected 90% of urea hydrolysis released significant amounts of CO<sub>2</sub> and ammonia in the aqueous phase during the shut-in period. The fresh CO<sub>2</sub> spontaneously transferred from the aqueous phase to nearby trapped oil droplets due to CO<sub>2</sub>'s order magnitude of greater oil solubility than in water (brine) solubility. Consequently, as oil swelling occurred, the entrapped oil droplets near residual oil saturation could be interconnected and eventually displaced out of the pores so that the water flooding after the shut-in showed a dramatic oil breakthrough in these tests, in contrast to the lack of tertiary oil produced when inadequate reaction time was provided.



**Figure 4-3 Effect of the gas generating agent concentration on the tertiary recovery of each shut-in stage and total tertiary recovery**

Figure 4-3 shows the tertiary recovery factors for each stage among the 5 urea concentrations used. The increase of total recovery was observed as urea concentrations increased. The total tertiary recovery curves reached a plateau beyond 10 wt. % of urea. Comparing to the case of 10 wt. % test, further increase of urea levels (15 wt. %) showed insignificant changes in the amount of tertiary recovery. The plateau of the tertiary recovery may indicate that the amounts of the generated CO<sub>2</sub> finally approached the solubility limit in both water and oil phases of the system. In the in situ CO<sub>2</sub> generation EOR process, the CO<sub>2</sub> molecules would first form in the aqueous phase after chemical decomposition. Because of the low chemical potential of CO<sub>2</sub> in the oil phase

initially, the CO<sub>2</sub> molecules would diffuse to the oil phase. Once the CO<sub>2</sub> concentrations reached CO<sub>2</sub> solubility limits in both oil and water, and assuming no gas phase was existing at operating temperature and pressure in the system, the migration of CO<sub>2</sub> between phases stopped. Without further CO<sub>2</sub> dissolution in the oil phase, the oil swelling behavior reached a limit, leading to a plateau level of potential tertiary recovery. Moreover, the chemical decomposition reactions reached equilibrium because the whole system reached the limit of CO<sub>2</sub> solubilities at test condition. In reality, the best system would not reach 100% tertiary recovery by simply increasing the amount of the delivered CO<sub>2</sub> because of the residual oil saturation under the immiscible displacement process using current formulations. Based on these data, if the target is to maximize the amount of tertiary recovery, the optimal urea concentration should be between 5 wt.% to 10 wt.% as the start of the plateau is close to 8 wt.%.

From the Figure 4-3, comparing the tertiary recovery between the first and the second chemical injection in all cases, the tertiary recoveries from the second PV chemical injection were much lower than those of the first injection. The second injection cycles in all the tests showed some additional oil removed. Therefore it is reasonable to say that injecting only 1 PV of urea was not enough for the system to reach its maximum oil swelling in this injection strategy. Among test 1 to test 5, the second injection cycles accounted for 29.9%, 23.8%, 19.3%, 11.3% and 13.5% of the total tertiary recovery, respectively. Use of a more concentrate chemical slug could provide additional CO<sub>2</sub> at test conditions; however, the effect of the second injection on the total recovery became less dramatic when the original urea concentration was already high. This implies that during the first urea slug injection a high urea concentration could generate

considerably more CO<sub>2</sub> than in the case of a low concentration slug. After the first injection event, the CO<sub>2</sub> dissolved in the oil phase reached much closer to the solubility limit in high concentration cases. Therefore, the amount of CO<sub>2</sub> that could be transferred to saturate the oil phase during the second injection event became lesser with increase of the chemical concentrations.

The amount of chemical use (or cost, indirectly) of this technique was also estimated as depicted in Figure 4-3. The estimation calculation only used the recovered oil volume from the first 1 PV injection because the efficiency of the second 1 PV injection was low, except for the 1 wt.% test. Therefore, if the target of the optimization was based on the consideration of cost efficiency, a 2.5 wt.% solution would be the optimized concentration (34 kg/barrel). The additional investment of this optimal formulation would be the combined transportation plus the chemical costs, and the savings of shorter project time frame.

**Table 4-3 pH measurement of the aqueous effluent for test 1-5**

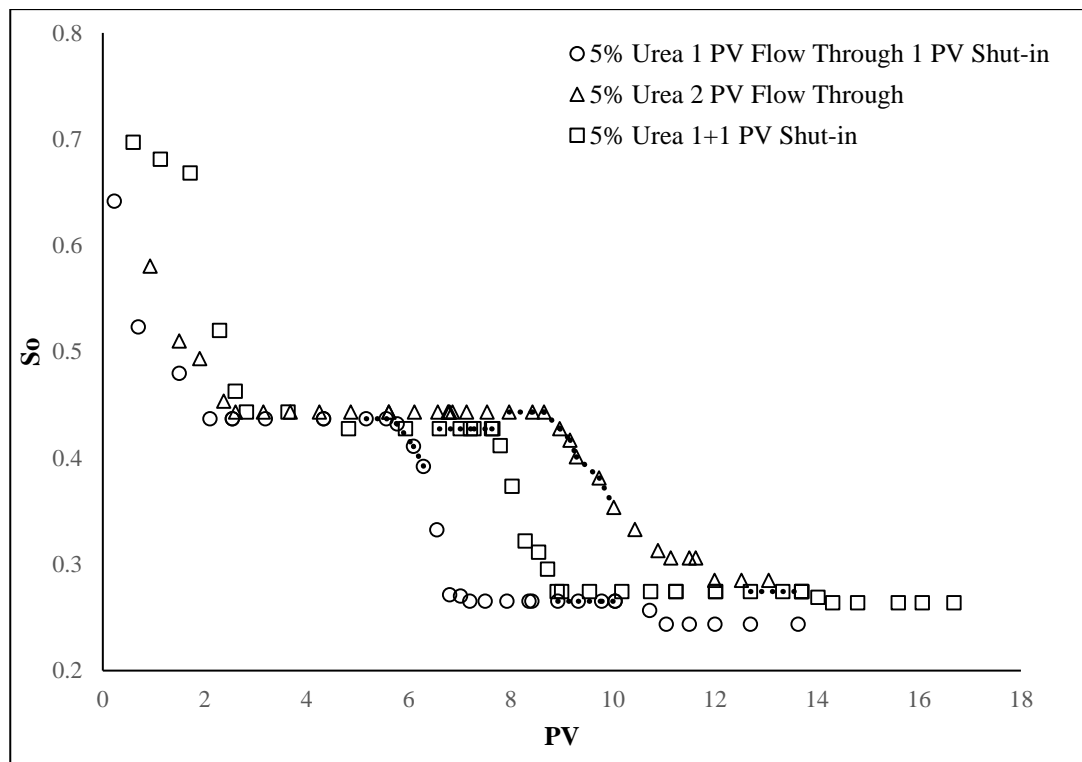
Urea Concentration, wt%	pH
0%	6.07
1%	9.34
3%	9.63
5%	9.92
10%	10.12
15%	10.13
35%	10.13

Table 4-3 shows the pH measurement of the aqueous effluent samples. Zero urea concentration samples were collected after the residual water saturation established during the brine flooding stage. Different tests showed identical pH reading during the brine flooding stage. The urea impacted samples were collected at the 0.5 pore volume



injection of the brine after the first shut-in stage in tests 1 to 5. The artificial seawater had a pH around neutral. A 1 wt.% urea hydrolysis drove pH of the effluent to 9.3. Further increase of the urea in feed solutions did not significantly alter the solution pH. The pH of the effluent reached a plateau at urea concentrations greater than 5 wt.%. Note that recent studies[33, 35] on use of ammonia EOR applications showed a similar trend of pH readings.

#### 4.4.4 The Optimized Injection Strategy



**Figure 4-4 Oil saturation VS time plot of 5 wt.% Urea injections with different injection strategy. The dashed lines between the dots indicate the injection of the gas generating agent slug. Cases: 5% Urea 1 PV flow through 1 PV Shut in (Test 6), 5% Urea 2 PV flow through (Test 7) and 5% Urea 1+1 PV shut-in (Test 3)**

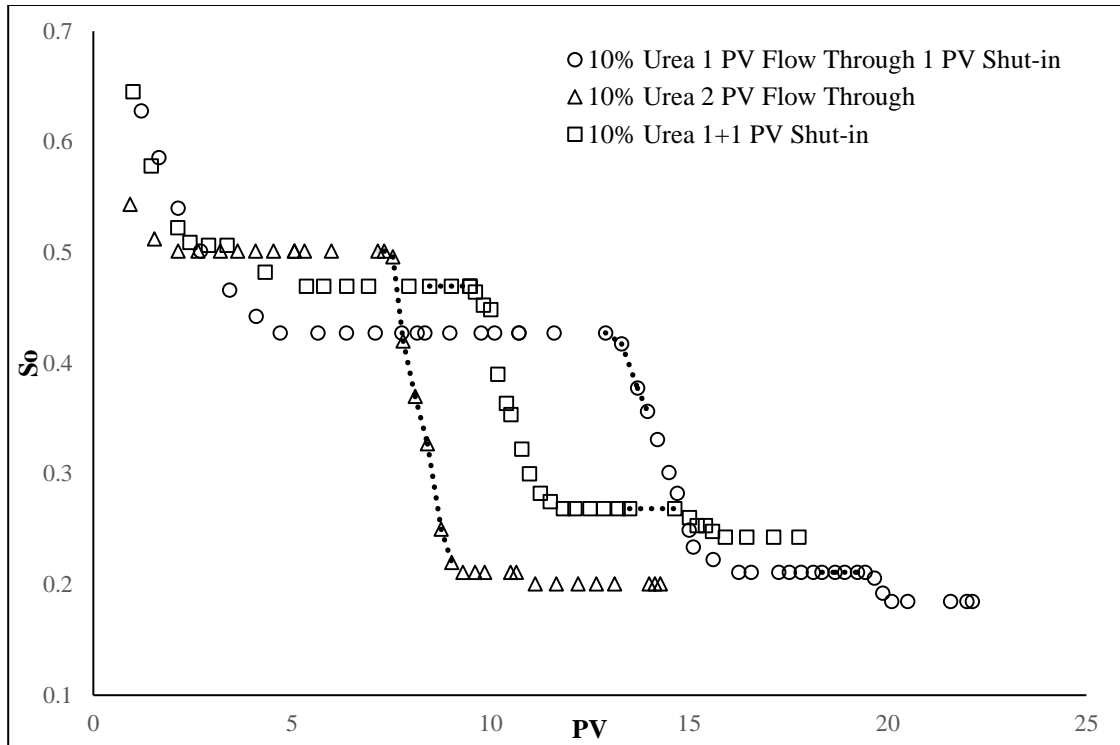


**Figure 4-5 Oil saturation VS time plot of 10 wt.% Urea injections with different injection strategy. The dashed lines between the dots indicate the injection of the gas generating agent slug. Cases: 10% Urea 1 PV flow through 1 PV Shut in (Test 8), 10% Urea 2 PV flow through (Test 9) and 10% Urea 1+1 PV shut-in (Test 4)**

Figure 4-4 and Figure 4-5 show the effects of different injection strategies on the tertiary recovery with two urea levels, 5 wt.% and 10 wt.%, respectively. Among these, Tests 3, 4, 6, 7, 8 and 9 used a constant total of 2 pore volume urea slugs by varying injection strategies to optimize the operation. Tests 3 and 4 were 1+1 PV shut-in tests. The injection sequence was described in the previous section. Tests 7 and 9 were 2 PV flow-through tests with no shut-in; however, the flow rate was reduced to 0.03 ml/min to allow longer chemical residence time. The chemical residence time was 10 hours at this lower flow rate. The first stage was 9 PVs brine flooding before urea injection to reach residual oil saturation. Then the tertiary recovery stage was a 2 PVs urea slug with

continuous injection followed by brine flooding till the oil cut in the effluent reached zero again. In contrast, Tests 6 and 8 were a 1 PV flow through plus a 1 PV shut-in test. The flow rate of these test was also 0.03 ml/min. After brine flooding, the first PV of the chemical slug was injected and followed by the brine flooding. Once the new residual oil saturation was reached, the second PV of the chemical slug was injected and followed by a 72 hours shut-in. Then brine flooding resumed after the shut-in.

By observing the details of the 5 wt.% tests in Figure 4-4, the 1 PV flow through plus 1 PV shut-in test provided the highest tertiary recovery. The 2 PVs continuous injection yielded the lowest tertiary recovery. The only difference between these 0.03 ml/min injection rate tests was the chemical residence time. By adding a shut-in cycle, the chemical residence time of the second PV increased from 10 hours to 82 hours. At the same temperature, longer residence time allowed a higher urea decomposition level. Since these tests were sand pack flooding test, the oil swelling was the dominant factor that contributed to the tertiary recovery. Therefore, the test that could thoroughly convert the urea to the CO<sub>2</sub> reasonably expected to have the best recovery. Because the decomposition of the urea was time-dependent at a specific temperature, in the continuous flow-through test, the urea decomposition ratio in the porous media was low. If the CO<sub>2</sub> formed in the preheating coil connected to the inlet of sand pack was not enough to fully saturate the aqueous phase, the oil mobilization ability of the chemical slug would be limited. After the in situ CO<sub>2</sub> EOR treatment, the zone close to the sand pack outlet could contribute more to the tertiary recovery. In reservoir condition, the residual oil at the near wellbore region would not contribute much to the tertiary recovery. The 1+1 PV shut-in test showed a recovery in the middle. Two 1 PV

chemical slug had a 73 hours residence time. Unlike the previously discussed two tests, the injection rate was 0.3ml/min. The effect of the slight increase of (10 X flow increase) capillary number at the higher flow rate was less significant on the recovery in this test than the increased reaction time at the lower flow rate.

In Figure 4-5 and the 10% urea cases, to our surprise, distinctly different recovery trends for different injection strategies were observed in the 5 wt.% cases, with the 2 PVs flow-through of 10% urea showing the best tertiary recovery. The worst 5 wt.% case was the 1+1 PV shut-in test. The tested injection strategies and conditions for 10 wt. % experiments were the same as the 5 wt.% tests. Therefore, the sharp contrasts between these two groups of tests are attributed to the urea concentration difference. With the same amount of hydrolysis time, a high concentration urea solution could generate more CO<sub>2</sub>. Based on the kinetic measurement of the urea decomposition without the catalyst in Figure 4-1, the half-life of the urea at 120 °C was 1290 min. Within a single half-life period, the 10 wt.% system could reach the maximum CO<sub>2</sub> delivery capability of the 5 wt.% system. From the Figure 4-2, the 10 wt. % chemical concentration was at the plateau of the curve. The urea decomposition ratio in these tests appeared to be no longer the primary limitation controlling the tertiary recovery. In a comparison of the 5 wt.% experiments, the tertiary recovery was likely controlled more by sweep efficiency than the amount of delivered CO<sub>2</sub> since the 10 wt.% should generate CO<sub>2</sub> faster than the 5% tests, based on the first order reaction model.

#### *4.4.5 Impact of High Divalent Ions Level*

The concentrated calcium ions tend to form carbonate precipitates with CO<sub>2</sub> under reservoir condition[86]. The divalent ions compatibility of the proposed in situ CO<sub>2</sub>

EOR system was reported in previously published work[102] and the tests with mimic seawater in this work. In general, the urea solubility was not affected by divalent ions in the artificial seawater at room temperature. After the decomposition of the urea in the sand pack flooding test, no signs of blockage or formation damage were detected in most cases. However, the hardness levels of the sea water were sometimes much lower than typical for formation water. Therefore, additional studies of high concentration divalent ion compatibility might be necessary. In this work, the gas generating agent slug was 10 wt.% urea, 2 wt.%  $\text{CaCl}_2$  and 8 wt.%  $\text{NaCl}$  solution, which was the example of an API brine condition. Before the flooding test, the urea solution was prepared and stabilized for 30 days with daily monitoring to make sure that no precipitate formed. For the sand pack flooding test, all the conditions were kept the same as previous 1+1 PV shut-in tests except that API brine replaced the mimic sea water.

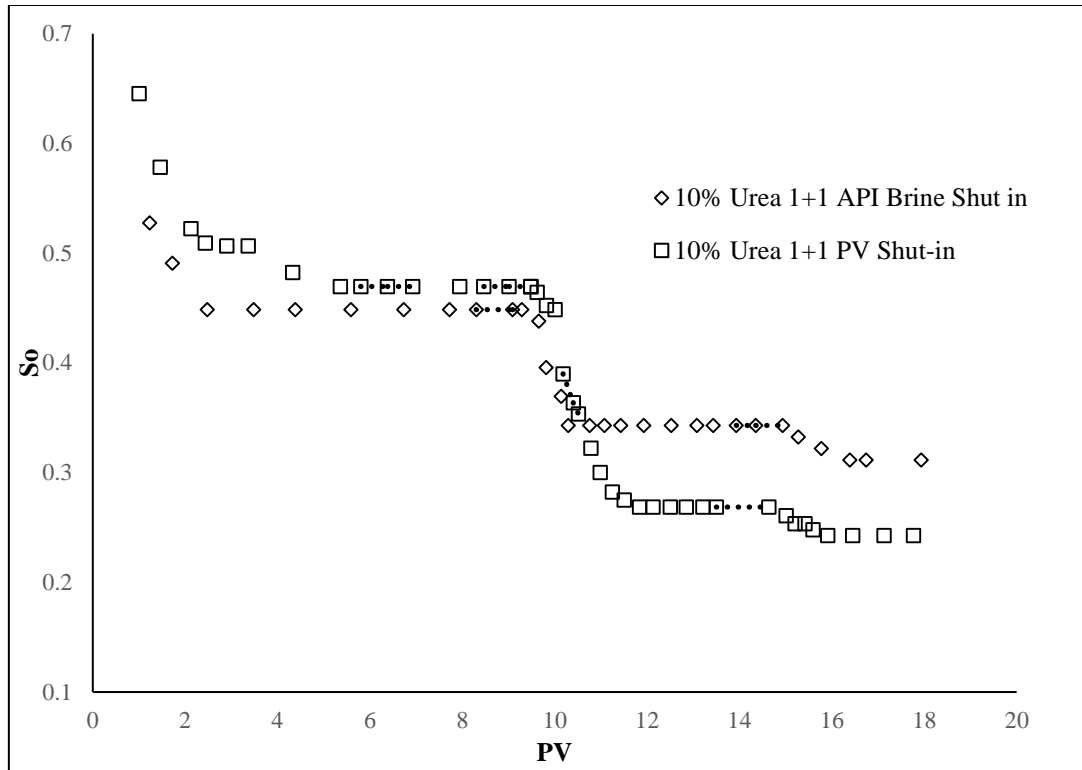


**Figure 4-6 Oil saturation VS time plot of 10 wt.% Urea with API brine and 10 wt.% Urea with seawater. Cases: 10% Urea API Brine 1+1PV Shut in (Test 10) and 10% Urea 1+1PV Shut in (Test 4)**

From Figure 4-6, the first 1 PV injection and shut-in contribute 76.9% of the total tertiary recovery (30.5%). Comparing to the 10 wt.% urea seawater tests, the tertiary recovery of API brine is relatively low. Because of excessive CO<sub>2</sub> consumptions by forming carbonate precipitate, the tertiary recovery and the oil recovery contribution from the second 1 PV injection of API brine 10 wt.% urea test were close to the seawater 2.5 wt.% case (tertiary recovery 24.4%). This result was an indication of the consumption of the generated CO<sub>2</sub> by the API brine. The Ca<sup>++</sup> concentration of API test case was 20 X that of the the seawater used in this work. The reactions between CO<sub>2</sub> and the Ca<sup>+2</sup> countered the potential of tertiary recovery strongly. By visual

observations of the effluent samples collected after the shut-in step, colloidal calcium carbonate precipitate was present in the brine, making the effluent cloudy (turbid). After applying 6000 rpm centrifugation for 20 minutes, most carbonate particles agglomerated and settled down to the bottom of the centrifuging vial while the supernatant became transparent. No larger carbonate crystals were observed in the precipitation. Based on the monitoring pressure data of the test, no noticeable blockage of the flow line and formation damage was recorded. However, the precipitation particles formed on the sand surface or suspended in brine might not have the ability to build up and block the relative large pore throats of the high permeability sand pack in this study (around 4 Darcy). Elevated divalent ions concentration application of the in situ CO<sub>2</sub> EOR technique was still questionable without further study of low permeability core and any occurrence of formation damage. Based on the collected data so far, the in situ CO<sub>2</sub> generation system using urea could tolerate divalent ions to a certain level (e.g., seawater level). If the divalent ions concentration was too high, it would lead to adverse effect of tertiary recovery performance or even formation damage.

#### *4.4.6 Low Temperature*

So far, all the experiments of this work were designed to run at 120 °C. If the in situ CO<sub>2</sub> EOR technique was only working in high-temperature condition, its practicability could be extremely limited. Proving the ability of in situ CO<sub>2</sub> generation EOR by using urea at low temperature significantly expands the field of its application. Based on the kinetic measurement of the urea decomposition in this work, the process was evaluated at 80 °C in this section. For the ease of the experiment running, the 35 wt.% gas

generating agent concentration was prepared in seawater to speed the reaction rate at low temperature.

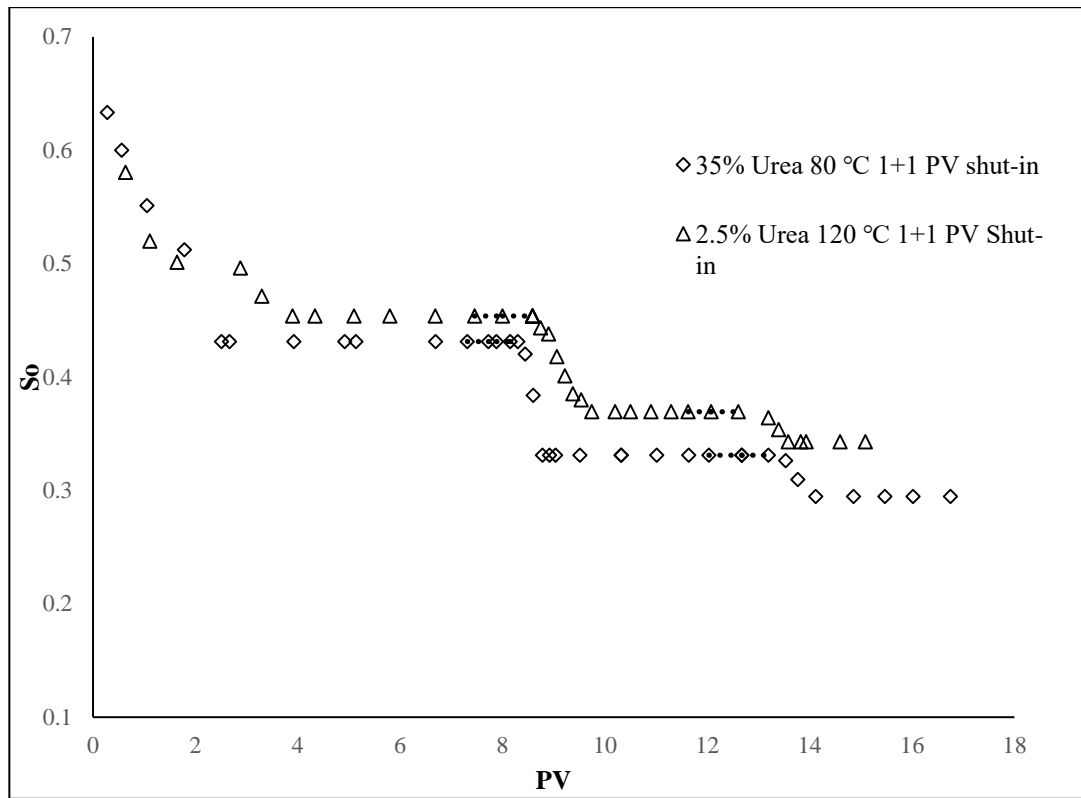


**Figure 4-7 Oil saturation VS time plot of 35 wt.% urea injection at 80°C and 2.5 wt.% urea injection at 120°C. Cases: 35% Urea 80°C 1+1PV Shut in (Test 11) and 2.5% Urea 1+1PV Shut in (Test 2)**

From the Figure 4-7, after two cycles of chemical injection and shut-in treatment, the tertiary recovery of this experiment was 31.71%. The second 1 PV injection and shut-in produced 26.68% oil of the total tertiary recovery. The characteristic of the oil breakthrough on the Figure 4-7 was similar to all the 1+1 PV shut-in tests at 120°C. Based on the urea hydrolysis kinetic measurement, 8% of the urea in 35 wt.% solution could be hydrolyzed after 73 hours heating, which was corresponding to 3 wt.% urea solutions hydrolyzed completely. Therefore, the result from 2.5 wt.% 1+1 PV shut-



in at 120 °C experiment was the most comparable test in this case, since the 90% of the urea in the 2.5 wt.% solution was hydrolyzed in test 2. The 80°C test generated slightly more CO<sub>2</sub> than the 2.5 wt.% 120°C test. Therefore, it was reasonable to see the tertiary recovery of the 80°C test was between the 2.5 wt.% and 5 wt.% tests at 120°C. Despite the temperature effect on the fluid property, the 35 wt.% 80°C test was almost identical to a 3 wt.% 120°C test. The amount of the generated CO<sub>2</sub> dramatically controlled the tertiary recovery. The 35 wt.% urea 120°C sand pack flooding test could be found in details at one of our previous work[102].

#### 4.5 Summary

**Table 4-4 Tertiary Recovery Summary**

	Test 1	Test 2	Test 3	Test 4	Test 5	Test 6	Test 7	Test 8	Test 9	Test 10	Test 11
Total Tertiary Recovery	11.0%	24.4%	38.3%	48.3%	50.0%	44.3%	35.7%	56.8%	60.0%	30.6%	31.7%
First PV Tertiary Recovery	7.7%	18.6%	30.9%	42.8%	43.2%	39.3%	\	50.6%	\	23.5%	23.2%
Second PV Tertiary Recovery	3.3%	5.8%	7.4%	5.5%	6.8%	5.0%	\	6.2%	\	7.1%	8.5%

Table 4-4 summarizes the performance of all the tested scenarios. It is clear to see that the divalent ions concentration adversely affected the tertiary recovery. Unless the urea concentration was very low, e.g. 1 wt.%, the second PV of urea injection did not contribute much to the final tertiary recovery.

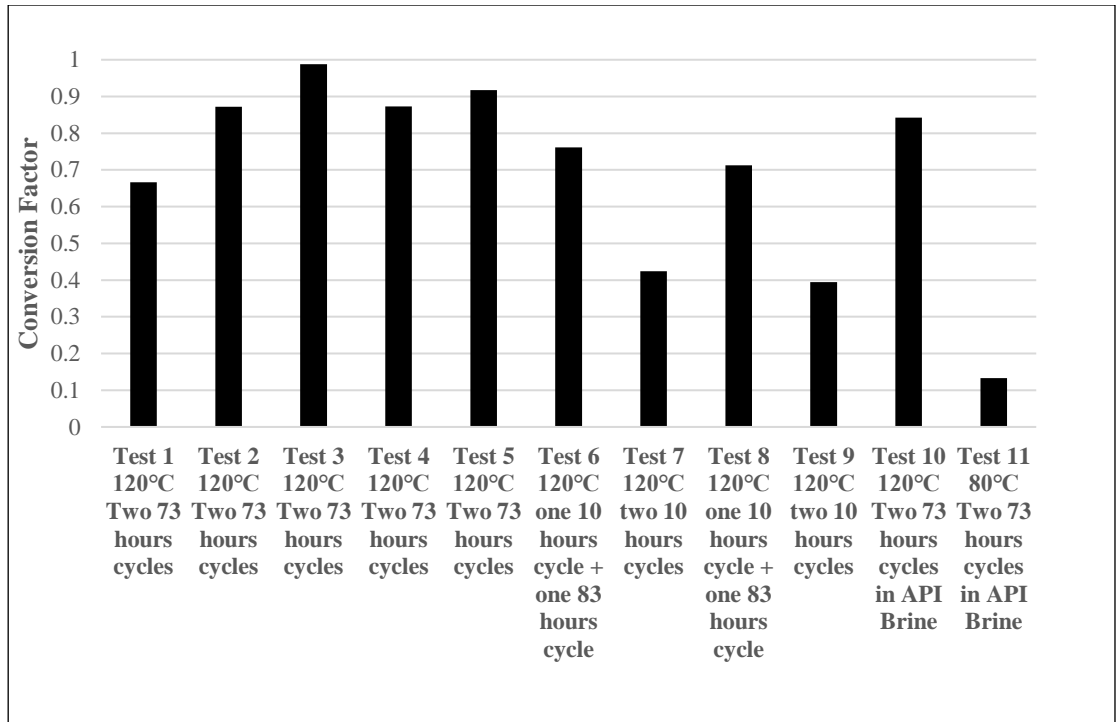


**Figure 4-8 Conversion factor of all the tests.**

Figure 4-8 shows all the data from the collected effluent urea concentration via HPLC analyses. Same injection strategy showed similar conversion factor for all concentrations. Among the 120°C tests, the 1+1 PV shut-in injection had the highest conversion factor. The conversion factor of the 2 PV flow-through tests was only half the conversion factor of the highest strategy. It could be attributed to the chemical residence time difference. The 80°C test showed a low conversion factor. The mass balance analysis coincided with the urea hydrolysis kinetic measurement. At low-temperature reservoir conditions, the potential of increasing the conversion factor was only a matter of time, such as the use of longer soaking time.

#### 4.6 Conclusion

The experiments reported in this study support the following conclusions:

1. The measured urea hydrolysis kinetic data can be used for in situ CO<sub>2</sub> generation prediction and process design.
2. NaOH could be used to increase the reaction rate of the urea hydrolysis.
3. Unlike miscible CO<sub>2</sub> flooding, the tertiary recovery ability of the in situ CO<sub>2</sub> generation was limited because of its immiscible flooding nature. With increasing urea concentration, the efficiency of the chemical reaches a plateau and then begins decreasing. There was an optimum concentration and injection strategy for a specific test condition.
4. The proposed system could provide significant tertiary recovery even in the presence of divalent ions.
5. If the divalent ions concentration was too high, the performance of the in situ CO<sub>2</sub> EOR would be adversely affected.
6. Low reservoir temperature is not a barrier for the in situ CO<sub>2</sub> EOR process if the chemical residence time could be manipulated to allow for adequate CO<sub>2</sub> generation.

## Chapter 5: Conclusions and Recommendations

From chapter 2, it can be concluded that ammonium carbamate can be used as the gas generating agent for the EOR purpose. The tertiary recovery of ammonium carbamate involved ICE process is significant compared with the published CWI and ICE system. This ICE process can work at a wide range of pressure(0 to 4000 psig) and temperature(96 to 133°C). Running experiment above the minimum miscibility pressure is not a critical criterion to receive a notable tertiary recovery. The ICE process only involves immiscible flooding. Unlike the CO<sub>2</sub> flooding, instead of producing lighter components in the crude oil, ICE process produces heavier components of the crude oil.

From chapter 3, after multiple sand pack flooding tests, the effectiveness of the urea as a gas generating agent in the ICE process is proved. Concentrated urea solution injection showed similar recovery as the concentrated ammonium carbamate solution. Under the same condition, ICE has better performance for lighter oil test than heavier oil. The tertiary recovery mechanism of the urea solution injection is the same as the ammonium carbamate solution. Urea solution can tolerate the cation concentration in the seawater. After the urea solution PVT test, it can be concluded that no separate CO<sub>2</sub> gas phase is forming during the ICE process.

From chapter 4, after the study on the urea hydrolysis reaction kinetics, the measured reaction rate can be used to design the chemical residence time. The reaction rate is higher than the base case with the adding of the NaOH as a catalyst. From the optimization of the chemical concentration, the urea consumption for barrel addition oil production can be as low as 34 kg. From the pH and mass balance analysis of the

effluent, the tertiary is strongly controlled by the generated CO<sub>2</sub> volume. Urea ICE can tolerate the divalent cations concentration in API brine. The reaction rate is enough for tertiary recovery at 80 °C.

The proposed ICE method revealed advantages against the traditional CO<sub>2</sub> EOR in this work. However, this work is only the initial study of this technique. The mechanisms and the applications of this technique have not been fully explored. If the research of ICE continues in the future, the full understanding of the whole system phase behavior is the priority work. Not like the phase behavior test for CWI, other than the oil, gas, and water the ICE phase behavior test should include the gas generating agent in the aqueous phase to explore the effect of water consumption during the chemical hydrolysis and the CO<sub>2</sub> solubility change from the dissolved chemical. Some corrections to the current phase behavior modeling tool are necessary after the phase behavior, and chemical kinetics mechanisms of the ICE are fully understood. Regarding the modeling work, the chemical reaction needs to be added to the current available CWI simulation to take the water consumption during the ICE process into account. The catalyst for urea hydrolysis is also important to expand the operating envelope to low-temperature reservoirs.

The new application of ICE EOR for other types of reservoirs would be possible. Not like traditional CO<sub>2</sub> flooding, no high concentration of carbonic acid is forming in the aqueous phase during the ICE process. Therefore, the tertiary recovery benefit of CO<sub>2</sub> could be applied to the carbonate reservoir without calcium carbonate precipitation near the production well. For liquid-rich shale reservoir EOR, the CO<sub>2</sub> bypassing issue of the

current CO<sub>2</sub> cyclic procedure is not happening in the ICE process. The shale matrix can be exposed to the CO<sub>2</sub> for a longer time. The ICE could be a promising solution for the liquid-rich shale EOR. It could be incorporated into the refracturing operation of the shale reservoir production. With enough amount of shut-in time, a significant amount of CO<sub>2</sub> could be generated to benefit the oil production and fracturing fluid flow back.

## References

- [1] J. Conti, P. Holtberg, J. Diefenderfer, A. LaRose, J.T. Turnure, L. Westfall, International Energy Outlook 2017, in, USDOE Energy Information Administration (EIA), Washington, DC (United States). Office of Energy Analysis, 2017.
- [2] L.S. Melzer, Carbon dioxide enhanced oil recovery (CO<sub>2</sub> EOR): Factors involved in adding carbon capture, utilization and storage (CCUS) to enhanced oil recovery, Center for Climate and Energy Solutions, (2012).
- [3] M.K. Verma, Fundamentals of Carbon Dioxide-enhanced Oil Recovery (CO<sub>2</sub>-EOR): A Supporting Document of the Assessment Methodology for Hydrocarbon Recovery Using CO<sub>2</sub>-EOR Associated with Carbon Sequestration, US Department of the Interior, US Geological Survey, 2015.
- [4] D.W. Green, G.P. Willhite, Enhanced Oil Recovery, Henry L. Doherty Memorial Fund of AIME, Society of Petroleum Engineers, 1998.
- [5] N. Mosavat, Utilization of Carbonated Water Injection (CWI) as a Means of Improved Oil Recovery in Light Oil Systems: Pore-Scale Mechanisms and Recovery Evaluation, in, Faculty of Graduate Studies and Research, University of Regina, 2014.
- [6] X. Wang, Q. Yuan, S. Wang, F. Zeng, The First Integrated Approach for CO<sub>2</sub> Capture and Enhanced Oil Recovery in China, in, Carbon Management Technology Conference, 2017.
- [7] L. Han, Y. Gu, Optimization of Miscible CO<sub>2</sub> Water-Alternating-Gas Injection in the Bakken Formation, *Energy & Fuels*, 28 (2014) 6811-6819.
- [8] H. Lei, S. Yang, L. Zu, Z. Wang, Y. Li, Oil Recovery Performance and CO<sub>2</sub> Storage Potential of CO<sub>2</sub> Water-Alternating-Gas Injection after Continuous CO<sub>2</sub> Injection in a Multilayer Formation, *Energy & Fuels*, 30 (2016) 8922-8931.
- [9] D.N. Rao, M.G. Girard, Induced Multiphase Flow Behaviour Effects in Gas Injection EOR Projects, (2002).
- [10] Y. Dong, B. Dindoruk, C. Ishizawa, E.J. Lewis, An experimental investigation of carbonated water flooding, in: SPE Annual Technical Conference and Exhibition, Society of Petroleum Engineers, 2011.
- [11] M. Sohrabi, M. Riazi, M. Jamiolahmady, N.I. Kechut, S. Ireland, G. Robertson, Carbonated water injection (CWI)—a productive way of using CO<sub>2</sub> for oil recovery and CO<sub>2</sub> storage, *Energy Procedia*, 4 (2011) 2192-2199.

- [12] N.I. Kechut, M. Jamiolahmady, M. Sohrabi, Numerical simulation of experimental carbonated water injection (CWI) for improved oil recovery and CO<sub>2</sub> storage, *Journal of Petroleum Science and Engineering*, 77 (2011) 111-120.
- [13] R. Christensen, Carbonated Waterflood Results--Texas And Oklahoma, in: *Annual Meeting of Rocky Mountain Petroleum Engineers of AIME, Society of Petroleum Engineers*, 1961.
- [14] C. Hickok, R. Christensen, H. Ramsay Jr, Progress review of the K&S carbonated waterflood project, *Journal of Petroleum Technology*, 12 (1960) 20-24.
- [15] J. Scott, C. Forrester, Performance of Domes Unit Carbonated Waterflood-First Stage, *Journal of Petroleum Technology*, 17 (1965) 1,379-371,384.
- [16] W.R. Shu, Carbonated waterflooding for viscous oil recovery, in, *Google Patents*, 1984.
- [17] M. Jödecke, Á. Pérez-Salado Kamps, G. Maurer, Experimental investigation of the solubility of CO<sub>2</sub> in (acetone+ water), *Journal of Chemical & Engineering Data*, 52 (2007) 1003-1009.
- [18] S. Bakhtiyarov, Technology on in-situ gas generation to recover residual oil reserves, in, *New Mexico Institute Of Mining And Technology*, 2008.
- [19] B.J.B. Shiau, T.-P. Hsu, B.L. Roberts, J.H. Harwell, Improved Chemical Flood Efficiency by In Situ CO<sub>2</sub> Generation, in: *SPE Improved Oil Recovery Symposium, Society of Petroleum Engineers*, 2010.
- [20] K. Gumersky, I. Dzhafarov, A.K. Shakhverdiev, Y.G. Mamedov, In-situ generation of carbon dioxide: New way to increase oil recovery, in: *SPE European Petroleum Conference, Society of Petroleum Engineers*, 2000.
- [21] L. Altunina, V. Kuvshinov, Evolution tendencies of physico-chemical EOR methods, in: *SPE European Petroleum Conference, Society of Petroleum Engineers*, 2000.
- [22] L.K. Altunina, V.A. Kuvshinov, Physicochemical methods for enhancing oil recovery from oil fields, *Russian Chemical Reviews*, 76 (2007) 971-987.
- [23] L. Altunina, V. Kuvshinov, Improved oil recovery of high-viscosity oil pools with physicochemical methods and thermal-steam treatments, *Oil & Gas Science and Technology-Revue de l'IFP*, 63 (2008) 37-48.



- [24] Y. Wang, J. Hou, Y. Tang, In-situ CO<sub>2</sub> generation huff-n-puff for enhanced oil recovery: Laboratory experiments and numerical simulations, *Journal of Petroleum Science and Engineering*, 145 (2016) 183-193.
- [25] Y. Li, K. Ma, Y. Liu, J. Zhang, X. Jia, B. Liu, Enhance Heavy Oil Recovery by In-Situ Carbon Dioxide Generation and Application in China Offshore Oilfield, in, *Society of Petroleum Engineers*, 2013.
- [26] M. Sohrabi, A. Emadi, S.A. Farzaneh, S. Ireland, A Thorough Investigation of Mechanisms of Enhanced Oil Recovery by Carbonated Water Injection, in: *SPE Annual Technical Conference and Exhibition*, Society of Petroleum Engineers, 2015.
- [27] N. Mosavat, F. Torabi, Experimental evaluation of the performance of carbonated water injection (CWI) under various operating conditions in light oil systems, *Fuel*, 123 (2014) 274-284.
- [28] D. Bonenfant, M. Mimeault, R. Hausler, Determination of the structural features of distinct amines important for the absorption of CO<sub>2</sub> and regeneration in aqueous solution, *Industrial & engineering chemistry research*, 42 (2003) 3179-3184.
- [29] N. McCann, M. Maeder, M. Attalla, Simulation of enthalpy and capacity of CO<sub>2</sub> absorption by aqueous amine systems, *Industrial & engineering chemistry research*, 47 (2008) 2002-2009.
- [30] R.A. Khatri, S.S. Chuang, Y. Soong, M. Gray, Thermal and chemical stability of regenerable solid amine sorbent for CO<sub>2</sub> capture, *Energy & Fuels*, 20 (2006) 1514-1520.
- [31] S. Wang, M. Kadhum, Q. Yuan, B.-J. Shiao, J.H. Harwell, Carbon Dioxide in Situ Generation for Enhanced Oil Recovery, in, *Carbon Management Technology Conference*, 2017.
- [32] N. Wen, M.H. Brooker, Ammonium carbonate, ammonium bicarbonate, and ammonium carbamate equilibria: a Raman study, *The Journal of Physical Chemistry*, 99 (1995) 359-368.
- [33] C. Flury, A. Afacan, M. Tamiz Bakhtiari, J. Sjoblom, Z. Xu, Effect of caustic type on bitumen extraction from Canadian oil sands, *Energy & Fuels*, 28 (2013) 431-438.
- [34] I. Fjelde, S.M. Asen, Wettability alteration during water flooding and carbon dioxide flooding of reservoir chalk rocks, in: *SPE EUROPEC/EAGE Annual Conference and Exhibition*, Society of Petroleum Engineers, 2010.

- [35] J.G. Southwick, E. van den Pol, C.H. van Rijn, D.W. van Batenburg, D. Boersma, Y. Svec, A. Anis Mastan, G. Shahin, K. Raney, Ammonia as Alkali for Alkaline/Surfactant/Polymer Floods, SPE Journal, 21 (2016) 10-21.
- [36] A. Steffens, Modeling and laboratory study of carbonated water flooding, in, TU Delft, Delft University of Technology, 2010.
- [37] Z. Duan, R. Sun, C. Zhu, I.-M. Chou, An improved model for the calculation of CO<sub>2</sub> solubility in aqueous solutions containing Na<sup>+</sup>, K<sup>+</sup>, Ca<sup>2+</sup>, Mg<sup>2+</sup>, Cl<sup>-</sup>, and SO<sub>4</sub><sup>2-</sup>, Marine Chemistry, 98 (2006) 131-139.
- [38] S. Hangx, Behaviour of the CO<sub>2</sub>-H<sub>2</sub>O system and preliminary mineralisation model and experiments, CATO Workpackage WP, 4 (2005).
- [39] A.M. Elsharkawy, S.G. Foda, EOS simulation and GRNN modeling of the constant volume depletion behavior of gas condensate reservoirs, Energy & Fuels, 12 (1998) 353-364.
- [40] T. Jindrová, J.i. Mikyška, A. Firoozabadi, Phase Behavior Modeling of Bitumen and Light Normal Alkanes and CO<sub>2</sub> by PR-EOS and CPA-EOS, Energy & Fuels, 30 (2015) 515-525.
- [41] R. Simon, D. Graue, Generalized correlations for predicting solubility, swelling and viscosity behavior of CO<sub>2</sub>-crude oil systems, Journal of Petroleum Technology, 17 (1965) 102-106.
- [42] G.W. Prosper, S.M.F. Ali, Scaled Model Studies Of The Immiscible Carbon Dioxide Flooding Process At Low Pressures, in, Petroleum Society of Canada, 1991.
- [43] N. De Nevers, A calculation method for carbonated water flooding, Society of Petroleum Engineers Journal, 4 (1964) 9-20.
- [44] L. Holm, CO<sub>2</sub> flooding: its time has come, Journal of Petroleum Technology, 34 (1982) 2,739-732,745.
- [45] G. Rojas, S. Ali, Dynamics of subcritical CO<sub>2</sub>/brine floods for heavy-oil recovery, SPE Reservoir Engineering, 3 (1988) 35-44.
- [46] M. Budhathoki, S.H.R. Barnee, B.-J. Shiau, J.H. Harwell, Improved oil recovery by reducing surfactant adsorption with polyelectrolyte in high saline brine, Colloids and Surfaces A: Physicochemical and Engineering Aspects, 498 (2016) 66-73.
- [47] X. Zhou, N.R. Morrow, S. Ma, Interrelationship of wettability, initial water saturation, aging time, and oil recovery by spontaneous imbibition and waterflooding, SPE Journal, 5 (2000) 199-207.

- [48] F. Wassmuth, K. Green, L. Randall, Details of in-situ foam propagation exposed with magnetic resonance imaging, *SPE Reservoir Evaluation & Engineering*, 4 (2001) 135-145.
- [49] J.J. Taber, F. Martin, R. Seright, EOR screening criteria revisited-Part 1: Introduction to screening criteria and enhanced recovery field projects, *SPE Reservoir Engineering*, 12 (1997) 189-198.
- [50] M. Emera, H. Sarma, A genetic algorithm-based model to predict co-oil physical properties for dead and live oil, in: *Canadian International Petroleum Conference*, Petroleum Society of Canada, 2006.
- [51] V. Darde, K. Thomsen, W.J.M. van Well, E.H. Stenby, Chilled ammonia process for CO<sub>2</sub> capture, *International Journal of Greenhouse Gas Control*, 4 (2010) 131-136.
- [52] V. Darde, W.J. van Well, E.H. Stenby, K. Thomsen, CO<sub>2</sub> capture using aqueous ammonia: kinetic study and process simulation, *Energy Procedia*, 4 (2011) 1443-1450.
- [53] D.W. Green, *Enhanced oil recovery*, Richardson, TX : Henry L. Doherty Memorial Fund of AIME, Society of Petroleum Engineers, Richardson, TX, 1998.
- [54] J.S. Buckley, T. Fan, Crude oil/brine interfacial tensions<sup>1</sup>, *Petrophysics*, 48 (2007).
- [55] H. Sharma, S. Dufour, G.W.P.P. Arachchilage, U. Weerasooriya, G.A. Pope, K. Mohanty, Alternative alkalis for ASP flooding in anhydrite containing oil reservoirs, *Fuel*, 140 (2015) 407-420.
- [56] C. Johnson Jr, Status of caustic and emulsion methods, *Journal of Petroleum Technology*, 28 (1976) 85-92.
- [57] M. Emera, J. Lu, Genetic Algorithm (GA)-Based Correlations Offer More Reliable Prediction of Minimum Miscibility Pressures (MMP) Between the Reservoir Oil and CO or Flue Gas, in: *Canadian International Petroleum Conference*, Petroleum Society of Canada, 2005.
- [58] E.J. Manrique, C.P. Thomas, R. Ravikiran, M. Izadi Kamouei, M. Lantz, J.L. Romero, V. Alvarado, EOR: current status and opportunities, in: *SPE improved oil recovery symposium*, Society of Petroleum Engineers, 2010.
- [59] P. Zuloaga-Molero, W. Yu, Y. Xu, K. Sepehrnoori, B. Li, Simulation Study of CO<sub>2</sub>-EOR in Tight Oil Reservoirs with Complex Fracture Geometries, *Scientific Reports*, 6 (2016).

- [60] H. Wang, Z. Lun, C. Lv, D. Lang, B. Ji, M. Luo, W. Pan, R. Wang, K. Gong, Measurement and Visualization of Tight Rock Exposed to CO<sub>2</sub> Using NMR Relaxometry and MRI, *Scientific Reports*, 7 (2017).
- [61] S. Kalra, W. Tian, X. Wu, A numerical simulation study of CO<sub>2</sub> injection for enhancing hydrocarbon recovery and sequestration in liquid-rich shales, *Petroleum Science*, (2017) 1-13.
- [62] T. Shen, R.G. Moghanloo, W. Tian, Ultimate CO<sub>2</sub> Storage Capacity of an Over-Pressurized 2D Aquifer Model, in: *EUROPEC 2015*, Society of Petroleum Engineers, 2015.
- [63] J.P. DiPietro, V. Kuuskraa, T. Malone, Taking CO<sub>2</sub> Enhanced Oil Recovery to the Offshore Gulf of Mexico: A Screening-Level Assessment of the Technically and Economically-Recoverable Resource, *SPE Economics & Management*, 7 (2015) 3-9.
- [64] T.W. Teklu, W. Alameri, R.M. Graves, H. Kazemi, A.M. AlSumaiti, Low-salinity water-alternating-CO<sub>2</sub> EOR, *Journal of Petroleum Science and Engineering*, 142 (2016) 101-118.
- [65] N.I. Kechut, M. Sohrabi, M. Jamiolahmady, Experimental and Numerical Evaluation of Carbonated Water Injection (CWI) for Improved Oil Recovery and CO<sub>2</sub> Storage, in: *SPE EUROPEC/EAGE Annual Conference and Exhibition*, Society of Petroleum Engineers, 2011.
- [66] N. Mosavat, F. Torabi, Performance of secondary carbonated water injection in light oil systems, *Industrial & Engineering Chemistry Research*, 53 (2013) 1262-1273.
- [67] N. Mosavat, F. Torabi, Application of CO<sub>2</sub>-saturated water flooding as a prospective safe CO<sub>2</sub> storage strategy, *Energy Procedia*, 63 (2014) 5619-5630.
- [68] Chemical Book, Urea, in, 2017.
- [69] L.P. Schell, Method of hydrolyzing urea contained in waste water streams, in, *Google Patents*, 1978.
- [70] M. Koebel, E.O. Strutz, Thermal and hydrolytic decomposition of urea for automotive selective catalytic reduction systems: thermochemical and practical aspects, *Industrial & engineering chemistry research*, 42 (2003) 2093-2100.
- [71] M. Rahimpour, A. Azarpour, Simulation of a urea thermal hydrolysis reactor, *Chem. Eng. Comm.*, 192 (2005) 155-167.

- [72] M. Barmaki, M. Rahimpour, A. Jahanmiri, Treatment of wastewater polluted with urea by counter-current thermal hydrolysis in an industrial urea plant, *Separation and Purification Technology*, 66 (2009) 492-503.
- [73] R.C. Warner, The kinetics of the hydrolysis of urea and of arginine, *Journal of Biological Chemistry*, 142 (1942) 705-723.
- [74] K.R. Lynn, Kinetics of Base-Catalyzed Hydrolysis of Urea, *The Journal of Physical Chemistry*, 69 (1965) 687-689.
- [75] A.N. Alexandrova, W.L. Jorgensen, Why urea eliminates ammonia rather than hydrolyzes in aqueous solution, *The journal of physical chemistry. B*, 111 (2007) 720.
- [76] J.N. Sahu, K. Mahalik, A.V. Patwardhan, B.C. Meikap, Equilibrium and Kinetic Studies on the Hydrolysis of Urea for Ammonia Generation in a Semibatch Reactor, *Industrial & Engineering Chemistry Research*, 47 (2008) 4689-4696.
- [77] M. Yao, W. Tu, X. Chen, C.-G. Zhan, Reaction pathways and free energy profiles for spontaneous hydrolysis of urea and tetramethylurea: unexpected substituent effects, *Organic & biomolecular chemistry*, 11 (2013) 7595-7605.
- [78] F. Zhu, J. Gao, X. Chen, M. Tong, Y. Zhou, J. Lu, Hydrolysis of Urea for Ammonia-Based Wet Flue Gas Desulfurization, *Industrial & Engineering Chemistry Research*, 54 (2015) 9072-9080.
- [79] A.M. Bernhard, D. Peitz, M. Elsener, T. Schildhauer, O. Kröcher, Catalytic urea hydrolysis in the selective catalytic reduction of NO<sub>x</sub>: catalyst screening and kinetics on anatase TiO<sub>2</sub> and ZrO<sub>2</sub>, *Catalysis Science & Technology*, 3 (2013) 942-951.
- [80] A.M. Bernhard, Catalytic urea decomposition, side-reactions and urea evaporation in the selective catalytic reduction of NO<sub>x</sub>, in, *University of Berne*, 2012.
- [81] N.V. Kaminskaia, N.M. Kostić, Kinetics and Mechanism of Urea Hydrolysis Catalyzed by Palladium(II) Complexes, *Inorganic Chemistry*, 36 (1997) 5917-5926.
- [82] L.P. Schell, Catalytic method for hydrolyzing urea, in, *Google Patents*, 1979.
- [83] E.H. Mayer, R. Earlougher Sr, A. Spivak, A. Costa, Analysis of heavy-oil immiscible CO<sub>2</sub> tertiary coreflood data, *SPE reservoir engineering*, 3 (1988) 69-75.
- [84] A. Fathollahi, B. Rostami, Carbonated water injection: Effects of silica nanoparticles and operating pressure, *The Canadian Journal of Chemical Engineering*, 93 (2015) 1949-1956.

- [85] Q. Yuan, S. Yao, X. Zhou, F. Zeng, K.D. Knorr, M. Imran, Miscible displacements with concentration-dependent diffusion and velocity-induced dispersion in porous media, *Journal of Petroleum Science and Engineering*, 159 (2017) 344-359.
- [86] J.T. Patton, N.M.S. University, N.E.T. Laboratory, U.S.D.o. Energy, M.E.T. Center, U.S.D.o.E.O.o. Scientific, T. Information, CO<sub>2</sub> Formation Damage Study. Final Report, National Energy Technology Laboratory (U.S.), 1983.
- [87] B. Hill, S. Hovorka, S. Melzer, Geologic carbon storage through enhanced oil recovery, *Energy Procedia*, 37 (2013) 6808-6830.
- [88] R.M. Enick, D.K. Olsen, J.R. Ammer, W. Schuller, Mobility and Conformance Control for CO<sub>2</sub> EOR via Thickeners, Foams, and Gels--A Literature Review of 40 Years of Research and Pilot Tests, in: SPE improved oil recovery symposium, Society of Petroleum Engineers, 2012.
- [89] L. koottungal, 2014 worldwide EOR survey, *Oil & Gas Journal*, (2014) 100-105.
- [90] B. Metz, O. Davidson, H. De Coninck, M. Loos, L. Meyer, IPCC special report on carbon dioxide capture and storage, in: Intergovernmental Panel on Climate Change, Geneva (Switzerland). Working Group III, 2005.
- [91] S. Rassenfoss, Shale EOR Works, But Will It Make a Difference?, *Journal of Petroleum Technology*, 69 (2017) 34-40.
- [92] K. Welkenhuysen, J. Rupert, T. Compennolle, A. Ramirez, R. Swennen, K. Piessens, Considering economic and geological uncertainty in the simulation of realistic investment decisions for CO<sub>2</sub>-EOR projects in the North Sea, *Applied Energy*, 185 (2017) 745-761.
- [93] D.E. Raifsnider, P.J. Raifsnider, In-situ formed co<sub>2</sub> drive for oil recovery, in, Google Patents, 1970.
- [94] C. Yang, Y. Lin, Z. Zhang, R. Deng, X. Wu, B. Niu, Z. Li, S. Ren, A Study on the Mechanism of Urea-assisted Steam Flooding in Heavy Oil Reservoirs, *Journal of Petroleum Science and Technology*, 5 (2015) 36-44.
- [95] P. Liu, W. Li, D. Shen, Experimental study and pilot test of urea-and urea-and-foam-assisted steam flooding in heavy oil reservoirs, *Journal of Petroleum Science and Engineering*, 135 (2015) 291-298.
- [96] K. Abdelgawad, M. Mahmoud, In-Situ Generation of CO<sub>2</sub> to Eliminate the Problem of Gravity Override in EOR of Carbonate Reservoirs, in: SPE Middle East Oil & Gas Show and Conference, Society of Petroleum Engineers, 2015.

- [97] M.A.N.E.D. Mahmoud, A.S. Sultan, K.Z. Abdelgawad, Method for enhanced oil recovery by in situ carbon dioxide generation, in, Google Patents, 2014.
- [98] M. Alam, M. Mahmoud, N. Sibaweih, A Slow Release CO<sub>2</sub> for Enhanced Oil Recovery in Carbonate Reservoirs, in: SPE Middle East Oil & Gas Show and Conference, Society of Petroleum Engineers, 2015.
- [99] V.N. Venkatesan, Oil recovery process employing CO<sub>2</sub> produced in situ, in, Google Patents, 1985.
- [100] D. Zhu, J. Hou, J. Wang, X. Wu, P. Wang, B. Bai, Acid-alternating-base (AAB) technology for blockage removal and enhanced oil recovery in sandstone reservoirs, *Fuel*, 215 (2018) 619-630.
- [101] S.I. Bakhtiyarov, A.K. Shakhverdiev, G.M. Panakhov, E.M. Abbasov, Effect of Surfactant on Volume and Pressure of Generated CO<sub>2</sub> Gas, in: Production and Operations Symposium, Society of Petroleum Engineers, 2007.
- [102] S. Wang, C. Chen, B. Shiau, J.H. Harwell, In-situ CO<sub>2</sub> generation for EOR by using urea as a gas generation agent, *Fuel*, 217 (2018) 499-507.
- [103] L. Holm, Miscibility and miscible displacement, *Journal of Petroleum Technology*, 38 (1986) 817-818.
- [104] F.O. Ajisafe, Microbial Waterflooding of the Third Earlsboro Unit, Seminole County, Oklahoma, University of Oklahoma, 2007.
- [105] J. Sahu, K. Mahalik, A. Patwardhan, B. Meikap, Equilibrium and kinetic studies on the hydrolysis of urea for ammonia generation in a semibatch reactor, *Industrial & Engineering Chemistry Research*, 47 (2008) 4689-4696.
- [106] L.P. Schell, Catalytic method for hydrolyzing urea, in, Google Patents, 1980.

## Appendix A: Representative Data

**Table A.1 Chapter 2 test 11**

Time	Inlet Pressure, psi	Back Pressure, psi	Temperature, °C	Time	Inlet Pressure, psi	Back Pressure, psi	Temperature, °C
4/3/2016 16:09	1323.9	1322.3	121.8	42466.67021	1319	1319.9	121.2
4/3/2016 17:29	1324.6	1321.9	121.4	4/6/2016 17:25	1328.1	1323.1	122.4
4/3/2016 18:48	1320.5	1319.1	121.9	4/6/2016 18:45	1323.5	1324.1	121.4
4/3/16 20:08	1321.5	1316.8	120.3	4/6/2016 20:03	1319.6	1316.3	123.1
4/3/16 21:28	1319.8	1315.4	120.4	4/6/2016 21:23	1309.7	1296.7	123.1
4/3/16 22:48	1311.1	1306.3	121.3	4/6/2016 22:43	1312.9	1306.9	122.4
4/4/16 0:08	1310.3	1305.4	121.4	4/7/2016 0:03	1315.8	1307.6	121.5
4/4/16 1:28	1302.3	1301.1	121.6	4/7/2016 1:23	1311.5	1313.1	121.8
4/4/16 2:48	1295.6	1292.7	120.4	4/7/2016 2:43	1304	1308.6	122.5
4/4/16 4:08	1299.6	1297	121.8	4/7/2016 4:03	1315	1313.5	122.1
4/4/16 5:28	1300.4	1296.1	121.8	4/7/2016 5:23	1322	1307.8	122.5
4/4/16 6:48	1302.8	1299.1	121.6	4/7/2016 6:43	1315.4	1310.5	121.6
4/4/16 8:08	1299.7	1297.9	121.6	4/7/2016 8:03	1320.9	1315.2	123
4/4/16 9:28	1303.3	1299.3	121.3	4/7/2016 9:23	1305.7	1290.8	122.6
4/4/16 10:48	1289.4	1284.7	122.1	4/7/2016 10:41	1321.7	1284.3	122.9
4/4/16 12:08	1299.3	1297.9	121.9	4/7/2016 12:01	1290.4	1307.3	122.1
4/4/16 13:28	1304.8	1301.8	122.3	4/7/2016 13:21	1259.6	1266.1	122.7
4/4/16 14:48	1302.4	1297.4	121.8	4/7/2016 14:41	1187.5	1205.1	122.7
4/4/16 16:08	1305.9	1304.3	121.7	4/7/2016 16:01	1154.6	1161.9	121.6
4/4/16 17:28	1304.3	1300.4	119.9	4/7/2016 17:21	1115.3	1102.3	122.8
4/4/16 18:48	1311.5	1306.9	121.7	4/7/2016 18:41	1101.1	1108.5	122.6
4/4/16 20:08	1311.9	1308.8	120.7	4/7/2016 20:01	1064.3	1033.9	123.5
4/4/16 21:26	1281.9	1278.2	121.3	4/7/2016 21:21	1047.2	1033.3	121.8
4/4/16 22:46	1296.2	1297.2	121.3	4/7/2016 22:41	992.9	972.9	123.2
4/5/16 0:06	1294.5	1289.7	121.1	4/8/2016 0:01	998.4	963.9	121.7
4/5/16 1:26	1299.9	1299.5	121.5	4/8/2016 1:21	957.1	963.4	122.3
4/5/16 2:46	1300.3	1312.6	121.8	4/8/2016 2:41	918.9	926.1	123.4
4/5/16 4:06	1313.4	1317.9	122.2	4/8/2016 4:01	905.2	904.4	122.9
4/5/16 5:26	1294.1	1283.9	122.1	4/8/2016 5:21	902.4	910.4	123
4/5/16 6:46	1309	1298.8	121.9	4/8/2016 6:41	892.4	895.8	122.2
4/5/16 8:06	1301.5	1314.7	122	4/8/2016 8:01	879.5	870.7	122.1
4/5/16 9:25	1313.4	1289.2	122.1	4/8/2016 9:21	862.8	858.6	122.2
4/5/16 10:45	1306	1283.4	122.8	4/8/2016 10:41	847	850.8	122.9
4/5/16 12:05	1306.8	1294.1	122.4	4/8/2016 11:58	1104.8	1143.8	123.2
4/5/16 13:25	1295.5	1285.8	122.8	4/8/2016 13:18	1330.2	1319.4	122.4
4/5/16 14:45	1304.4	1286.9	123.2	4/8/2016 14:38	1300.5	1294.6	124.2
4/5/16 16:05	1293.8	1296	123.1	4/8/2016 15:58	1317.4	1311.6	123.2
4/5/16 17:25	1325.9	1321.1	121.3	4/8/2016 17:17	1325.2	1314.4	121.7
4/5/16 18:45	1336.5	1310.8	122.1	4/8/2016 18:37	1313.4	1306	121.5
4/5/16 20:05	1334.8	1310.5	123	4/8/2016 19:57	1311.6	1305	122.9
4/5/16 21:25	1322.7	1321.8	123.1	4/8/2016 21:17	1310.5	1313.1	122
4/5/16 22:45	1324.9	1322.8	122.7	4/8/2016 22:37	1330.5	1326.4	122.4
4/6/16 0:05	1316.4	1315.3	123.2	4/8/2016 23:57	1328.1	1327.2	122.5
4/6/16 1:25	1313.4	1314	122.7	4/9/2016 1:17	1330.1	1324.3	122.3
4/6/16 2:45	1323.9	1322.4	123.1	4/9/2016 2:37	1325.5	1325.7	123.3
4/6/16 4:05	1324.8	1313.1	122.7	4/9/2016 3:57	1325.7	1325.4	122.6
4/6/16 5:25	1285.4	1279.7	122	4/9/2016 5:17	1326.7	1324.9	122.9
4/6/16 6:45	1295.7	1297.2	122.8	4/9/2016 6:37	1298.7	1309	123.6
4/6/16 8:05	1305.6	1298.2	122	4/9/2016 7:57	1299.8	1296.5	123.1
4/6/16 9:25	1285.8	1279.2	122.9	4/9/2016 9:17	1305.6	1295.9	122.3
4/6/16 10:45	1288	1286.6	122.8	4/9/2016 10:37	1205.3	1247.9	122.6
4/6/16 12:05	1304	1322	122.7	4/9/2016 11:57	283.2	1245.9	122.4
4/6/16 13:25	1325.3	1318.5	122.6	4/9/2016 13:17	211	1246.2	122
4/6/16 14:45	1307.2	1307.7	122.5	4/9/2016 14:37	170	1246.7	121.4



**Table A. 2 Chapter 3 test 3**

Time	Inlet Pressure, psi	Back Pressure, psi	Temperature, °C	Time	Inlet Pressure, psi	Back Pressure, psi	Temperature, °C
9/4/2016 22:27	7.3	9.1	24.1	9/8/2016 17:58	4012.2	4013.7	120.6
9/4/2016 22:29	340.2	747.2	24.1	9/8/2016 19:38	4009.5	4009	120.3
9/4/2016 22:38	3589.7	3591.8	50.5	9/8/2016 21:18	4012.3	4011.4	121.1
9/5/16 0:00	4029	4031.8	122.5	9/8/2016 22:58	4011.1	4012.6	120.2
9/5/16 1:40	4028	4026.7	121.6	9/9/2016 0:38	4011.5	4011.4	121.6
9/5/16 3:20	4013.8	4013.4	120.9	9/9/2016 2:18	4011.1	4012.7	121.4
9/5/16 5:00	4029.4	4028.7	121.7	9/9/2016 3:58	4006.3	4006.8	122.1
9/5/16 6:40	4026.3	4026	122.5	9/9/2016 5:38	3994	4001.1	122
9/5/16 8:20	4024.2	4028.4	122.1	9/9/2016 7:18	3999.8	3997.4	122.2
9/5/16 10:00	4012	4012.2	120.2	9/9/2016 8:58	4015.3	3995.1	120.5
9/5/16 11:40	4007.7	4009.1	121.2	9/9/2016 10:38	4018.4	4010.4	122.1
9/5/16 13:20	4010.8	4011	121.8	9/9/2016 12:18	4012.5	4011	120.8
9/5/16 15:00	4022.5	4021.8	122.4	9/9/2016 13:58	4016.6	4015.6	120.4
9/5/16 16:40	4025	4026.6	121.5	9/9/2016 15:38	4015.8	4016.1	120.1
9/5/16 18:20	4022.8	4021	121.4	9/9/2016 17:18	4014.6	4012.3	121.8
9/5/16 20:00	4007.8	4007	122.7	9/9/2016 18:58	4002.9	4002.8	121.5
9/5/16 21:40	4023.4	4015.5	122.5	9/9/2016 20:38	3917.5	3930.1	121.1
9/5/16 23:20	3862.5	3857.8	122.3	9/9/2016 22:18	3851.3	3831.4	122.1
9/6/16 1:00	4021.1	4022.9	122.3	9/9/2016 23:58	3772.1	3766.2	122.2
9/6/16 2:40	4018.9	4018.2	121.6	9/10/2016 1:38	3683.6	3661.5	121.6
9/6/16 4:20	4002.7	4001.5	122.1	9/10/2016 3:18	3602.4	3583.6	121.8
9/6/16 6:00	4024.4	4019.4	120.6	9/10/2016 4:58	3532.3	3538.6	120.6
9/6/16 7:40	4018.4	4017.9	121.9	9/10/2016 6:38	3536.1	3522.8	121.6
9/6/16 9:20	4001.2	4003.3	120.5	9/10/2016 8:18	3487.2	3467.7	121.3
9/6/16 11:00	3986.6	3985	122.9	9/10/2016 9:58	3448.5	3432.4	121.3
9/6/16 12:40	4018.8	4018	121.9	9/10/2016 11:38	3398.7	3373.4	122.1
9/6/16 14:20	4022.3	4019	122.2	9/10/2016 13:18	3343.3	3357.9	120.2
9/6/16 16:00	3998	3997.4	121.8	9/10/2016 14:58	3336.9	3362.5	122
9/6/16 17:40	3908.4	3908.4	121.2	9/10/2016 16:38	3340.2	3335.1	121.6
9/6/16 19:20	4016.7	4002.5	120.5	9/10/2016 18:18	3924.5	3942.6	121.3
9/6/16 21:00	3996.9	3992.5	120.6	9/10/2016 19:58	4028.7	4019.3	121.6
9/6/16 22:40	3982.8	3981.1	121	9/10/2016 21:38	4015.7	4015	121.2
9/7/16 0:20	4015	4014.2	121.2	9/10/2016 23:18	4035.8	4034.5	121.4
9/7/16 2:00	4012.7	4011.9	120.2	9/11/2016 0:58	4029.1	4035.1	122.2
9/7/16 3:40	4011	4008.4	121.3	9/11/2016 2:38	4035.7	4035.1	121.3
9/7/16 5:20	4018	4017.2	121.2	9/11/2016 4:18	4035.7	4030.5	121.8
9/7/16 7:00	3983.3	3985.1	120.4	9/11/2016 5:58	4037.9	4036.7	120.7
9/7/16 8:40	4005.9	4004.8	121.1	9/11/2016 7:38	4039.5	4039.4	121.3
9/7/16 10:20	4014.4	4013.3	120.4	9/11/2016 9:18	4040.5	4039.6	122.6
9/7/16 12:00	4021.3	4020.8	121.7	9/11/2016 10:58	4029.5	4028.9	122.4
9/7/16 13:40	3953.3	3951.8	120	9/11/2016 12:38	4034.8	4032.3	122.7
9/7/16 15:20	4007.7	4007.4	121.5	9/11/2016 14:18	4036.7	4036.9	121.5
9/7/16 17:00	3978.1	3977.9	122.1	9/11/2016 15:58	4034.1	4033.6	121.6
9/7/16 18:40	4003.9	4006	121.6	9/11/2016 17:38	4030.7	4030.7	122.5
9/7/16 20:20	4011.5	4011.6	120.6	9/11/2016 19:18	4018	4019.4	121.4
9/7/16 22:00	4008.9	4005.5	120.3	9/11/2016 20:58	4024	4019.4	121.9
9/7/16 23:40	4013.3	4012.9	122.5	9/11/2016 22:38	4032.6	4031.3	122.8
9/8/16 1:20	4015.2	4014.5	122.1	9/12/2016 0:18	4030.9	4029.2	122.7
9/8/16 3:00	4011.4	4010.4	120.4	9/12/2016 1:58	4031.7	4031.2	122.6
9/8/16 4:40	4013.3	4012.6	120.4	9/12/2016 3:38	4032	4031.3	122.8
9/8/16 6:20	4011.7	4011.5	120.2	9/12/2016 5:18	4029.9	4029.9	122.5
9/8/16 8:00	4015.2	4014.3	120.4	9/12/2016 6:58	4030	4029.4	122.9
9/8/16 9:40	4013.5	4012.7	121.8	9/12/2016 8:38	4028.6	4030.4	120.6
9/8/16 11:18	4012.5	4011.1	121.9	9/12/2016 10:18	4030.5	4030.1	122
42621.54095	4014.6	4014.2	121.9	9/12/2016 11:58	4032.9	4031.8	122.6
9/8/2016 14:38	4005.4	4007.7	120.4	9/12/2016 13:38	4028.4	4027.2	121.9
9/8/2016 16:18	4011.7	4010	121.9	9/12/2016 15:18	3444.2	3430.2	25

**Table A. 3 Chapter 4 test 4**

Time	Inlet Pressure, psi	Back Pressure, psi	Temperature, °C	Time	Inlet Pressure, psi	Back Pressure, psi	Temperature, °C
4/18/17 15:33	1.5	0.8	24.4	4/22/17 4:31	1460.9	714.9	118.6
4/18/17 17:11	1549.4	1549.2	118.4	4/22/17 6:11	1445.6	716.2	120.1
4/18/17 18:51	1539.6	1538.1	119.4	4/22/17 7:51	1439.4	720.9	117.7
4/18/17 20:31	1577	1575.5	119.1	4/22/17 9:31	1445.3	718.5	120.2
4/18/17 22:11	1305.7	1304.2	117.1	4/22/17 11:11	1441.9	715.8	119.1
4/18/17 23:51	1264.2	1262.9	118.7	4/22/17 12:51	1477.1	1530.5	119.5
4/19/17 1:31	1313.7	1311.1	118.1	4/22/17 14:31	1433.7	1491.7	119.4
4/19/17 3:11	1506	1504.5	119.6	4/22/17 16:11	1556.8	1555.8	117.5
4/19/17 4:51	1503.6	1502.1	117.9	4/22/17 17:51	1479.2	1477.9	119.7
4/19/17 6:31	1263.7	1262.3	118.7	4/22/17 19:31	1434.5	1433	119.7
4/19/17 8:11	1510	1508.4	119	4/22/17 21:11	1514.6	897.8	117.3
4/19/17 9:51	1486.4	1484.8	117.7	4/22/17 22:51	1508.6	910.2	120
4/19/17 11:31	1555.2	1553.8	119.4	4/23/17 0:31	1504.7	897.2	119.9
4/19/17 13:11	1555.8	1554.5	119.6	4/23/17 2:11	1485.4	887.2	120.2
4/19/17 14:51	1541.7	1001.8	118.5	4/23/17 3:51	1481.5	904.4	120.6
4/19/17 16:31	1541.5	1006.1	117.6	4/23/17 5:31	1479.5	917.1	120.5
4/19/17 18:11	1549.1	1006.4	119.9	4/23/17 7:11	1467.8	905.1	118.2
4/19/17 19:51	1544	986	119.2	4/23/17 8:51	1445.9	890	118.4
4/19/17 21:31	1528.1	971.8	118.1	4/23/17 10:31	1443	925.2	120.2
4/19/17 23:11	1536.3	968.6	119.8	4/23/17 12:11	1439.7	926.2	117.7
4/20/17 0:51	1517.7	956.9	117.2	4/23/17 13:51	1434.1	905.9	120.4
4/20/17 2:31	1513.4	955.6	118.8	4/23/17 15:31	1440.3	944.9	117.5
4/20/17 4:11	1504.4	944	118.3	4/23/17 17:11	1436.7	946.8	119.1
4/20/17 5:51	1512.1	938.7	117.7	4/23/17 18:51	1430.5	928.2	120.1
4/20/17 7:31	1507.3	937.8	120	4/23/17 20:31	1436.6	950.2	120.2
4/20/17 9:11	1501.5	944.9	120.4	4/23/17 22:11	1422	953.3	119.8
4/20/17 10:51	1492.1	946.2	117.4	4/23/17 23:51	1426.6	935.8	120.8
4/20/17 12:31	1490.4	909	119.4	4/24/17 1:31	1406.4	911.2	120.5
4/20/17 14:11	1471.6	893.7	118	4/24/17 3:11	1402.6	932	120.8
4/20/17 15:51	1470.6	905.8	117.3	4/24/17 4:51	1395.1	937.3	120.5
4/20/17 17:31	1469.5	906.7	119.6	4/24/17 6:31	1402.5	926.9	118.6
4/20/17 19:11	1450.5	898.7	118.2	4/24/17 8:11	1396.9	921.6	117.6
4/20/17 20:51	1451.4	882.4	119	4/24/17 9:51	1511	934.8	120.3
4/20/17 22:31	1432.4	864.7	117.7	4/24/17 11:31	1513.2	955	120.4
4/21/17 0:11	1437.9	856.6	119.9	4/24/17 13:11	1522.9	941.5	120.4
4/21/17 1:51	1422.5	847.7	119.6	4/24/17 14:51	1531.9	961.4	117.8
4/21/17 3:31	1414.8	831.7	118.1	4/24/17 16:31	1533.4	989.7	118.4
4/21/17 5:11	1422.2	823.3	119	4/24/17 18:11	1540.7	991	120.6
4/21/17 6:51	1402.5	809.7	117.9	4/24/17 19:51	1553.1	1017	119.5
4/21/17 8:31	1382.4	784.3	117.6	4/24/17 21:31	1547.6	988.6	120.5
4/21/17 10:11	1376.6	763.3	119.3	4/24/17 23:11	1558.7	1010.2	117.9
4/21/17 11:51	1217.1	775.2	82.7	4/25/17 0:51	1556.8	992.3	118.6
4/21/17 13:31	1355.2	796.1	120	4/25/17 2:31	1542.6	978.3	120.3
4/21/17 15:11	1352.3	780.7	119.5	4/25/17 4:11	1553.5	1000.2	118
4/21/17 16:51	1532.8	779.9	119.2	4/25/17 5:51	1549.6	994.8	118.3
4/21/17 18:31	1520.2	766	119.3	4/25/17 7:31	1552.9	1007.3	117.3
4/21/17 20:11	1519.1	742.4	118.4	4/25/17 9:11	1536.2	1005.1	120.3
4/21/17 21:51	1502.7	724.4	118.8	4/25/17 10:51	1293.4	1292.4	117.5
4/21/17 23:31	1488.1	724.2	118	4/25/17 12:31	1570.6	1569.2	119.2
4/22/17 1:11	1472.6	717.9	118.9	4/25/17 14:11	1299.5	1297.9	61.3
4/22/17 2:51	1471.6	716.5	118.8				